Published for SISSA by Springer

Received: January 8, 2025
Accepted: February 20, 2025
Published: April 11, 2025

Triple real-emission contribution to the zero-jettiness soft function at N3LO in QCD

Daniel Baranowski,[a] **Maximilian Delto**,[b,d] **Kirill Melnikov**,[c] **Andrey Pikelner**[c] **and Chen-Yu Wang**[d]

[a] *Physik Institut, Universität Zürich, Winterthurerstrasse 190, 8057 Zürich, Switzerland*
[b] *Physics Department, Technical University of Munich, James-Franck-Strasse 1, 85748 Garching, Germany*
[c] *Institute for Theoretical Particle Physics (TTP), Karlsruhe Institute of Technology, Wolfgang-Gaede-Str. 1,76131 Karlsruhe, Germany*
[d] *Max-Planck Institute for Physics, Boltzmannstr. 8, 85748 Garching, Germany*

E-mail: daniel.baranowski@physik.uzh.ch, maximilian.delto@tum.de, kirill.melnikov@kit.edu, andrey.pikelner@kit.edu, cywang@mpp.mpg.de

Abstract: Recently, we have presented the result for the zero-jettiness soft function at next-to-next-to-next-to-leading order (N3LO) in perturbative QCD [1], without providing technical details of the calculation. The goal of this paper is to describe the most important element of that computation, the triple real-emission contribution. We present a detailed discussion of the many technical aspects of the calculation, for which a number of methodological innovations was required. Although some elements of the calculation were discussed earlier [2–6], this paper is intended to provide a complete summary of the methods used in the computation of the triple real-emission contribution to the soft function.

Keywords: Factorization, Renormalization Group, Higher-Order Perturbative Calculations

ArXiv ePrint: 2412.14001

https://doi.org/10.1007/JHEP04(2025)084

Contents

1 Introduction

Experiments at the LHC and its high-luminosity upgrade will continue the exploration of the Standard Model and searches for physics beyond it through precise measurements. Eventually, interpretations of such measurements will be dominated by theoretical systematics, and improvements in the description of hard hadron collisions are therefore called for. Such improvements require advancements in computations of two- and three-loop amplitudes for high multiplicities, and in dealing with real-emission processes which are needed to cancel infra-red divergences present in loop amplitudes [7–9].[1]

The crucial difference between loop amplitudes and real-emission contributions is that infra-red divergencies in virtual amplitudes appear explicitly after integrating over the loop momenta, manifesting themselves as poles in the dimensional regularization parameter $\epsilon = (4-d)/2$, with d being the dimensionality of space-time. On the contrary, real-emission contributions involve complex observables and cannot be analytically integrated over the entire phase space. Because of that, infra-red divergences need to be extracted before the numerical integration.

It is possible to do that because divergences only appear in phase-space regions where additional radiation (with respect to Born processes) becomes soft and collinear and, therefore, unresolved. Since infra-red safe observables are, by definition, not sensitive to soft- and collinear radiation, and since matrix elements exhibit universal factorization in these limits, it becomes possible to extract infra-red divergences in a process-independent manner. Consequently, various *slicing and subtraction* schemes that isolate, extract, and cancel infra-red poles in cross-section calculations, have been proposed and employed at NLO [10–20], NNLO [21–70] and N3LO [71–75]. Additionally, fully-numerical approaches exist which combine loop- and real-emission integrands before the integration [76–82]. Further discussion of advanced computational methods in QCD and their applications can be found in ref. [83].

Modern slicing and subtraction schemes require integration of well-defined functions encapsulating soft- and collinear dynamics, over phase spaces of unresolved emissions. These integrals differ because of phase-space constraints which are particular to a specific scheme. In this paper, we consider the N-jettiness observable $\mathcal{T}_N$ [84, 85], which can be used as a slicing variable for lepton- and hadron-collider processes with final-state jets. The N-jettiness slicing scheme has already been used in a number of high-profile NNLO QCD computations [29–32, 72, 75].

In case of N-jettiness, integrals over unresolved phase-space regions are further split into the so-called soft, beam and jet functions. Beam and jet functions describe collinear emissions off incoming and outgoing hard partons. These functions are process-independent and are currently known through N3LO in perturbative QCD [86–93].

The *soft function* describes soft QCD radiation at large angles. For this reason, it is sensitive to color charges in the full event. This fact makes the soft function a much more complex quantity to calculate. The complexity of the soft function is further exacerbated by the definition of the N-jettiness variable which requires one to find the minima of certain combinations of scalar products between soft and hard partons. The traditional approach

[1] Collinear divergencies associated with the initial-state radiation are absorbed into the parton distribution functions.

to computing the N-jettiness soft function, that goes back to the early papers on this subject [84, 85], involves explicit resolution of the N-jettiness constraint by an additional phase-space partitioning. Since the complexity of such a partitioning strongly increases with the number of external particles, the N-jettiness soft function was first calculated for processes with two, three and four hard partons [2, 94–100].

Recently, new computational approaches were developed which allowed the calculation of the N-jettiness soft function for an *arbitrary* number of hard partons N [101, 102]. This fact makes the N-jettiness slicing scheme the first scheme in which all unresolved real-emission ingredients are known analytically for arbitrary collider processes (with massless partons) at NNLO QCD. We note in passing that the computation of ref. [102] represents a notable departure from the original methods, because divergences are regulated at the level of the entire soft function and the N-jettiness is treated as *any other* infra-red safe observable. Practically, one employs nested soft-collinear subtraction scheme [103] and the integrated double-soft subtraction term computed in ref. [104].

One may dream of replicating this success also at N3LO QCD but, given a rather limited understanding of soft and collinear singularities at that perturbative order, and a complex nature of the N-jettiness soft function, calculations at N3LO have naturally focused on the $N = 0$ case [3–6]. The explicit partitioning of the radiative phase space into sectors where the N-jettiness assumes a definite value, remains manageable in such a case. However, instead of integrating the resulting expressions numerically using the sector decomposition method [105], as was done in NNLO QCD computations for the $N = 0, 1, 2$ soft functions [96–100], we use techniques developed for multi-loop computations, such as the integration-by-parts (IBP) relations [106, 107] and the method of differential equations [108–112], and adapt them for our purposes.

In this paper, we discuss the triple-real contribution to the N3LO QCD zero-jettiness soft function, accounting for both ggg and $gq\bar{q}$ soft final-state partons. We aim at explaining how to overcome the technical challenges described in ref. [1], where the result for the zero-jettiness soft function at N3LO has been presented.

The outline of the paper is as follows. In section 2, we define the zero-jettiness soft function, explain how the soft limits of tree-level matrix elements are computed, and determine the integrand for the soft function computation. In section 3 we argue that some integrals, required for the computation of the soft function, are not regulated dimensionally. We also describe a constructive procedure called filtering, which allows us to remove such integrals from the calculation. In section 4 we explain how the integration-by-parts method works for phase-space integrals with Heaviside functions. In sections 5 and 6, we discuss computation of master integrals. We find it necessary to divide them into two classes. The first class contains no integrals with the propagator $1/k_{123}^2$, where k_{123} is the sum of three soft-parton momenta. The second class comprises integrals *with* this propagator. Integrals that belong to the first class are discussed in section 5; we compute them by integrating over the phase space of three soft partons, subject to the zero-jettiness constraint. Integrals of the second type are too complicated for a direct integration. In section 6, we explain how we introduce an auxiliary parameter and derive differential equations for such integrals. Calculation of the boundary conditions is discussed in section 7. We elaborate on the numerical checks in section 8, provide results for the soft function in section 9 and conclude in section 10. Some elements of the calculations and the various quantities used there are presented in several appendices.

2 Definition of the soft function and the soft limits of squared amplitudes

The zero-jettiness observable describes processes with exactly two hard partons. It is defined as follows [84, 85]

$$\mathcal{T}_0(n) = \sum_{i=1}^{n} \min\left[\frac{2p_a \cdot k_i}{P}, \frac{2p_b \cdot k_i}{P}\right]. \tag{2.1}$$

In eq. (2.1), $p_{a,b}$ are the four-momenta of hard partons, either incoming or outgoing, k_i, $i \in \{1,\dots,n\}$ are the momenta of additional (soft) partons, and P is an arbitrary parameter of mass-dimension one. The zero-jettiness soft function can be written as

$$S_\tau = \sum_{n=0}^{\infty} S_\tau^{(n)}, \tag{2.2}$$

where $S_\tau^{(n)}$ describes a partonic process with n soft particles in the final state. It reads

$$S_\tau^{(n)} = \frac{1}{\mathcal{N}_{\rm sym}} \int \prod_{i=1}^{n} [\mathrm{d}k_i]\; \delta(\tau - \mathcal{T}_0(n))\; \mathrm{Eik}(p_a, p_b, \{k_1,\dots,k_n\}). \tag{2.3}$$

In eq. (2.3), $\mathcal{N}_{\rm sym}$ is a symmetry factor to account for identical particles in the final state, $[\mathrm{d}k] = \mathrm{d}^d k/(2\pi)^{d-1}\delta(k^2)\theta(k^0)$, and the eikonal function is defined as follows

$$\mathrm{Eik}(p_a, p_b, \{k_1,\dots,k_n\}) = \lim_{\lambda\to 0} \lambda^{2n} \frac{|\mathcal{M}(p_a, p_b, \{\lambda k_1,\dots,\lambda k_n\})|^2}{|\mathcal{M}(p_a,p_b)|^2}, \tag{2.4}$$

which corresponds to the leading soft approximation of the matrix element $\mathcal{M}$.[2] Each eikonal function receives virtual corrections which also have to be computed in the leading soft approximation; it follows that at leading order $S_\tau^{(n)} \sim \alpha_s^n$.

Hence, to obtain the N3LO contribution to the zero-jettiness soft function, one requires ingredients that are familiar from computations of partonic cross sections at that perturbative order. They include the radiation of three soft partons, the one-loop corrections to the double-real emission, and the two-loop corrections to the single-real emission. The notable difference to ordinary N3LO computations is that the three-loop (purely virtual) corrections become scaleless in the soft limit and vanish. For the case when soft partons are gluons, the relevant contributions are shown in figure 1. The two non-vanishing virtual corrections (RRV and RVV) have been computed in refs. [3, 5]. In the RRV case both phase-space and loop integrations were treated on the same footing. In contrast, the RVV contribution was computed directly by integrating eq. (2.3) for $n = 1$. Such an integration is straightforward thanks to the simple form of the single-soft current for two hard partons at two loops [113–115]. We discuss the calculation of the RVV contribution in appendix B.

[2] In eq. (2.4) $|\mathcal{M}|^2$ refers to the matrix element squared summed over colors and polarizations of all particles involved.

In this paper, we elaborate on the computation of the triple real-emission contribution, the most challenging part of the calculation of the zero-jettiness soft function at N3LO. We begin with the explanation of how the four-momenta of soft and hard partons are parametrized in this case. Since we aim at simplifying the zero-jettiness measurement function and since this function depends on projections of momenta k_i on $p_{a,b}$, it is convenient to introduce light-cone (Sudakov) coordinates. The two hard momenta $p_{a,b}$ define two light-cone directions. We write

$$p_a = \frac{\sqrt{s_{ab}}}{2} n, \qquad p_b = \frac{\sqrt{s_{ab}}}{2} \bar{n}, \tag{2.5}$$

where $s_{ab} = 2p_a \cdot p_b$. It follows that $n^2 = \bar{n}^2 = 0$ and $n \cdot \bar{n} = 2$. The momenta of soft partons read

$$k_i^\mu = \frac{\alpha_i}{2} n^\mu + \frac{\beta_i}{2} \bar{n}^\mu + k_{\perp,i}^\mu, \qquad i = 1,2,3. \tag{2.6}$$

We note that since $k_i^2 = 0$, $k_{\perp,i}^\mu = \sqrt{\alpha_i \beta_i}\, e_{\perp,i}^\mu$, with $e_{\perp,i} \cdot n = e_{\perp,i} \cdot \bar{n} = 0$, and $(e_{\perp,i})^2 = -1$. It follows that $\alpha_i = k_i \cdot \bar{n}$ and $\beta_i = k_i \cdot n$. We use the above definitions, take $P = \sqrt{s_{ab}}$, and re-write eq. (2.1) as

$$\mathcal{T}_0(n) = \sum_{i=1}^{n} \min\left[\alpha_i, \beta_i\right]. \tag{2.7}$$

As can be seen from eq. (2.6), the minimum function differentiates between soft partons emitted into the forward and the backward hemisphere, defined with respect to the collision axis. In order to project the different phase-space regions onto a unique value of $\mathcal{T}_0(n)$ without the minimum function, we insert a partition of unity for each of the soft partons and write

$$1 = \prod_{i=1}^{3} \left[\theta(\alpha_i - \beta_i) + \theta(\beta_i - \alpha_i)\right]. \tag{2.8}$$

Upon expanding the product, eq. (2.8) splits into eight terms. These terms can be arranged in two groups. In the first group (two terms) all soft partons are emitted into the same hemisphere whereas in the second group two partons are emitted into the same hemisphere and one parton into the opposite hemisphere (six terms). Assuming that the eikonal function is symmetric under the permutation of soft partons,[3] and under the exchange of forward and backward directions ($n \leftrightarrow \bar{n}$), we only need to consider two of the eight phase-space configurations, which we refer to as "nnn" and "$nn\bar{n}$". The phase-space measures for the two cases read[4]

$$\mathrm{d}\Phi_{\theta\theta\theta} = \frac{1}{\mathcal{N}_\varepsilon^3} \left(\prod_{i=1}^{3} [\mathrm{d}k_i]\right) \times \delta(1 - \beta_{123}) \times \left(\prod_{i=1}^{3} \theta(\alpha_i - \beta_i)\right), \tag{2.9}$$

$$\mathrm{d}\Phi_{\theta\theta\bar{\theta}} = \frac{1}{\mathcal{N}_\varepsilon^3} \left(\prod_{i=1}^{3} [\mathrm{d}k_i]\right) \times \delta(1 - \beta_{12} - \alpha_3) \times \left(\prod_{i=1}^{2} \theta(\alpha_i - \beta_i)\right) \times \theta(\beta_3 - \alpha_3). \tag{2.10}$$

[3] This is the case for three soft gluons, in case of soft gluon plus soft quark-antiquark pair emission we symmetrize the integrand.

[4] We note that we have set $\tau = 1$ in eqs. (2.9), (2.10) and in what follows. The dependence on τ can be restored by means of simple dimensional analysis, whenever required.

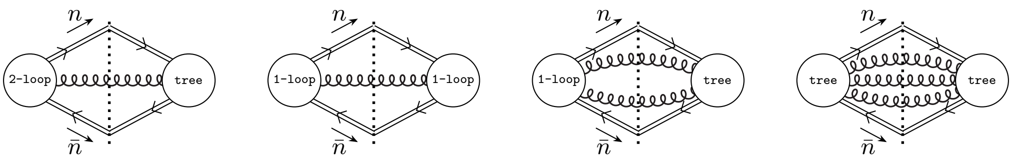

Figure 1. Different contributions to the zero-jettiness soft function at N3LO, see text for details. Only contributions with final-state gluons are shown. Diagrams to the right of the cut are complex-conjugated.

We assumed that in the $nn\bar{n}$ case, cf. eq. (2.10), partons $1,2$ are emitted into the same hemisphere and parton 3 into the opposite one. Furthermore, we have introduced a normalization factor

$$\mathcal{N}_\varepsilon = \frac{\Omega^{(d-2)}}{4(2\pi)^{d-1}} = \frac{(4\pi)^\varepsilon}{16\pi^2\Gamma(1-\varepsilon)}\,. \tag{2.11}$$

The N3LO triple-real emission contribution to eq. (2.3) is then written as

$$S_\tau^{(3)}\Big|_{\alpha_s^3} \equiv S_\tau^{RRR} = \mathcal{N}_\varepsilon^3\left[2\left(S_{nnn}^{ggg} + S_{nnn}^{gq\bar{q}}\right) + 6\left(S_{nn\bar{n}}^{ggg} + S_{nn\bar{n}}^{gq\bar{q}}\right)\right]. \tag{2.12}$$

This leaves us with four quantities to compute; they read

$$S_{nnn}^{ggg} = \frac{1}{3!}\int \mathrm{d}\Phi_{\theta\theta\theta}\Big[|J_{ggg}(n,\bar{n},k_1,k_2,k_3)|^2 + (n\leftrightarrow\bar{n})\Big], \tag{2.13}$$

$$S_{nn\bar{n}}^{ggg} = \frac{1}{3!}\int \mathrm{d}\Phi_{\theta\theta\bar{\theta}}\Big[|J_{ggg}(n,\bar{n},k_1,k_2,k_3)|^2 + (n\leftrightarrow\bar{n})\Big], \tag{2.14}$$

$$S_{nnn}^{gq\bar{q}} = \int \mathrm{d}\Phi_{\theta\theta\theta}\Big[|J_{gq\bar{q}}(n,\bar{n},k_1,k_2,k_3)|^2 + (n\leftrightarrow\bar{n})\Big], \tag{2.15}$$

$$S_{nn\bar{n}}^{gq\bar{q}} = \frac{1}{3}\int \mathrm{d}\Phi_{\theta\theta\bar{\theta}}\Big[\Big(|J_{gq\bar{q}}(n,\bar{n},k_1,k_2,k_3)|^2 + (k_2\leftrightarrow k_3) + (k_1\leftrightarrow k_3)\Big) + \Big(n\leftrightarrow\bar{n}\Big)\Big]. \tag{2.16}$$

The eikonal functions $J_{ggg}(n,\bar{n},k_1,k_2,k_3)$ and $J_{gq\bar{q}}(n,\bar{n},k_1,k_2,k_3)$ describe the soft limit $k_1\sim k_2\sim k_3\to 0$ of the tree level matrix elements squared of the processes $f_a(p_a)+f_b(p_b)\to X+g(k_1)+g(k_2)+g(k_3)$ and $f_a(p_a)+f_b(p_b)\to X+g(k_1)+q(k_2)+\bar{q}(k_3)$, respectively, where X is an arbitrary color-neutral state. These quantities are known; the three-gluon eikonal function was computed in ref. [116] and the eikonal function for the $gq\bar{q}$ emission can be found in refs. [117, 118].

We have re-calculated both eikonal functions for the required case of two hard partons. To do this, we generated all required diagrams for the above processes using `DIANA` [119], which internally calls `QGRAF` [120], employed the "soft-gluon rules" [121] and manipulated resulting expressions using `FORM` [122–125]. Complete agreement with the results in the literature [116–118] was found.

The eikonal functions that need to be integrated over zero-jettiness phase space contain the following inverse propagators

$$1/D_i \in \{q\cdot k_i, q\cdot k_{ij}, q\cdot k_{123}, k_{ij}^2, k_{123}^2\},\quad q=n,\bar{n},\quad i\neq j=1,2,3\,, \tag{2.17}$$

where $k_{ij} = k_i + k_j$ and $k_{123} = k_1 + k_2 + k_3$. In section 4 we explain how to use the integration-by-parts technology [106] to express integrals in eqs. (2.13)–(2.16) through a smaller set of master integrals. However, before doing this, we will discuss a peculiar issue that we encountered while working on the computation of the soft function, namely the existence of integrals that are not regulated dimensionally.

3 Integrals not regulated dimensionally

In refs. [4, 5] we have pointed out that some master integrals required for the triple-real contribution to the N3LO zero-jettiness soft function *are not regulated dimensionally.*[5] Our calculation is not the first one to face this problem in QCD perturbation theory [126–128]. The standard way to treat this problem is to introduce an analytic regulator into the integration measure for all integrals. Unfortunately, the new regulator — which appears alongside with the dimensional one — makes the required computations significantly more complex, so that finding ways to avoid ill-defined integrals becomes important.

Our experience with computing the N3LO real-emission master integrals for the soft function indicates that several conditions need to be satisfied for such integrals to become unregulated. In particular, it is necessary that one of the Sudakov variables is small, and the other one is large, that their product is $\mathcal{O}(1)$ and that it appears in one of the propagators. This can be understood from the fact that the integration measure $\mathrm{d}\Phi$ depends on the dimensional regularization parameter through a factor $\prod_{i=1}^{3} (\alpha_i \beta_i)^{-\varepsilon}$. Obviously, if $\alpha_i \sim 1/\alpha_j$, $\beta_i \sim 1/\beta_j$ or $\alpha_i \sim 1/\beta_j$, the dimensional regulator becomes ineffective.

To understand if such scalings lead to integrals with a non-vanishing support, we can assume, without loss of generality, that the smallest variable is $\beta_1 \sim \lambda \to 0$ and that the largest variable is either $\alpha_1 \sim \lambda^{-1}$ or $\alpha_2 \sim \lambda^{-1}$, or $\beta_2 \sim \lambda^{-1}$. We are interested in finding integrals where the $\lambda \to 0$ limit is non-trivial, and leads to non-vanishing integrals that are not regulated dimensionally.

Consider the case $\beta_1 \sim \lambda$ and $\alpha_1 \sim 1/\lambda$, with $\lambda \to 0$. Inverse propagators with non-trivial dependence on α_1 and β_1 become

$$\alpha_1 + x \cdots \to \alpha_1,\; \beta_1 + x \to x,\; k_{12}^2 \to \alpha_1 \beta_2, \quad k_{13}^2 \to \alpha_1 \beta_3, \quad k_{123}^2 \to \alpha_1(\beta_2 + \beta_3), \tag{3.1}$$

where x denotes a generic $\mathcal{O}(1)$ quantity composed of Sudakov parameters of the soft partons. We also drop β_1 from the δ-function constraining the zero-jettiness. It follows that integrations over α_1 and β_1 factorize, which implies that the region with $\beta_1 \sim \lambda, \alpha_1 \sim \lambda^{-1}$ has no support.

We continue with the region $\beta_1 \sim \lambda, \beta_2 \sim \lambda^{-1}$, where the following relations for inverse propagators hold

$$\beta_2 + x \cdots \to \beta_2,\; \beta_1 + x \to x,\; k_{12}^2 \to \beta_2 \alpha_1, \quad k_{23}^2 \to \beta_2 \alpha_3, \quad k_{123}^2 \to \beta_2(\alpha_1 + \alpha_3). \tag{3.2}$$

Similar to the previous case, the factorization of β_1 and β_2 integrations implies that this region has no support.

[5] Note that this problem did not arise for the real-emission contributions with *two* real partons both at NNLO and N3LO [2, 6].

For the remaining option $\beta_1 \sim \lambda, \alpha_2 \sim 1/\lambda$, the main difference compared to the previous cases is that the propagator

$$k_{12}^2 = \alpha_1\beta_2 + \alpha_2\beta_1 - 2\sqrt{\alpha_1\beta_1\alpha_2\beta_2}\cos\phi_{12}, \tag{3.3}$$

does not simplify, because all terms on the right-hand side of eq. (3.3) are of the same order. Since we are interested in the region $\beta_1 \ll \alpha_1$ and $\beta_2 \ll \alpha_2$, partons 1 and 2 are emitted into the same hemisphere. Incorporating the zero-jettiness constraints for the two partons, $\theta(\alpha_1 - \beta_1)\theta(\alpha_2 - \beta_2)$, we change the integration variables $\beta_1 \to r_1\alpha_1, \alpha_2 \to \beta_2/r_2$, with $r_{1,2} \in [0,1]$.

As we already mentioned, the critical new element in this region is the inverse propagator k_{12}^2 which does not simplify. This propagator depends on the relative angle between directions of the transverse components of the four-vectors $k_{1,2}$. To perform the integration over $k_{1,2}$, we write

$$k_{12}^2 = \alpha_1\beta_2\left(1+\frac{r_1}{r_2}\right)(\rho\cdot\rho_{12}), \tag{3.4}$$

where we have introduced two $(d-1)$-dimensional vectors ρ and ρ_{12} such that $\rho^2 = 0$ and $\rho_{12}^2 = 1 - 4r_1r_2/(r_1+r_2)^2$. The required integral over angles is then easily computed using eq. (D.32). We find

$$X_n = \int \frac{\mathrm{d}\Omega_1^{(d-2)}}{\Omega_{(d-2)}}\frac{\mathrm{d}\Omega_2^{(d-2)}}{\Omega_{(d-2)}}\frac{1}{(k_{12}^2)^n} = \frac{I^{(1)}_{d-2;n}(\rho_{12}^2)}{\alpha_1^n\beta_2^n\left(1+\frac{r_1}{r_2}\right)^n}, \tag{3.5}$$

where $I^{(1)}_{d-2;n}(\rho^2)$ can be extracted from eq. (D.36). Using eq. (E.4), the result can be simplified, and we obtain

$$\begin{aligned} X_n = \frac{1}{(\alpha_1\beta_2)^n}\Big[&\theta(r_2-r_1)\,{}_2F_1\left(n,n+\varepsilon;1-\varepsilon;\frac{r_1}{r_2}\right) \\ &+\left(\frac{r_2}{r_1}\right)^n\theta(r_1-r_2)\,{}_2F_1\left(n,n+\varepsilon;1-\varepsilon;\frac{r_2}{r_1}\right)\Big]. \end{aligned} \tag{3.6}$$

Next, we need to integrate over r_1, r_2. The generic integral reads

$$\begin{aligned} \Xi^{(n)}_{a,b} = &\int_0^1 \mathrm{d}r_2 \int_0^{r_2} \mathrm{d}r_1\, r_1^{a-\varepsilon} r_2^{b+\varepsilon}\,{}_2F_1\left(n,n+\varepsilon;1-\varepsilon;\frac{r_1}{r_2}\right) \\ &+ \int_0^1 \mathrm{d}r_1 \int_0^{r_1} \mathrm{d}r_2\, r_1^{a-\varepsilon} r_2^{b+\varepsilon}\left(\frac{r_2}{r_1}\right)^n {}_2F_1\left(n,n+\varepsilon;1-\varepsilon;\frac{r_2}{r_1}\right), \end{aligned} \tag{3.7}$$

where a and b are integers, and powers of ε arise from the integration measure after the variable transformation. We change the integration variables as $r_1 = zy, r_2 = y$, and $r_2 = zy$, $r_1 = y$ in the first and the second integral, respectively. We find

$$\Xi^{(n)}_{a,b} = \int_0^1 \frac{\mathrm{d}y}{y}\, y^{a+b+2}\int_0^1 \mathrm{d}z\left(z^{a-\varepsilon} + z^{b+\varepsilon+n}\right){}_2F_1(n,n+\varepsilon;1-\varepsilon,z). \tag{3.8}$$

The integral over z is regulated dimensionally, but the integral over y is not. In fact, the integral exists for $a+b+2>0$ but not for other values.

To obtain a *fully-regulated integral*, we need an additional regulator. We do that by introducing a factor $\beta_1^\nu\beta_2^\nu\beta_3^\nu$ into the measure for nnn integrals and $\beta_1^\nu\beta_2^\nu\alpha_3^\nu$ for $nn\bar{n}$ integrals. Of course, in the above discussion only the β_1^ν factor is relevant, but since we aim at modifying the measure in such a way that *all* integrals are regulated, momenta components of all soft partons must appear. Since $\beta_1^\nu = (r_1\alpha_1)^\nu$, the computation proceeds unaffected, except that in eqs. (3.7), (3.8) a becomes $a+\nu$ and the potential divergences for $2+a+b\le 0$ are regulated. The integral in eq. (3.8) with $a\to a+\nu$ evaluates to

$$\Xi^{(n)}_{a+\nu,b} = \frac{{}_3F_2\left(n,n+\varepsilon,1+a+\nu-\varepsilon;1-\varepsilon,2+a+\nu-\varepsilon;1\right)}{(1+a+\nu-\varepsilon)(2+a+\nu+b)} + \frac{{}_3F_2\left(n,n+\varepsilon,1+b+n+\varepsilon;1-\varepsilon,2+b+n+\varepsilon;1\right)}{(1+b+\varepsilon+n)(2+a+\nu+b)}. \tag{3.9}$$

The $1/\nu$ pole arises for $2+a+b=0$.

We note in passing that even if the equation $a+b=-2$ is satisfied, this does not immediately imply that a particular integral has a $1/\nu$ divergence. The reason for this is that such a divergence may be multiplied by an unconstrained (scaleless) integral over another Sudakov parameter, or that the residue of $\Xi^{(n)}_{a+\nu,b}$ at $\nu=0$ vanishes.

For the particular choice of small and large parameters that we discussed above, the first option may occur because of the integration over α_1. Hence, unregulated integrals in this case *must* involve denominators of the form α_1+x. The master formula for such integrals reads

$$\int\limits_0^\infty \frac{\mathrm{d}\alpha_1}{\alpha_1}\frac{\alpha_1^{n_1}}{(\alpha_1+x)^{n_2}} = \frac{\Gamma\left(n_1\right)\Gamma\left(n_2-n_1\right)}{\Gamma\left(n_2\right)}x^{n_1-n_2}, \tag{3.10}$$

where x stands for other $\mathcal{O}(1)$ Sudakov parameters. Note that in our example, x in eq. (3.10) can only be α_3, which shows that one needs at least three partons for the unregulated term to occur.

The above analysis can be used to identify integrals that are not regularized dimensionally, and to remove all IBP relations that involve them from the system of equations that one employs to find master integrals. We refer to this procedure as *filtering*. To determine affected integrals, we find all integrals that contain at least one propagator $1/k_{ij}^2$, make sure that θ-functions' constraints are such that partons i and j are emitted into the same hemisphere, consider the two cases $\beta_i\sim 1/\alpha_j\to 0$ and $\beta_j\sim 1/\alpha_i\to 0$, expand remaining propagators assuming that all other Sudakov parameters are $\mathcal{O}(1)$ and determine parameters n,a and b that appear in the function $\Xi^{(n)}_{a,b}$. If for a particular integral $a+b+2\le 0$, it is declared to be ill-defined without the regulator and all equations that contain such an integral are removed the system of IBP equations. If, however, the condition $a+b+2>0$ holds, all equations that contain such integrals are retained and used in the course of the reduction to master integrals. This procedure can be conveniently summarized as a set of power-counting rules for the denominators listed in table 1. We emphasize that, for this analysis, it is important to derive the IBP relations keeping the analytic regulator non-vanishing, $\nu\neq 0$, since an ill-defined integral may have a coefficient that is proportional to ν. Finally, we note that the

D_i	$\beta_1 \sim \lambda,\, \alpha_2 \sim \lambda^{-1}$	
	integrand	scaling
k_{12}^2	k_{12}^2	1
k_{13}^2	$\alpha_1\beta_3$	1
k_{23}^2	$\alpha_2\beta_3$	λ^{-1}
k_{123}^2	$\alpha_2\beta_3$	λ^{-1}
$\alpha_1+\alpha_2$	α_2	λ^{-1}
$\alpha_1+\alpha_3$	$\alpha_1+\alpha_3$	1
$\alpha_2+\alpha_3$	α_2	λ^{-1}
$\alpha_1+\alpha_2+\alpha_3$	α_2	λ^{-1}
$\beta_1+\beta_2$	β_2	1
$\beta_1+\beta_3$	β_3	1
$\beta_2+\beta_3$	$\beta_2+\beta_3$	1
$\beta_1+\beta_2+\beta_3$	$\beta_2+\beta_3$	1
α_1	α_1	1
α_2	α_2	λ^{-1}
α_3	α_3	1
β_1	β_1	λ
β_2	β_2	1
β_3	β_3	1

Table 1. Scalings of all possible propagators that appear in the soft function. All other configurations can be obtained through permutations of soft momenta k_i. To classify an integral, one can simply replace all inverse propagators with their λ-scalings and read off the overall factor λ^p. Integrals with $p > 0$ are well-defined without the regulator, while those with $p \leq 0$ are ill-defined. Integrals with $p = 0$ are potentially $1/\nu$-divergent which can be checked directly without much effort.

redundancy of IBP equations and a very specific set of conditions that integrals must fulfill to be ill-defined, ensures that only a small set of ν-dependent master integrals[6] is needed at the end of the calculation. Such master integrals are explicitly computed in section 5.2.

4 Integral reduction in the presence of theta functions and additional regulators

It is well-known [129] that one can simplify the calculation of phase-space integrals by mapping them onto loop integrals and treating them using conventional multi-loop methods. In this section, we explain how to do this for the integrals of the eikonal functions in eqs. (2.13)–(2.16). We would like to express integrals that are needed for the computation of the soft function through a smaller number of independent "master integrals". Computational methods that we use to achieve that have been discussed in ref. [4]; we repeat them here for completeness.

Reduction to master integrals simplifies the computation in multiple ways. On the one hand, it minimizes the number of integrals that we need to calculate; on the other hand, it also decreases the complexity of the calculation because master integrals are often

[6] Furthermore, only divergent parts of those integrals are needed.

simpler than the original ones. Furthermore, the reduction establishes algebraic relations between integrals offering the flexibility in choosing which integrals to compute and which to obtain from such relations. Also, availability of the reduction enables useful crosschecks by comparing explicit computation of integrals with their expressions through master integrals. Finally, a working reduction is the prerequisite for deriving differential equations satisfied by master integrals, see section 6.

The reduction to master integrals follows Laporta's algorithm [130] and proceeds in the following way. One derives a large-enough system of linear relations among the integrals relevant for the problem at hand using integration-by-parts (IBP) identities [106] and symmetries of the integrals. Then, introducing a measure to order integrals in complexity, one solves the homogeneous linear system using the Gauss' elimination method, expressing many complex integrals, in terms of a few simpler integrals. These remaining integrals are called "master integrals".

We note that the general approach described above is well-known and broadly used for perturbative calculations in quantum field theory. However, it proved to be very challenging to realize it for integrals that are needed to compute the soft function. Below we describe the challenges and explain how they are overcome.

IBP relations. Linear relations between integrals are obtained using the IBP technology [106], based on the observation that for properly regularized integrals the following formula is valid

$$0 = \int \prod_i \mathrm{d}^d k_i \, \frac{\partial}{\partial k_j^\mu} \left(v^\mu \, f(\{k\},\{p\}) \right) . \tag{4.1}$$

In the above equation, v is either one of the loop momenta k_i or one of the external momenta p_i, and the integrand f is a product of propagators (see eq. (2.17)) raised to arbitrary powers, δ-functions that ensure that partons are on-shell and that the zero-jettiness has a definite value, and θ-functions that allow us to resolve the zero-jettiness constraint.[7] In principle, computing derivatives under the integral sign in eq. (4.1) is straightforward and, once this is done, that equation provides algebraic relations between different integrals that we seek to exploit. In practice, there is a problem of differentiating δ- and θ-functions that we now discuss.

We deal with all δ-functions by employing the reverse unitarity idea [129, 131], which amounts to writing

$$\delta(g(x)) = \lim_{\sigma\to 0} \frac{i}{2\pi} \left[\frac{1}{g(x)+i\sigma} - \frac{1}{g(x)-i\sigma} \right] \equiv \left[\frac{1}{g(x)} \right]_{\mathrm{c}} . \tag{4.2}$$

The "cut propagators" appearing on the right-hand side of the above equation can be easily accommodated into the IBP technology.

It is useful to classify appearing integrals in terms of the integral families, defined by complete and linearly-independent sets of generalized propagators with respect to algebraic relations that involve scalar products of all four-vectors in the problem. Such a classification allows one to re-write scalar products that appear in the numerators of phase-space integrals

[7] As we already mentioned, not all integrals that are needed for computing the soft function are regularized dimensionally. However, once the analytic regulator is employed, IBP relations are applicable.

uniquely through the denominators, and to represent integrals in a compact way using denominators raised to positive or negative powers. We will explain shortly how the integral families for the computation of the soft function are constructed.

However, before doing that, we discuss how the θ-functions, that determine a hemisphere into which a particular soft parton is emitted, are incorporated into the IBP formalism. Schematically, modified IBP relations can be written as follows

$$\begin{aligned} 0 &= \int \left(\prod_i \mathrm{d}^d k_i\right) \, \frac{\partial}{\partial k_j^\mu} v^\mu \, f \, \theta\, [g] \\ &= \int \left(\prod_i \mathrm{d}^d k_i\right) \left\{ d \, \delta_{v,k_j} \, f \, \theta[g] + \theta[g] \, v^\mu \frac{\partial}{\partial k_j^\mu} f + f \, \delta[g] \, v^\mu \frac{\partial}{\partial k_j^\mu} g \right\}. \end{aligned} \tag{4.3}$$

The three terms that appear on the right-hand side of the above equation are quite different. In the first two terms the original θ-function is unaffected, which means that they would not change even if the θ-function constraint was removed from the integrand. The last term in eq. (4.3), where the θ-function has turned into a δ-function with the same argument, is the contribution of the boundary that now occurs at finite values of partons' momenta.

Making use of this observation, we derive IBP relations that connect integrals with a certain number of θ- and δ-functions to integrals with the same number of θ- and δ-functions, *as well as* integrals where the number of θ-functions is decreased and the number of δ-functions is increased by one. Repeated application of IBP relations to boundary-type integrals decreases the number of θ-functions further, until we arrive at integrals where all θ-functions are replaced by δ-functions. Integrals with δ-functions and no θ-functions close under the integration-by-parts identities thanks to reverse unitarity, so once this stage is achieved, no new types of integrals appear. To incorporate both θ- and δ-functions with arguments $\pm(\alpha_i - \beta_i)$, we generalize the notation for the phase-space in eqs. (2.9), (2.10) and write

$$\mathrm{d}\Phi_{f_1 f_2 f_3} = \frac{1}{\mathcal{N}_\varepsilon^3} \left(\prod_{i=1}^3 [\mathrm{d}k_i]\right) \times \delta(1-\beta_{123}) \times \left(\prod_{i=1}^3 f_i(\alpha_i - \beta_i)\right), \tag{4.4}$$

$$\mathrm{d}\Phi_{f_1 f_2 \bar{f}_3} = \frac{1}{\mathcal{N}_\varepsilon^3} \left(\prod_{i=1}^3 [\mathrm{d}k_i]\right) \times \delta(1-\beta_{12}-\alpha_3) \times \left(\prod_{i=1}^2 f_i(\alpha_i - \beta_i)\right) \times f_3(\beta_3 - \alpha_3). \tag{4.5}$$

The functions $f_{1,2,3}$ represent θ- and δ-function constraints.

As an example, consider the IBP relation[8]

$$\begin{aligned} 0 = \int \frac{\partial}{\partial k_2^\mu} \frac{\bar{n}^\mu \mathrm{d}\Phi_{\theta\theta\bar{\theta}}}{(k_1\cdot k_2)(k_{12}\cdot\bar{n})^2(k_2\cdot n)(k_1\cdot\bar{n})} &= \int \frac{\mathrm{d}\Phi_{\theta\theta\bar{\theta}} \, \bar{n}_\mu}{(k_1\cdot k_2)(k_{12}\cdot\bar{n})^2(k_2\cdot n)(k_1\cdot\bar{n})} \\ \times \left[-\frac{2k_2^\mu}{[k_2^2]_{\mathrm{c}}} - \frac{n^\mu}{[1-k_{12}\cdot n - k_3\cdot\bar{n}]_{\mathrm{c}}} - \frac{k_1^\mu}{(k_1\cdot k_2)} - \frac{\bar{n}^\mu}{(k_{12}\cdot\bar{n})} - \frac{n^\mu}{(k_2\cdot n)} \right] \\ - (n\cdot\bar{n}) \int \prod_{i=1}^3 [\mathrm{d}k_i] \, \frac{\delta(1-\beta_{12}-\alpha_3)\theta(\alpha_1-\beta_1)\theta(\beta_3-\alpha_3)}{(k_1\cdot k_2)(k_{12}\cdot\bar{n})^2(k_2\cdot n)(k_1\cdot\bar{n})} \delta(k_2\cdot\bar{n} - k_2\cdot n). \end{aligned} \tag{4.6}$$

[8]We note that the derivative on the left-hand side does not act on the volume differential $\mathrm{d}^d k_2$. Furthermore, recall that $\alpha_i = k_i \cdot \bar{n}$ and $\beta_i = k_i \cdot n$.

The first five terms on the right-hand side of eq. (4.6) arise when the derivative acts on either an eikonal or a cut propagator from the phase space; we will refer to such terms as "homogeneous". The last — "inhomogeneous" — term in eq. (4.6) describes the non-zero boundary contribution. Writing the δ-function which originated from the derivative of the θ-function as a cut propagator, it is easy to see that the resulting propagators cease being linearly independent. Although the presence of linearly-dependent propagators is in itself not fatal for the IBP technology, it does create multiple inconveniences because of hidden linear dependencies between integrals which may significantly increase the complexity of intermediate expressions.

To get rid of these problems, we perform a partial fraction decomposition by multiplying the last term in eq. (4.6) by $1 = [k_1 \cdot \bar{n} + (k_2 \cdot \bar{n} - k_2 \cdot n) + k_2 \cdot n] \,/\, [k_{12} \cdot \bar{n}]$. We arrive at[9]

$$
\begin{aligned}
0 = &\int \frac{\mathrm{d}\Phi_{\theta\theta\bar{\theta}}}{(k_1 \cdot k_2)(k_{12} \cdot \bar{n})^2 (k_2 \cdot n)(k_1 \cdot \bar{n})} \\
&\times \left[-\frac{2(k_{12} \cdot \bar{n} - k_1 \cdot \bar{n})}{[k_2^2]_{\mathrm{c}}} - \frac{n \cdot \bar{n}}{[1 - k_{12} \cdot n - k_3 \cdot \bar{n}]_{\mathrm{c}}} - \frac{k_1 \cdot \bar{n}}{(k_1 \cdot k_2)} - \frac{n \cdot \bar{n}}{(k_2 \cdot n)} \right] \\
&- (n \cdot \bar{n}) \int \frac{\mathrm{d}\Phi_{\theta\delta\bar{\theta}}}{(k_1 \cdot k_2)(k_{12} \cdot \bar{n})^3} \left[\frac{1}{(k_2 \cdot n)} + \underbrace{\frac{(k_2 \cdot \bar{n} - k_2 \cdot n)}{(k_2 \cdot n)(k_1 \cdot \bar{n})}}_{=0} + \frac{1}{(k_1 \cdot \bar{n})} \right].
\end{aligned}
\tag{4.7}
$$

After this step, all propagators in the two integrals in the above equations are linearly independent, and we proceed with defining the integral families. The primary distinction between families is the number of θ- and δ-functions, and the types of propagators they contain. We show the IBP relations and the way they connect the various types of integral families in figure 2.

Analytic regulator. In section 3, we have argued that some integrals, needed to compute the zero-jettiness soft function, are not regularized dimensionally. We have also explained that one can regularize such integrals by introducing the analytic regulator ν. The modified measures read

$$
\mathrm{d}\Phi^{\nu}_{f_1 f_2 f_3} = \frac{1}{\mathcal{N}_\varepsilon^3} \left(\prod_{i=1}^{3} [\mathrm{d}k_i] \right) \times \delta(1 - \beta_{123}) \times \left(\prod_{i=1}^{3} f_i(\alpha_i - \beta_i) \beta_i^{\nu} \right), \tag{4.8}
$$

$$
\mathrm{d}\Phi^{\nu}_{f_1 f_2 \bar{f}_3} = \frac{1}{\mathcal{N}_\varepsilon^3} \left(\prod_{i=1}^{3} [\mathrm{d}k_i] \right) \times \delta(1 - t_{123}) \times \left(\prod_{i=1}^{2} f_i(\alpha_i - \beta_i) \beta_i^{\nu} \right) \times f_3(\beta_3 - \alpha_3) \alpha_3^{\nu}, \tag{4.9}
$$

where $t_{123} = \beta_{12} + \alpha_3$. A significant drawback in using the analytic regulator is that it changes the IBP relations. To illustrate this, consider the same IBP relation as before, but with the analytic regulator. We find

$$
\begin{aligned}
0 &= \int \left(\prod_i \mathrm{d}^d k_i \right) \frac{\partial}{\partial k_j^{\mu}} v^{\mu} f \theta[g] (k_j \cdot q)^{\nu} \\
&= \int \left(\prod_i \mathrm{d}^d k_i \right) \left\{ d \delta_{v,k_j} f \theta + \theta v^{\mu} \frac{\partial}{\partial k_j^{\mu}} f + f \delta[g] v^{\mu} \frac{\partial}{\partial k_j^{\mu}} f + \frac{\nu f \theta[g] (v \cdot q)(k_j \cdot q)^{\nu}}{(k_j \cdot q)} \right\},
\end{aligned}
\tag{4.10}
$$

[9]We note that the second term in the last line of eq. (4.7) has the form $\sim x\delta(x)$ and integrates to zero.

where $q = n, \bar{n}$ depending on the choice of k_j and the configuration of the integral. The last term on the r.h.s. of eq. (4.10) is caused by the regulator and, generally, also requires an additional partial fraction decomposition.

Symmetry relations. In addition to linear relations provided by the IBP equations, there are also symmetry relations between integrals. In the nnn case, the phase space is symmetric under the re-labeling of partons' momenta. In the $nn\bar{n}$ case, the phase space is symmetric under the relabeling $k_1 \leftrightarrow k_2$.

In the $nn\bar{n}$ case, integrals with δ-functions can be simplified further. For example, interchanging $k_2 \leftrightarrow k_3$ and $n \leftrightarrow \bar{n}$ leaves the $\delta\theta\bar{\theta}$ phase space unchanged. Furthermore, there are two types of $nn\bar{n}$ integrals that can be mapped onto the nnn configuration *entirely*. First, for integrals with $f_3 = \delta$, we can write

$$\delta(1 - \beta_{12} - \alpha_3)\delta(\alpha_3 - \beta_3) = \delta(1 - \beta_{123})\delta(\beta_3 - \alpha_3) \,. \tag{4.11}$$

Second, for $f_1 = f_2 = \delta$, we find

$$\begin{aligned} &\delta(1 - \beta_{12} - \alpha_3)\delta(\alpha_1 - \beta_1)\delta(\alpha_2 - \beta_2)f_3(\beta_3 - \alpha_3) \\ \overset{n\leftrightarrow\bar{n}}{=} \; &\delta(1 - \alpha_{12} - \beta_3)\delta(\beta_1 - \alpha_1)\delta(\beta_2 - \alpha_2)f_3(\alpha_3 - \beta_3) \\ = \; &\delta(1 - \beta_{123})\delta(\alpha_1 - \beta_1)\delta(\alpha_2 - \beta_2)f_3(\alpha_3 - \beta_3). \end{aligned} \tag{4.12}$$

Hence, we only need to consider integrals of the $\theta\theta\bar{\theta}$-, $\delta\theta\bar{\theta}$- and $\theta\delta\bar{\theta}$-type for the configuration $nn\bar{n}$. The symmetry relations are also illustrated in figure 2; they are heavily used to simplify the reduction.

Details of the technical implementation. Following the sequence of steps described below, we express the phase-space integrals in eqs. (2.13)–(2.16) through fewer and less complex master integrals.

- Using the partial fraction decomposition to resolve dependencies between the zero-jettiness constraining δ-function and the eikonal propagators, we map all $\theta\theta\theta$ integrals onto a set of $\mathcal{O}(100)$ families. They are constructed in such a way that they close under IBP relations with the analytic regulator ν.

- Starting from these families, we determine all lower-level families which arise when θ-functions turn into δ-functions. Again, these families are constructed in such a way, that they close when the term with the analytic regulator in the measure is differentiated. We arrive at additional $\mathcal{O}(100)$ and $\mathcal{O}(200)$ integral families for the nnn and $nn\bar{n}$ configuration, respectively. The partial fraction decompositions we use in this step are not unique; to ensure that these definitions suffice to uniquely identify integrals in terms of families in the entire IBP setup, we had to choose a global ordering of propagators that we keep through the entire calculation.

- It is easy to derive the *homogeneous* parts of the IBP relations for generic powers of propagators for each integral family. To obtain a complete IBP relation, we need to add terms that arise from the derivatives of Heaviside functions and measure factors raised to power ν. We add these terms on-the-fly, while generating relations for a specific set of indices (i.e. for a particular seed integral) which makes this step rather slow. We do so, because inhomogeneous terms require partial fraction decomposition, using the chosen ordering, as well as the integral-family identification.

The issue of generating sufficiently many linear relations, to have a reduction to the minimal set of master integrals, did play a crucial role in the calculation. Choosing a large-enough seed-list for complete reduction to occur, yet the seed-list that we could still handle with available resources, proved non-trivial and required a significant amount of trial and error.

- We use `Feynson` [132] to derive symmetry relations between integrals.
- We use `Kira⊕FireFly` [133–135] to solve the resulting linear system of equations as a function of d and ν. Since we expect that the soft function is regular in the limit $\nu \to 0$, it is useful to choose master integrals in such a way, that they remain independent in the $\nu \to 0$ limit. Good candidates for such basis can be found by studying the system at $\nu = 0$ and requiring that the $\nu = 0$ master integrals remain master integrals also in the $\nu \neq 0$ case. With this informed choice of basis, the reduction requires a runtime of about 10 days on 32 cores, compared to about 70 days without this optimization.

Proceeding along the lines described above, we arrive at the following result for the soft function[10]

$$S^{ggg;gq\bar{q}}_{nnn,nn\bar{n}} = \sum_{i=1}^{123} a_i I_i^{\cancel{k^2_{123}}} + \sum_{i=1}^{139} b_i I_i^{k^2_{123}} + \nu \sum_{i=1}^{4} c_i I_i^{1/\nu} + \mathcal{O}(\nu)\,, \tag{4.13}$$

where we have taken the $\nu \to 0$ limit wherever possible, such that the reduction coefficients a_i, b_i, c_i only depend on ε. Using the power counting rules from section 3, we find four integrals $\{I_i^{1/\nu}\}$ that contain a $1/\nu$ singularity but, thanks to the choice of basis, they appear in the soft function with a prefactor ν. Furthermore, in eq. (4.13), we have separated ν-regular integrals according to whether or not they contain the $1/k^2_{123}$ propagator.

The reason for this separation is that these three classes of integrals are computed differently. Indeed, in the following section, we will show that direct integration allows us to compute master integrals without the $1/k^2_{123}$ propagator $\{I_i^{\cancel{k^2_{123}}}\}$, as well as the $1/\nu$ parts of master integrals $\{I_i^{1/\nu}\}$. After that, we consider the most complicated set of integrals $\{I_i^{k^2_{123}}\}$, which we compute by modifying these master integrals through the introduction of an auxiliary parameter, followed by constructing and solving differential equations with respect to this parameter that the modified master integrals satisfy.

5 Integrals without $1/k^2_{123}$ propagator and $1/\nu$-divergent integrals

In this section we discuss the calculation of master integrals without the $1/k^2_{123}$ propagator, and the $1/\nu$-divergent integrals. These integrals are computed by a direct integration over the light-cone coordinates of soft partons α and β. All in all, 127 integrals are calculated in this way.

[10] We note that not all integrals contribute to all channels/configurations, so some of the a_i, b_i, c_i are zero.

JHEP04(2025)084

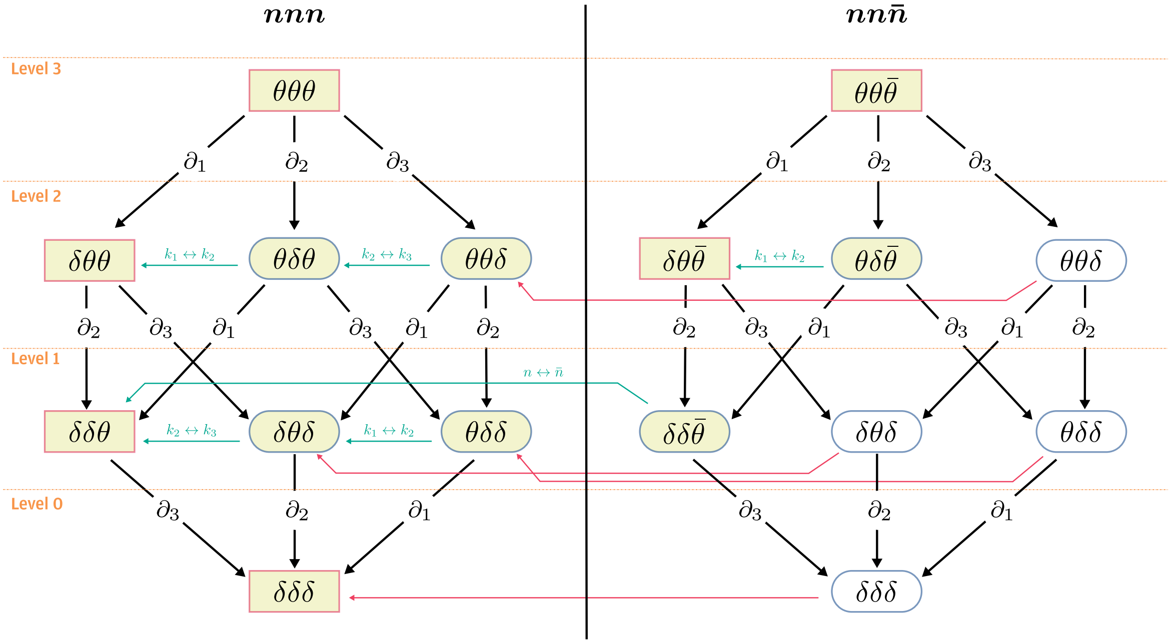

Figure 2. Relations between integrals. IBP identities relate integrals to those where one of the θ-functions is replaced by a δ-function, as illustrated by black arrows. Rectangular boxes represent sets of integrals which are processed using integration by parts, and no mapping onto other integral families is performed. Oval-shaped empty boxes are mapped into the same-hemisphere configuration as indicated by red arrows. After momenta re-naming, shown above the green arrows, filled oval-shaped boxes are mapped onto unique topologies.

	f_1	f_2	f_3	Variable change	Splitting
$\mathrm{d}\Phi_{\delta\theta\theta}$	$\delta(\alpha_1-\beta_1)$	$\theta(\alpha_2-\beta_2)$	$\theta(\alpha_3-\beta_3)$	$\alpha_1\to\beta_1, \alpha_2\to\frac{\beta_2}{r_2}, \alpha_3\to\frac{\beta_3}{r_3}$	—
$\mathrm{d}\Phi_{\delta\theta\bar{\theta}}$	$\delta(\alpha_1-\beta_1)$	$\theta(\alpha_2-\beta_2)$	$\theta(\beta_3-\alpha_3)$	$\alpha_1\to\beta_1, \alpha_2\to\frac{\beta_2}{r_2}, \beta_3\to\frac{\alpha_3}{r_3}$	—
$\mathrm{d}\Phi_{\theta\delta\delta}$	$\theta(\alpha_1-\beta_1)$	$\delta(\alpha_2-\beta_2)$	$\delta(\alpha_3-\beta_3)$	$\alpha_1\to\frac{\beta_1}{r_1}, \alpha_2\to\beta_2, \alpha_3\to\beta_3$	—
$\mathrm{d}\Phi_{\theta\delta\theta}$	$\theta(\alpha_1-\beta_1)$	$\delta(\alpha_2-\beta_2)$	$\theta(\alpha_3-\beta_3)$	$\alpha_1\to\frac{\beta_1}{r_1}, \alpha_2\to\beta_2, \alpha_3\to\frac{\beta_3}{r_3}$	$r_1 \vert r_3$
$\mathrm{d}\Phi_{\theta\delta\bar{\theta}}$	$\theta(\alpha_1-\beta_1)$	$\delta(\alpha_2-\beta_2)$	$\theta(\beta_3-\alpha_3)$	$\alpha_1\to\frac{\beta_1}{r_1}, \alpha_2\to\beta_2, \beta_3\to\frac{\alpha_3}{r_3}$	—
$\mathrm{d}\Phi_{\theta\theta\bar{\theta}}$	$\theta(\alpha_1-\beta_1)$	$\theta(\alpha_2-\beta_2)$	$\theta(\beta_3-\alpha_3)$	$\alpha_1\to\frac{\beta_1}{r_1}, \alpha_2\to\frac{\beta_2}{r_2}, \beta_3\to\frac{\alpha_3}{r_3}$	$r_1 \vert r_2$
$\mathrm{d}\Phi_{\bar{\theta}\delta\theta}$	$\theta(\beta_1-\alpha_1)$	$\delta(\alpha_2-\beta_2)$	$\theta(\alpha_3-\beta_3)$	$\beta_1\to\frac{\alpha_1}{r_1}, \alpha_2\to\beta_2, \beta_3\to\frac{\alpha_3}{r_3}$	—
$\mathrm{d}\Phi_{\bar{\theta}\theta\theta}$	$\theta(\beta_1-\alpha_1)$	$\theta(\alpha_2-\beta_2)$	$\theta(\alpha_3-\beta_3)$	$\beta_1\to\frac{\alpha_1}{r_1}, \alpha_2\to\frac{\beta_2}{r_2}, \beta_3\to\frac{\alpha_3}{r_3}$	—

Table 2. Summary of applied variable changes and integral splittings according to $\delta-$ and θ-function constraints f_i. Splitting of the integration domain into $r_i < r_j$ and $r_j < r_i$ sectors is required only if the integral contains the propagator $1/k_i \cdot k_j$.

5.1 Integrals that do not need an analytic regulator

An important property of the eikonal function is that all integrals without the $1/k_{123}^2$ propagator, needed for computing the N3LO contribution to the soft function, can have up to two scalar products between momenta of different soft partons. Hence, owing to the possibility of relabelling soft momenta, we write such integrals as

$$I_{nm} = \int \frac{\mathrm{d}\Phi_{f_1 f_2 f_3}\, R(\{\alpha\},\{\beta\})}{[2k_1\cdot k_2]^n\,[2k_1\cdot k_3]^m} = \int \prod_{i=1}^{3} \left(\frac{\mathrm{d}\alpha_i \mathrm{d}\beta_i}{(\alpha_i\beta_i)^{\varepsilon}} f_i(\alpha_i,\beta_i) \right) R(\{\alpha\},\{\beta\})\,\Omega_{nm}. \tag{5.1}$$

In the above equation, the phase-space measure $\mathrm{d}\Phi_{f_1 f_2 f_3}$ is given in eqs. (4.4), (4.5), and we used the Sudakov decomposition in eq. (2.6) to express all denominators other than $2k_1k_2$ and $2k_1k_3$ through $\{\alpha\}$ and $\{\beta\}$, collecting them into the rational function R. The non-trivial dependence on the relative azimuthal angles between soft-parton momenta is encapsulated in the angular integral Ω_{nm}. It reads

$$\Omega_{nm} = \frac{1}{\left(\Omega^{(d-2)}\right)^3} \int \frac{\mathrm{d}\Omega_{k_1}^{(d-2)}\mathrm{d}\Omega_{k_2}^{(d-2)}\mathrm{d}\Omega_{k_3}^{(d-2)}}{[2k_1\cdot k_2]^n\,[2k_1\cdot k_3]^m}. \tag{5.2}$$

To compute this integral we use the fact that we can integrate over angles of partons 2 and 3 independently. Furthermore,

$$\frac{1}{\Omega^{(d-2)}} \int \frac{\mathrm{d}\Omega_{k_i}^{(d-2)}}{[2k_i\cdot k_j]^n} = \frac{I_{d-2;n}^{(1)}(\rho_{ij}^2)}{(\alpha_i\beta_j+\alpha_j\beta_i)^n}, \tag{5.3}$$

where $I_{d,n}^{(1)}$ can be found in eq. (D.36) and $\rho_{ij}^2 = (\alpha_i\beta_j - \alpha_j\beta_i)^2 / (\alpha_i\beta_j+\alpha_j\beta_i)^2$. It follows that

$$\Omega_{nm} = \frac{I_{d-2;n}^{(1)}(\rho_{12}^2)}{(\alpha_1\beta_2+\alpha_2\beta_1)^n}\,\frac{I_{d-2;m}^{(1)}(\rho_{13}^2)}{(\alpha_1\beta_3+\alpha_3\beta_1)^m}. \tag{5.4}$$

For each specific set of the jettiness constraints represented by functions f_i in eq. (5.1), we change integration variables following table 2. We then simplify the hypergeometric functions appearing in functions $I^{(1)}$ by applying the transformation in eq. (E.4). For configurations where two soft partons are emitted into the same hemisphere we split the integration region and introduce new variables r_i, cf. table 2, to map the integration regions onto the intervals $[0,1]$.

We note that the transformation eq. (E.4) that we apply to simplify angular integrals involves the *absolute value* of ρ_{ij}. In principle, ρ_{ij} does not need to be positive-definite, but there are cases when it can be. Indeed, this happens if the two constraints f_i and f_j are $f_i f_j \in \{\delta\theta, \theta\delta, \theta\bar{\theta}\}$. Then, using variables defined in table 2, we easily find

$$\left|\rho_{ij}^{\delta\theta}\right| = \frac{1-r_j}{1+r_j}, \qquad \left|\rho_{ij}^{\theta\delta}\right| = \frac{1-r_i}{1+r_i}, \qquad \left|\rho_{ij}^{\theta\bar{\theta}}\right| = \frac{1-r_i r_j}{1+r_i r_j}, \tag{5.5}$$

where $0 \le r_{i,j} \le 1$. Superscripts in the above equations are introduced to indicate constraints on partons i and j. However, if $f_i f_j = \theta\theta$, so that the two partons are emitted into the same hemisphere, we find $|\rho_{ij}| = |r_i - r_j|/(r_i+r_j)$. In this case, we have to write

$$|\rho_{ij}| = \theta(r_i - r_j)\,\frac{r_i - r_j}{r_i + r_j} + \theta(r_j - r_i)\,\frac{r_j - r_i}{r_j + r_i}, \tag{5.6}$$

to get rid of the absolute value.

Hence, after integrating over azimuthal angles in integrals I_{nm} in eq. (5.1), and changing the integration variables as in table 2, we obtain integrals over variables α_i, β_i, r_i which are at most six-dimensional. Furthermore, at least one of the integrations can be performed by removing the δ function that fixes the zero-jettiness value.

Calculation of several representative I_{nm} integrals for the nnn case were discussed in ref. [4]. Below, we will consider examples of new master integrals with three θ functions, which appear for the first time in the $nn\bar{n}$ configuration. We begin by considering an integral without scalar products between momenta k_i and k_j. The integral reads

$$J = \int \frac{\mathrm{d}\Phi_{\theta\theta\bar{\theta}}}{(k_{123} \cdot n)\,(k_{123} \cdot \bar{n})}. \tag{5.7}$$

We choose the parametrization according to table 2 and note that for this integral the splitting of integration variables $r_{1,2}$ into $r_1 < r_2$ and $r_2 < r_1$ is not necessary. We then integrate over α_3 to remove the zero-jettiness constraint, and change the integration variables, $\beta_1 \to x\ y$ and $\beta_2 \to x\ (1-y)$. We obtain

$$J = \int_0^1 \mathrm{d}x \mathrm{d}y \mathrm{d}r_1 \mathrm{d}r_2 \mathrm{d}r_3 \frac{(1-x)^{1-2\varepsilon} x^{3-4\varepsilon} r_1^{-1+\varepsilon} r_2^{-1+\varepsilon} r_3^{-1+\varepsilon} (1-y)^{1-2\varepsilon} y^{1-2\varepsilon}}{(x r_2 y + r_1 (r_2(1-x) + x(1-y)))\,(1 - x + r_3 x)}. \tag{5.8}$$

The integrations over r_1 and r_3 can be performed in terms of the hypergeometric functions. We find

$$\begin{aligned} J = \frac{1}{\varepsilon^2} \int_0^1 & \mathrm{d}x \mathrm{d}y \mathrm{d}r_2 (1-x)^{-2\varepsilon} x^{2-4\varepsilon} r_2^{-2+\varepsilon} (1-y)^{1-2\varepsilon} y^{-2\varepsilon} \\ & \times {}_2F_1\left(1, \varepsilon; 1+\varepsilon; -\tfrac{x}{1-x}\right) {}_2F_1\left(1, \varepsilon; 1+\varepsilon; -\tfrac{r_2(1-x)+x(1-y)}{x r_2 y}\right). \end{aligned} \tag{5.9}$$

We note that arguments of the hypergeometric functions in the above equation look complicated, suggesting an increased difficulty compared to integrals needed for the nnn case discussed in ref. [4]. However, upon closer inspection, the singularity structure of the integrand in eq. (5.9) turns out to be quite simple, as could be expected on general grounds. Indeed, since the hypergeometric functions in eq. (5.9) diverge logarithmically at the integration boundaries, the singularity structure is entirely determined by the double pole at $r_2 = 0$. To isolate it, we apply the transformation shown in eq. (E.3) to both hypergeometric functions. We then find

$$\begin{aligned} J = \frac{1}{\varepsilon^2} \int_0^1 & \mathrm{d}x\ \mathrm{d}y\ \mathrm{d}r_2\ (1-x)^{-\varepsilon} x^{2-3\varepsilon} r_2^{-2+2\varepsilon} \left(r_2 + x(1-r_2)(1-y)\right)^{-\varepsilon} \\ & \times (1-y)^{1-2\varepsilon} y^{-\varepsilon} {}_2F_1\left(\varepsilon, \varepsilon; 1+\varepsilon; x\right) {}_2F_1\left(\varepsilon, \varepsilon; 1+\varepsilon; \tfrac{r_2+x(1-r_2-y)}{r_2+x(1-r_2)(1-y)}\right). \end{aligned} \tag{5.10}$$

To subtract the double-pole singularity at $r_2 = 0$, we need to extract the different $r_2 \to 0$ branches that are contained in the last hypergeometric function in eq. (5.10). This can be easily done using eq. (E.2), and we find

$$J = J^{(a)} + J^{(b)}, \tag{5.11}$$

where

$$J^{(a)} = \frac{\Gamma(1-\varepsilon)}{\Gamma(1+\varepsilon)} \int_0^1 \mathrm{d}x\mathrm{d}y\mathrm{d}r_2 \, (1-x)^{-\varepsilon} x^{2-3\varepsilon} r_2^{-2+2\varepsilon} (1-y)^{1-2\varepsilon} y^{-\varepsilon} \\ \times (r_2 + x(1-r_2-y))^{-\varepsilon} \, {}_2F_1(\varepsilon, \varepsilon; 1+\varepsilon; x) \,, \tag{5.12}$$

$$J^{(b)} = \frac{1}{\varepsilon(\varepsilon-1)} \int_0^1 \mathrm{d}x\mathrm{d}y\mathrm{d}r_2 \, (1-x)^{-\varepsilon} x^{3-3\varepsilon} r_2^{-1+2\varepsilon} (1-y)^{1-2\varepsilon} y^{1-2\varepsilon} \\ \times \frac{{}_2F_1(\varepsilon, \varepsilon; 1+\varepsilon; x)}{(r_2 + x(1-r_2)(1-y))} {}_2F_1\left(1, 1; 2-\varepsilon; \tfrac{x \; y \; r_2}{(r_2+x(1-r_2)(1-y))}\right). \tag{5.13}$$

Integral $J^{(a)}$ can be integrated over r_2 using eq. (E.7); the result reads

$$J^{(a)} = \frac{\Gamma(1-\varepsilon)\Gamma(\varepsilon)}{\varepsilon(2\varepsilon-1)} \int_0^1 \mathrm{d}x\mathrm{d}y (1-x)^{-\varepsilon} x^{2-4\varepsilon} (1-y)^{1-3\varepsilon} y^{-\varepsilon} \\ \times {}_2F_1(\varepsilon, \varepsilon; 1+\varepsilon; x) {}_2F_1\left(\varepsilon, -1+2\varepsilon; 2\varepsilon; \frac{x-1}{x(1-y)}\right). \tag{5.14}$$

The integrand of $J^{(b)}$ has a simple pole at $r_2 = 0$ which can be easily subtracted. Finally, we expand the integrand for $J^{(a)}$ in eq. (5.14) and the subtracted integrand for $J^{(b)}$ in ε using the package `HypExp` [136, 137], and integrate order by order in ε with the help of `HyperInt` [138]. The result for the full integral reads

$$J = -\frac{5}{12\varepsilon^2} - \frac{215}{72\varepsilon} + \left(\frac{11}{72}\pi^2 - \frac{343}{24}\right) + \varepsilon\left(-\frac{1999}{36} + \frac{7}{8}\pi^2 + \frac{14}{3}\zeta_3\right) + \mathcal{O}\left(\varepsilon^2\right). \tag{5.15}$$

We continue with the discussion of an integral involving two scalar products of different soft-parton momenta

$$I = \int \frac{\mathrm{d}\Phi_{\theta\theta\bar{\theta}}}{(k_{13} \cdot \bar{n})\,(k_2 \cdot \bar{n})\,(k_1 \cdot k_3)\,(k_2 \cdot k_3)}. \tag{5.16}$$

Proceeding as discussed earlier, we integrate over the azimuthal angles of the three partons, change the integration variables following table 2, and integrate over α_3 removing the zero-jettines δ function. We find

$$I = 4 \int_0^1 \mathrm{d}\beta_1 \mathrm{d}\beta_2 \, \theta(1-\beta_{12}) \int_0^1 \mathrm{d}r_1 \mathrm{d}r_2 \mathrm{d}r_3 \frac{\beta_1 \,(r_1 r_2 r_3)^{\varepsilon}}{\left(\beta_1 \beta_2 \bar{\beta}_{12}\right)^{1+2\varepsilon} \left(\beta_1 + r_1 \bar{\beta}_{12}\right)} \\ \times {}_2F_1(1, 1+\varepsilon; 1-\varepsilon; r_1 r_3) \, {}_2F_1(1, 1+\varepsilon; 1-\varepsilon; r_2 r_3) \,, \tag{5.17}$$

where $\bar{\beta}_{12} = 1 - \beta_{12}$. We change the integration variable $\beta_1 = t(1-\beta_2)$, integrate over r_2 using the definition of the generalized hypergeometric function in eq. (E.8), and obtain

$$I = \frac{4}{(1+\varepsilon)} \int_0^1 \mathrm{d}\beta_2 \mathrm{d}t \mathrm{d}r_1 \mathrm{d}r_3 \frac{(1-\beta_2)^{-1-4\varepsilon} \beta_2^{-1-2\varepsilon} (1-t)^{-1-2\varepsilon} t^{-2\varepsilon}}{r_1 + t - r_1 t} \\ \times {}_2F_1(1, 1+\varepsilon; 1-\varepsilon; r_1 r_3) \; {}_3F_2(1, 1+\varepsilon, 1+\varepsilon; 1-\varepsilon, 2+\varepsilon; r_3) \,. \tag{5.18}$$

This expression can be further integrated over β_2 and t. Integration over β_2 results in Γ-functions, and integration over t leads to an ${}_2F_1$ function with the argument $1-1/r_1$, which can be simplified using eq. (E.3). Proceeding along these lines, we obtain

$$I = \frac{2\Gamma^3(-2\varepsilon)}{(1+\varepsilon)\Gamma(-6\varepsilon)} \int_0^1 \mathrm{d}x\mathrm{d}y \left(\frac{y}{x}\right)^{\varepsilon} {}_2F_1\left(1, 1+\varepsilon; 1-\varepsilon; xy\right) \\ \times {}_2F_1\left(1-2\varepsilon, -4\varepsilon; 1-4\varepsilon; 1-x\right) {}_3F_2\left(1, 1+\varepsilon, 1+\varepsilon; 1-\varepsilon, 2+\varepsilon; y\right). \tag{5.19}$$

Since this integral is finite, we compute it by expanding the integrand in ε and integrating the resulting expression. To do this, we use the packages `HypExp` [136, 137] and `HyperInt` [138]. The final result reads

$$I = \frac{\pi^2}{2\varepsilon^2} - \left(\frac{3}{2}\pi^2 - 18\zeta_3\right)\frac{1}{\varepsilon} + \left(\frac{9}{2}\pi^2 - 54\zeta_3 + \frac{1}{120}\pi^4\right) \\ - \varepsilon\left(\frac{27}{2}\pi^2 - 162\zeta_3 + \frac{1}{40}\pi^4 + \frac{125}{2}\pi^2\zeta_3 - \frac{837}{2}\zeta_5\right) + \mathcal{O}\left(\varepsilon^2\right). \tag{5.20}$$

The above examples demonstrate how the calculation of integrals that are regulated dimensionally and do not contain the $1/k_{123}^2$ propagator is performed. Although these computations are not easy and, quite often, integral representations for $nn\bar{n}$ integrals look quite complex, in comparison with their nnn counterparts they have a simpler structure of singularities and require a smaller number of subtractions before the expansion of integrands in ε can be performed.

5.2 $1/\nu$-divergent integrals

There are 4 master integrals that become divergent if the analytic regulator is sent to zero. They are

$$I_1^{1/\nu} = \int \frac{\mathrm{d}\Phi_{\theta\theta\delta}\left(\beta_1\beta_2\beta_3\right)^{\nu}}{k_{123}^2(k_1\cdot k_2)(\alpha_1+\alpha_3)\beta_1}, \tag{5.21}$$

$$I_2^{1/\nu} = \int \frac{\mathrm{d}\Phi_{\theta\theta\delta}\left(\beta_1\beta_2\beta_3\right)^{\nu}}{(k_1\cdot k_2)(\alpha_1+\alpha_3)\alpha_2\beta_1}, \tag{5.22}$$

$$I_3^{1/\nu} = \int \frac{\mathrm{d}\Phi_{\theta\theta\bar{\theta}}\left(\beta_1\beta_2\alpha_3\right)^{\nu}}{k_{123}^2(k_1\cdot k_2)(\alpha_1+\alpha_3)(\beta_1+\beta_2+\beta_3)\beta_1}, \tag{5.23}$$

$$I_4^{1/\nu} = \int \frac{\mathrm{d}\Phi_{\theta\theta\bar{\theta}}\left(\beta_1\beta_2\alpha_3\right)^{\nu}}{(k_1\cdot k_2)(\alpha_1+\alpha_3)\alpha_2(\beta_1+\beta_2+\beta_3)\beta_1}. \tag{5.24}$$

The integrals $I_{1,2}^{1/\nu}$ have been computed previously in ref. [4]; they read

$$I_1^{1/\nu} = \nu^{-1}\frac{\Gamma^2(-2\varepsilon)\Gamma(-4\varepsilon-1)\Gamma(1+2\varepsilon)}{\Gamma(-6\varepsilon-1)}C(\varepsilon) + \mathcal{O}(\nu^0), \tag{5.25}$$

$$I_2^{1/\nu} = \nu^{-1}\frac{\Gamma^2(-2\varepsilon)\Gamma(-4\varepsilon)\Gamma(1+2\varepsilon)}{\Gamma(-6\varepsilon)}C(\varepsilon) + \mathcal{O}(\nu^0), \tag{5.26}$$

where

$$C(\varepsilon) = \lim_{\nu\to 0}\left[\nu\Xi^{(1)}_{\nu-1,-1}\right] \\ = \frac{{}_3F_2(1,1+\varepsilon,1+\varepsilon;1-\varepsilon,2+\varepsilon;1)}{1+\varepsilon} - \frac{{}_3F_2(1,1+\varepsilon,-\varepsilon;1-\varepsilon,1-\varepsilon;1)}{\varepsilon}. \tag{5.27}$$

We have discussed the origin of the $1/\nu$ singularities in section 3, and described steps required to extract them. Although those steps are sufficient for obtaining the $1/\nu$ poles of $I_{3,4}^{1/\nu}$, we find it instructive to discuss the calculation of the $1/\nu$ poles of these integrals in detail.

We begin with $I_4^{1/\nu}$. The $1/\nu$ singularity in this case originates from the integration region $\beta_1 \sim \alpha_2^{-1} \to 0$. We integrate over the relative azimuthal angle between k_1 and k_2, and obtain

$$\begin{aligned} I_4^{1/\nu} = &\int\limits_0^\infty \mathrm{d}\beta_1 \mathrm{d}\beta_2 \mathrm{d}\alpha_3 \beta_1^{-2\varepsilon+\nu} \beta_2^{-2\varepsilon+\nu} \alpha_3^{-2\varepsilon+\nu} \int\limits_0^1 \mathrm{d}r_1 \mathrm{d}r_2 \; r_1^{\varepsilon-2} r_2^{\varepsilon-2} \int\limits_{\alpha_3}^\infty \mathrm{d}\beta_3 \beta_3^{-\varepsilon} \\ &\times \frac{\delta(1-\beta_1-\beta_2-\alpha_3)}{(\beta_1/r_1+\alpha_3)(\beta_2/r_2)(\beta_1+\beta_2+\beta_3)\beta_1} \, 2\Big[\, r_2 \, \theta(r_1-r_2) \\ &\times {}_2F_1\left(1,1+\varepsilon;1-\varepsilon;\frac{r_2}{r_1}\right) + r_1 \theta(r_2-r_1) {}_2F_1\left(1,1+\varepsilon;1-\varepsilon;\frac{r_1}{r_2}\right)\Big], \end{aligned} \tag{5.28}$$

where $r_i = \beta_i/\alpha_i$ are the new integration variables. Because of the scaling relation between β_1 and α_2, and since other Sudakov variables are $\mathcal{O}(1)$, we find $r_1 \sim \beta_1 \to 0$ and $r_2 \sim \alpha_2^{-1} \to 0$. Approximating the integrand, we find

$$\begin{aligned} I_4^{1/\nu} \sim &\int\limits_0^\infty \mathrm{d}\beta_1 \mathrm{d}\beta_2 \mathrm{d}\alpha_3 \beta_1^{-2\varepsilon+\nu} \beta_2^{-2\varepsilon+\nu} \alpha_3^{-\varepsilon+\nu} \int\limits_0^1 \mathrm{d}r_1 \mathrm{d}r_2 \; r_1^{\varepsilon-2} r_2^{\varepsilon-2} \int\limits_{\alpha_3}^\infty \mathrm{d}\beta_3 \beta_3^{-\varepsilon} \\ &\times \frac{\delta(1-\beta_2-\alpha_3)}{(\beta_1/r_1+\alpha_3)(\beta_2/r_2)(\beta_2+\beta_3)\beta_1} \, 2\Big[r_2 \theta(r_1-r_2) \\ &\times {}_2F_1\left(1,1+\varepsilon;1-\varepsilon;\frac{r_2}{r_1}\right) + r_1 \theta(r_2-r_1) {}_2F_1\left(1,1+\varepsilon;1-\varepsilon;\frac{r_1}{r_2}\right)\Big]. \end{aligned} \tag{5.29}$$

The integral over β_1 is easily computed using eq. (3.10). Keeping the $1/\nu$ pole, we write

$$\begin{aligned} I_4^{1/\nu} = &\, 2\Gamma(-2\varepsilon)\Gamma(1+2\varepsilon) \, \frac{C(\varepsilon)}{\nu} \\ &\times \left[\int\limits_0^1 \mathrm{d}\beta_2 \mathrm{d}\alpha_3 \beta_2^{-2\varepsilon} \alpha_3^{-3\varepsilon-1} \delta(1-\beta_2-\alpha_3) \int\limits_{\alpha_3}^\infty \mathrm{d}\beta_3 \beta_3^{-\varepsilon} \frac{1}{\beta_2+\beta_3} \frac{1}{\beta_2} \right] + \mathcal{O}(\nu^0), \end{aligned} \tag{5.30}$$

where we have used eq. (5.27) to express $\Xi_{\nu-1,-1}^{(1)}$ in terms of $C(\varepsilon)$. The last integral in eq. (5.30) can be easily calculated. We obtain

$$\begin{aligned} &\int\limits_0^1 \mathrm{d}\beta_2 \mathrm{d}\alpha_3 \beta_2^{-2\varepsilon} \alpha_3^{-3\varepsilon-1} \delta(1-\beta_2-\alpha_3) \int\limits_{\alpha_3}^\infty \mathrm{d}\beta_3 \beta_3^{-\varepsilon} \frac{1}{\beta_2+\beta_3} \frac{1}{\beta_2} \\ &= \frac{\Gamma(-2\varepsilon)\Gamma(1-4\varepsilon)}{\varepsilon\Gamma(1-6\varepsilon)} \; {}_3F_2\left(1,1,-2\varepsilon;1+\varepsilon,1-6\varepsilon;1\right). \end{aligned} \tag{5.31}$$

Finally, combining the various contributions and extracting the $1/\nu$ pole, we find

$$I_4^{1/\nu} = \frac{\Gamma^2(-2\varepsilon)\Gamma(1+2\varepsilon)\Gamma(1-4\varepsilon)}{\nu\varepsilon\Gamma(1-6\varepsilon)} \; C(\varepsilon) \; {}_3F_2\left(1,1,-2\varepsilon;1+\varepsilon,1-6\varepsilon;1\right) + \mathcal{O}(\nu^0), \tag{5.32}$$

where the function $C(\varepsilon)$ is given in eq. (5.27).

The computation of integral $I_3^{1/\nu}$ proceeds analogously. The only difference in comparison to $I_4^{1/\nu}$ is the presence of the propagator $1/k_{123}^2$, which simplifies to $1/(\alpha_2\beta_3)$ in the region responsible for producing the $1/\nu$ singularity. We find

$$I_3^{1/\nu} = \frac{\Gamma(1+2\varepsilon)\Gamma(-4\varepsilon)\Gamma^2(-2\varepsilon)}{\nu\Gamma(-6\varepsilon)(1+\varepsilon)}\, C(\varepsilon)\; {}_3F_2\left(1,1,-2\varepsilon;-6\varepsilon,2+\varepsilon;1\right) + \mathcal{O}(\nu^0). \tag{5.33}$$

The four integrals discussed above are the only $1/\nu$-divergent integrals that are required for computing the N3LO QCD contribution to the soft function.

6 Computing integrals with $1/k_{123}^2$ propagators using differential equations

It remains to compute 139 integrals that contain the $1/k_{123}^2$ propagator. Since we did not find a way to calculate them by direct integration, we follow the approach described in ref. [4] and modify this propagator by introducing an auxiliary parameter m^2,

$$\frac{1}{k_{123}^2} \to \frac{1}{k_{123}^2 + m^2}. \tag{6.1}$$

This step, applied to an original master integral $I(\varepsilon)$ transforms it to an m^2-dependent integral $J(\varepsilon, m^2)$.

There are two reasons for introducing m^2 in this way. First, it allows us to derive differential equations for the integrals $\boldsymbol{J}(\varepsilon, m^2)$, to solve them with high numerical precision and to extrapolate solutions to the point $m^2 = 0$. Second, inclusion of m^2 into the propagator $1/k_{123}^2$ enables computation of boundary conditions for the differential equations at the point $m^2 = \infty$, where significant simplifications occur. Although these simplifications are not as radical as may be naively expected, they are sufficient for an analytic computation of the required boundary constants, as we explain in section 7.

6.1 Constructing the differential equations

The differential equations are constructed following the standard procedure.

1. After the reduction of all integrals needed to compute the soft function, we select a set of dimensionally-regulated master integrals that contain the $1/k_{123}^2$ propagator. We will refer to this set as $\{I^{k_{123}^2}(\varepsilon)\}$.

2. For integrals from this set, we modify the $1/k_{123}^2$ propagator as in eq. (6.1). We will refer to this new set as $\{J^{k_{123}^2}(\varepsilon, m^2)\}$.

3. For $\{J^{k_{123}^2}(\varepsilon, m^2)\}$ integrals, we generate a system of linear equations using the integration-by-parts method, following the discussion in section 4. We need to extend the list of integrals that we consider and include additional integrals with $1/(k_{123}^2 + m^2)$ and also integrals without this propagator, to ensure that integration-by-parts identities close. We will refer to the new list of integrals as $\{J(\varepsilon, m^2)\}$. We note that the presence of the parameter m^2 does not affect the classification of integral families.

4. Computing derivatives of integrals from $\{J^{k_{123}^2}(\varepsilon, m^2)\}$ with respect to m^2, and expressing them through master integrals, we obtain a linear system of first-order differential equations
$$\frac{\partial}{\partial m^2}\boldsymbol{J}(\varepsilon, m^2) = \boldsymbol{M}(\varepsilon, m^2)\boldsymbol{J}(\varepsilon, m^2). \tag{6.2}$$

In principle, the above procedure should be performed for integrals defined with the analytic regulator. We have attempted to do that and found that the construction of differential equations becomes extremely complicated, as the reduction to master integrals involves three parameters d, ν and m^2 making it very slow and inefficient. However, it is important to realize that it is *unnecessary* to do that. Indeed, since the set of integrals $I^{k_{123}^2}(\varepsilon)$ includes integrals that *are* regularized dimensionally, and since introduction of m^2 cannot affect this property, derivatives of $J(\varepsilon, m^2)$ integrals cannot depend on ν as well. Hence, it should be possible to construct a ν-independent system of differential equations that these integrals satisfy. Our experience shows that the construction of such a system is possible but highly non-trivial. To achieve this, we relied heavily on the idea of *filtering* described at the end of section 3, which allows us to remove ill-defined integration-by-parts identities from the sets of linear equations and set $\nu = 0$ everywhere *before* attempting to solve it. We note that we have performed extensive checks of the filtering process by comparing exact ν-dependent reductions with reductions performed using a filtered system of IBP relations.

Remarkably, the filtered reduction actually achieves a more "complete" reduction than the ν-dependent reduction. In a test of the filtered reduction, we reduce those well-defined integrals needed for the computation of the soft function and compare the result with the ν-dependent reduction.[11] Some of the integrals are reduced to well-defined master integrals, which we reproduce exactly, while other integrals are reduced to the four $1/\nu$-divergent integrals $I^{1/\nu}$ discussed in section 5.2 with $\mathcal{O}(\nu^1)$ reduction coefficients. We find that the filtered IBP system reduces all such integrals, equivalently, to *two* well-defined integrals with $\mathcal{O}(\nu^0)$ reduction coefficients instead. It turns out that there are linear relations among the $1/\nu$ poles of the four integrals $I^{1/\nu}$

$$I_1^{1/\nu} = \frac{1+6\varepsilon}{1+4\varepsilon} I_2^{1/\nu} + \mathcal{O}(\nu^0), \tag{6.3}$$
$$I_3^{1/\nu} = -\frac{1+6\varepsilon}{1+3\varepsilon} I_4^{1/\nu} + \frac{1+7\varepsilon}{\varepsilon(1+3\varepsilon)} I_2^{1/\nu} + \mathcal{O}(\nu^0). \tag{6.4}$$

In the ν-dependent reduction, the $I^{1/\nu}$ integrals are independent, which is understandable since higher order terms in the expansion in ν of these integrals are unrelated to each other. This fact shows that the filtered reduction correctly captures the contributions that are relevant for the soft function and avoids the redundancies introduced by the analytic regulator ν.

6.2 Solving the differential equation and constructing solutions at $m^2 = 0$

In the previous section we described the construction of the system of differential equations for integrals that contain the $1/k_{123}^2$ propagator. Any system of differential equations requires

[11] Note that in our setup, the soft function is expressed as a linear combination of both well-defined integrals and ill-defined integrals. The filtered IBP system can only work with well-defined integrals.

boundary conditions. We find it convenient to compute them at $m^2 \to \infty$; we discuss the details of their computation in section 7. In this section we assume that the boundary conditions are known, explain how to solve the system of differential equations numerically, and recover the $m^2 = 0$ master integrals $I(\varepsilon)$ that we actually require.

The system of differential equations reads

$$\partial_{m^2} \boldsymbol{J}(\varepsilon, m^2) = \boldsymbol{M}(\varepsilon, m^2)\boldsymbol{J}(\varepsilon, m^2). \tag{6.5}$$

It contains 630 integrals. Our goal is to solve it numerically, starting from $m^2 = \infty$, and obtaining the desired $m^2 = 0$ integrals as

$$\boldsymbol{I}(\varepsilon) = \lim_{m^2 \to 0^+} \boldsymbol{J}(\varepsilon, m^2). \tag{6.6}$$

In deriving the system of differential equations it is critical to choose a basis of master integrals that keeps the differential equations simple. In particular, it is important to ensure that the matrix $\boldsymbol{M}(\varepsilon, m^2)$ contains no denominators which mix ϵ and m^2. We were able to achieve this for the system of equations that we have to solve. Even for good bases, elements of the matrix $\boldsymbol{M}$ are rational functions of m^2, comprised of high-degree polynomials with many poles in the complex m^2-plane.

Before describing how the system of differential equations can be solved, it is useful to make a few remarks about singularities of the integrals $\boldsymbol{J}(\varepsilon, m^2)$. Since these are phase-space integrals with $k_{123}^2 > 0$, the mass dependent propagator $1/(k_{123}^2 + m^2)$ cannot develop any non-analyticity for real positive values of m^2, except for $m^2 = 0$ and $m^2 = \infty$. Hence, in principle, as long as we stay away from the negative real axis in the complex m^2-plane, we can reach the point $m^2 = 0$ without having to worry about crossing singular surfaces, where values of integrals can branch.

However, it is to be noted that the matrix $\boldsymbol{M}(\varepsilon, m^2)$, that appears in the differential equation, does have singularities also in the half-plane where $\mathrm{Re}(m^2) > 0$. Altogether, there are 38 poles at various values of m^2 in the matrix $\boldsymbol{M}(\varepsilon, m^2)$, coming from 29 different polynomials in the denominator. These polynomials read

$$\begin{aligned}
&m^2, \pm1+m^2, \pm1+2m^2, \pm1+4m^2, \pm1+8m^2, \pm9+16m^2, 4+m^2, -16+m^2,\\
&1+16m^2, 1+3m^2, -9+4m^2, -3+4m^2, 1+5m^2, -3+8m^2, 4+9m^2, 1+64m^2,\\
&1+4m^4, 1+4m^2+16m^4, 4\pm13m^2+32m^4, -27+64m^4, -7-36m^2+96m^4,\\
&16+87m^2+1024m^4, 1+108m^2-304m^4+64m^6.
\end{aligned} \tag{6.7}$$

Among the zeros of these polynomials, there is a branch point at the origin, which is our target point. There are 22 singularities located at the half-plane with $\mathrm{Re}(m^2) < 0$ or on the imaginary axis of m^2

$$\begin{aligned}
m^2 \approx \{&-4, \quad -1, \quad -0.649511, \quad -0.5625, \quad -0.5, \quad -0.444,\\
&-0.33, \quad -0.25, \quad -0.203125 \pm 0.289379i, \quad -0.2,\\
&-0.1412, \quad -0.125, \quad -0.125 \pm 0.21651i, \quad -0.0625,\\
&-0.042480 \pm 0.11756i, \quad -0.015625, \quad -0.00903, \quad \pm 0.5i\}.
\end{aligned} \tag{6.8}$$

JHEP04(2025)084

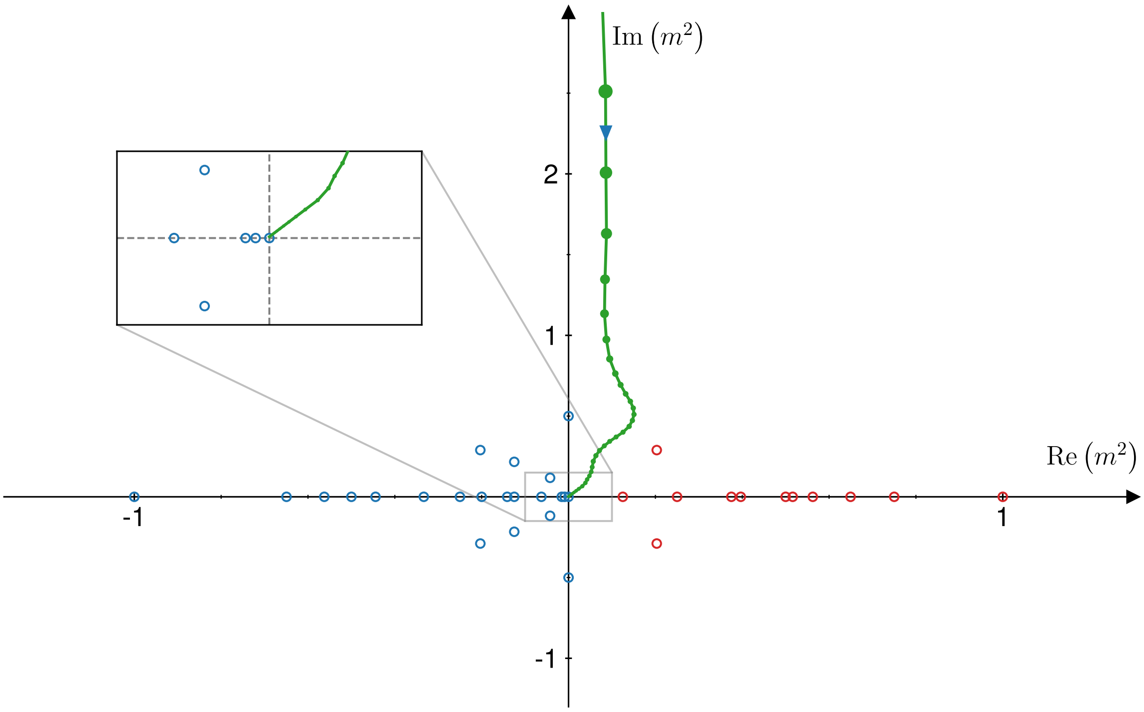

Figure 3. Singularities of $\boldsymbol{M}(\varepsilon, m^2)$ in the vicinity of $m^2 = 0$. The singularities located in the right half-plane of m^2 are colored in red, while other singularities are colored in blue. The path that we follow to move from $m^2 = \infty$ to $m^2 = 0$ is shown in green.

Finally, there are 15 poles in the half-plane where $\mathrm{Re}(m^2) > 0$,

$$\begin{aligned} m^2 \approx \{&0.125, \quad 0.25, \quad 0.203125 \pm 0.289379i, \quad 0.375, \\ &0.3966835638, \quad 0.5, \quad 0.5162444550, \quad 0.5625, \\ &0.6495190528, \quad 0.75, \quad 1, \quad 2.25, \quad 4.362345770, \quad 16\}. \end{aligned} \tag{6.9}$$

These different singularities of the matrix $\boldsymbol{M}$ are illustrated in figure 3, and, as we already mentioned, all $\boldsymbol{J}(\varepsilon, m^2)$ integrals have to remain regular in the half-plane to the right of the imaginary axis.

Furthermore, when m^2 is real and positive, the phase-space integrals should also be real. While this sounds completely obvious, it provides a useful consistency check for the solutions of the differential equations, especially if one starts at complex infinity and moves towards a positive real axis.

The solution at $m^2 = \infty$ takes the following form

$$\begin{aligned} \boldsymbol{J}_\infty(\varepsilon, m^2) = \sum_{nlk} \left(m^2\right)^{-n-l\varepsilon} \log^k m^2 \boldsymbol{B}_{nlk}(\varepsilon) &= \sum_n \left(m^2\right)^{-n} \boldsymbol{B}_n^0(\varepsilon) \\ &+ \left(m^2\right)^{-\varepsilon} \left[\sum_n \left(m^2\right)^{-n} \boldsymbol{B}_n^{-\varepsilon}(\varepsilon) + \sum_n \left(m^2\right)^{-n} \log m^2 \boldsymbol{B}_n^{-\varepsilon,\log}(\varepsilon)\right] \\ &+ \left(m^2\right)^{-2\varepsilon} \left[\sum_n \left(m^2\right)^{-n} \boldsymbol{B}_n^{-2\varepsilon}(\varepsilon) + \sum_n \left(m^2\right)^{-n} \log m^2 \boldsymbol{B}_n^{-2\varepsilon,\log}(\varepsilon)\right. \\ &\left. + \sum_n \left(m^2\right)^{-n} \log^2 m^2 \boldsymbol{B}_n^{-2\varepsilon,\log^2}(\varepsilon)\right], \end{aligned} \tag{6.10}$$

where in the second step we write the relevant terms of the expansion *actually* allowed by the differential equations.

We find that we require 49 constants of the type $\boldsymbol{B}_i^0$, 28 constants of the type $\boldsymbol{B}_i^{-\varepsilon}$, 26 constants of the type $\boldsymbol{B}_i^{-2\varepsilon}$, and 1 constant of the type $\boldsymbol{B}_i^{-\varepsilon,\log}$ to fully specify the solution. Integrals, from which these constants are determined, can be chosen arbitrarily, but simpler integrals are preferred.

Having determined a sufficient number of the expansion coefficients in eq. (6.10), we can evaluate $\boldsymbol{J}_\infty(\varepsilon, m^2)$ at a point $m^2 = m_i^2$ that is different from infinity. To choose this point, we need to determine the radius of convergence of the expansion in eq. (6.10), which is controlled by the closest singularity to $m^2 = \infty$ in the complex m^2-plane, or the farthest singularity away from the origin. For our equation $m^2 = 16$ dictates the radius of convergence of the solution at the boundary eq. (6.10), any m^2 that satisfies $|m^2| > 16$ is a valid choice of m_i^2. In practice m_i^2 is taken to be $64i$. Having chosen the first evaluation point m_i^2, within the radius of convergence, we obtain $\boldsymbol{J}(\varepsilon, m_i^2) = \boldsymbol{J}_\infty(\varepsilon, m_i^2)$. To move forward, we represent solutions of the differential equation as Taylor series

$$\boldsymbol{J}_{m_i^2}(\varepsilon, m^2) = \sum_{n=0} \left(m^2 - m_i^2\right)^n \boldsymbol{c}_n(\varepsilon), \tag{6.11}$$

which is possible since m_i^2 is a regular point of the differential equation. It should be apparent that $\boldsymbol{c}_0(\varepsilon) = \boldsymbol{J}(\varepsilon, m_i^2)$ and that other coefficients in the above equation are

$$c_n(\varepsilon) = \frac{1}{n!}\frac{\mathrm{d}^n\, \boldsymbol{J}_\infty(\varepsilon, m^2)}{\mathrm{d}m^{2n}}\Big|_{m^2=m_i^2}. \tag{6.12}$$

We find it convenient to compute these derivative by utilizing the differential equation. The n-th derivative satisfies

$$\frac{\mathrm{d}^n\, \boldsymbol{J}(\varepsilon, m^2)}{\mathrm{d}m^{2n}} = \sum_{k=0}^{n-1} \frac{(n-1)!}{(n-1-k)!k!}\left[\frac{\mathrm{d}^k \boldsymbol{M}}{\mathrm{d}m^{2k}}\; \frac{\mathrm{d}^{(n-1-k)}\, \boldsymbol{J}(\varepsilon, m^2)}{\mathrm{d}m^{2(n-1-k)}}\right]. \tag{6.13}$$

Using these equations recursively, we easily obtain the coefficients $c_n(\varepsilon)$.[12] We then use eq. (6.11) to move away from the point m_i^2, staying within its radius of convergence, and then repeat the above procedure at another regular point.

Continuing this process, after about 50 steps we reach a point within the radius of convergence of the solution at $m^2 = 0$. We will refer to this last regular point as m_f^2. The point $m^2 = 0$ is a singular point of the differential equation, so the expansion around this point has a power-logarithmic form

$$\boldsymbol{J}_0(\varepsilon, m^2) = \sum_{lnk} \left(m^2\right)^{n+l\varepsilon} \log^k m^2 \boldsymbol{c}_{nlk}(\varepsilon). \tag{6.14}$$

We compute coefficients of the expansion in eq. (6.14) by comparing it with the value of the Taylor-expanded integrals $\boldsymbol{J}(\varepsilon, m_f^2)$ at m_f^2. We emphasize that in the formal solution

[12] In practice, $c_n(\varepsilon)$ can be evaluated efficiently by casting the differential equation system into a system of linear recurrence relations and solving it order by order.

shown in eq. (6.14) we include all branches that are consistent with the behavior of the differential equation eq. (6.5) at $m^2 = 0$.

Finally, we take the limit $m^2 \to 0$ *at fixed* ε, recovering original massless integrals

$$\boldsymbol{I}(\varepsilon) = \lim_{\varepsilon \to 0} \lim_{m^2 \to 0^+} \boldsymbol{J}_0(\varepsilon, m^2) = \boldsymbol{c}_{000}(\varepsilon), \tag{6.15}$$

where the limit $\varepsilon \to 0$ is understood as an expansion through the required order in ε.

It is interesting to note that there are more independent integrals in the list $\boldsymbol{J}(\varepsilon, m^2)$ than in $\boldsymbol{I}(\varepsilon)$. This means that the massless integrals that we obtain as the limit of massive integrals are not independent and relations between them can be found using the IBP relations for massless integrals. This provides an opportunity for a highly non-trivial and powerful check, and we find that our solutions do pass it.

To conclude this section, we note that in comparison to our previous work [4, 5], where both parameters d and ν were retained in the differential equations, the current approach is simpler and more transparent. The reason for this is that it is difficult to construct the ν-dependent differential equations and to analyze the behavior of the solutions around singular points $m^2 = 0$ and ∞. For example, the solution $\boldsymbol{J}_0(\varepsilon, \nu, m^2)$ of the ν-dependent system of differential equations at $m^2 = 0$ depends on both regulators ε and ν, and the original massless integrals are recovered in the following way[13]

$$\boldsymbol{I}(\varepsilon, \nu) = \lim_{\varepsilon \to 0} \lim_{\nu \to 0} \lim_{m^2 \to 0^+} \boldsymbol{J}_0(\varepsilon, \nu, m^2). \tag{6.16}$$

The need to compute these limits forces us to develop full understanding of the ν dependence of master integrals at the singular points, which is highly non-trivial. Furthermore, evolving solutions of the differential equations from $m^2 = \infty$ to $m^2 = 0$ is much more challenging in the presence of the ν regulator.

Previously [4, 5], we observed that the ν-dependent solutions $(m^2)^{n+l\varepsilon+l'\nu} \log^k m^2$ take a relatively simple form and, in the limit $\nu \to 0$, can be accounted for correctly without the need of explicitly introducing the regulator ν to the differential equation. This allows us to take the $\nu \to 0$ limit before starting to solve the differential equations, making it similar to cases where dimensional regularization is sufficient. However, due to an increased complexity of master integrals, this was hardly a viable option for the $nn\bar{n}$ case. The use of a filtered reduction was crucial for solving the problem, as all integrals $\boldsymbol{I}(\varepsilon)$ that appear in that case are guaranteed to be well-defined without the need of an additional regulator.

7 Boundary conditions

In the previous section, we have assumed that all the boundary conditions at $m^2 = \infty$ are known. In this section we discuss how they are computed. By analyzing the matrix $\boldsymbol{M}(\varepsilon, m^2)$ at $m^2 \to \infty$, it is possible to identify the possible branches for various integrals and deduce the minimal set of constants for the boundary conditions. Many of these branches provide vanishing contributions, and only three branches $(m^2)^{-n\varepsilon}$ with $n = 0, 1, 2$, which have already appeared in the nnn case [4, 5], contribute.

[13] The $\varepsilon \to 0$ and $\nu \to 0$ limits should be understood as the expansion of integrals through an appropriate order in these variables.

D_i	$\alpha_1 \sim m^2$	$\alpha_2 \sim m^2$	$\alpha_3 \sim m^2$	$\beta_3 \sim m^2$
$k_{12} \cdot n$	β_{12}	β_{12}	β_{12}	β_{12}
$k_{23} \cdot n$	β_{23}	β_{23}	β_{23}	$\boldsymbol{\beta_3}$
$k_{13} \cdot n$	β_{13}	β_{13}	β_{13}	$\boldsymbol{\beta_3}$
$k_{123} \cdot n$	β_{123}	β_{123}	β_{123}	$\boldsymbol{\beta_3}$
$k_{12} \cdot \bar{n}$	$\boldsymbol{\alpha_1}$	$\boldsymbol{\alpha_2}$	α_{12}	α_{12}
$k_{23} \cdot \bar{n}$	α_{23}	$\boldsymbol{\alpha_2}$	$\boldsymbol{\alpha_3}$	α_{23}
$k_{13} \cdot \bar{n}$	$\boldsymbol{\alpha_1}$	α_{13}	$\boldsymbol{\alpha_3}$	α_{13}
$k_{123} \cdot \bar{n}$	$\boldsymbol{\alpha_1}$	$\boldsymbol{\alpha_2}$	$\boldsymbol{\alpha_3}$	α_{123}
k_{12}^2	$\boldsymbol{\alpha_1 \beta_2}$	$\boldsymbol{\alpha_2 \beta_1}$	k_{12}^2	k_{12}^2
k_{23}^2	k_{23}^2	$\boldsymbol{\alpha_2 \beta_3}$	$\boldsymbol{\alpha_3 \beta_2}$	$\boldsymbol{\beta_3 \alpha_2}$
k_{13}^2	$\boldsymbol{\alpha_1 \beta_3}$	k_{13}^2	$\boldsymbol{\alpha_3 \beta_1}$	$\boldsymbol{\beta_3 \alpha_1}$
$k_{123}^2 + m^2$	$\boldsymbol{\alpha_1 \beta_{23}} + m^2$	$\boldsymbol{\alpha_2 \beta_{13}} + m^2$	$\boldsymbol{\alpha_3 \beta_{12}} + m^2$	$\boldsymbol{\beta_3 \alpha_{12}} + m^2$

Table 3. Scalings in the region $(m^2)^{-\varepsilon}$.

7.1 The Taylor branch

Since we discuss phase-space integrals and consider the limit $m^2 \to \infty$, the most natural contribution arises from the Taylor expansion of integrands in $1/m^2$. This implies

$$\frac{1}{k_{123}^2 + m^2} \to \frac{1}{m^2} + \mathcal{O}(k_{123}^2/m^2), \tag{7.1}$$

and the complicated denominator k_{123}^2 disappears from the computation entirely. Integrals that appear in the calculation of the Taylor branch can be computed by direct integration in the same way as the master integrals discussed in section 5.

7.2 Region $(\boldsymbol{m^2})^{-\varepsilon}$

A peculiar feature of *phase-space* integrals required for the computation of the soft function is their *ultra-violet* sensitivity, manifesting itself in the appearance of non-trivial branches in the $m^2 \to \infty$ limit. We start with the discussion of the $(m^2)^{-\varepsilon}$ branch. This branch occurs when a larger light-cone component of one of the partons' momenta is $\mathcal{O}(m^2)$ and all other momenta components and momenta of other partons are $\mathcal{O}(1)$. This can only happen if at least one θ-function is present in the integrand.

In table 3 we provide original and simplified expressions for all inverse propagators, for different choices of the large light-cone coordinate. It follows from that table, that there is one (and only one) case-specific scalar product of two four-momenta that cannot be simplified. These scalar products depend on the relative angle between momenta of two partons, and it is this dependence that makes the computation of boundary conditions for this branch challenging.

We denote two partons, whose momenta scale as $\mathcal{O}(1)$, as i and j, and the parton with one $\mathcal{O}(m^2)$ Sudakov component as h. We also assume that the larger momentum component is $\tilde{\gamma}_h$ and the smaller one is γ_h. It follows from table 3 that any integral that provides the $(m^2)^{-\varepsilon}$ branch can be written as

$$J \sim \frac{1}{\mathcal{N}_\varepsilon^2} \int\limits_0^\infty \mathrm{d}\gamma_h \, \gamma_h^{-\varepsilon} \int [\mathrm{d}k_i][\mathrm{d}k_j] \frac{f_i f_j R_0(\alpha_i,\beta_i,\alpha_j,\beta_j,\gamma_h)}{[k_{ij}^2]^n} \int\limits_0^\infty \frac{\mathrm{d}\tilde{\gamma}_h \, \tilde{\gamma}_h^{-\varepsilon}}{\tilde{\gamma}_h^{n_1} \, (\tilde{\gamma}_h \, x_{ij} + m^2)^{n_2}}, \tag{7.2}$$

where the rational function $R_0(\alpha_i,\beta_i,\alpha_j,\beta_j,\gamma_h)$ contains the zero-jettiness δ-function, and depends on the light-cone components of all partons. The polynomial x_{ij} that depends on the light-cone components of momenta $k_{i,j}$ can be read off from table 3. The integral over $\tilde{\gamma}_h$ gives

$$\int\limits_0^\infty \frac{\mathrm{d}\tilde{\gamma}_h \, \tilde{\gamma}_h^{-\varepsilon}}{\tilde{\gamma}_h^{n_1} \, (\tilde{\gamma}_h \, x_{ij} + m^2)^{n_2}} = (m^2)^{1-\varepsilon-n_1-n_2} \frac{\Gamma(n_1+n_2-1+\varepsilon)\Gamma(1-n_1-\varepsilon)}{\Gamma(n_2)} \, x_{ij}^{n_1-1+\varepsilon}. \tag{7.3}$$

As the next step, we discuss integration over momenta of partons i and j and consider the following integral

$$J_{ij} = \frac{1}{\mathcal{N}_\varepsilon^2} \int [\mathrm{d}k_i][\mathrm{d}k_j] \frac{1}{[k_{ij}^2]^n} \, f_i \, f_j \, R(\alpha_i,\beta_i,\alpha_j,\beta_j,\gamma_h). \tag{7.4}$$

In eq. (7.4) we have introduced a new function $R(\alpha_i,\beta_i,\alpha_j,\beta_j,\gamma_h) = x_{ij}^{n_1-1+\varepsilon} R_0(\alpha_i,\beta_i,\alpha_j,\beta_j,\gamma_h)$. The inverse propagator k_{ij}^2 reads

$$k_{ij}^2 = 2k_i \cdot k_j = (\alpha_i\beta_j + \alpha_j\beta_i) \left(1 - 2\frac{\sqrt{\alpha_i\beta_j\alpha_j\beta_i}}{\alpha_i\beta_j + \alpha_j\beta_i} \vec{e}_{\perp,i} \cdot \vec{e}_{\perp,j} \right) = (\alpha_i\beta_j + \alpha_j\beta_i) \, (\rho \cdot \rho_m) \, , \tag{7.5}$$

where ρ and ρ_m are two $(d-1)$-dimensional *Minkowski* vectors. The vector ρ is light-like, $\rho^2 = 0$, and the vector ρ_m is time-like with

$$\rho_m^2 = \frac{(\alpha_i\beta_j - \alpha_j\beta_i)^2}{(\alpha_i\beta_j + \alpha_j\beta_i)^2}. \tag{7.6}$$

The angular integration in the transverse space is easily performed with the help of eq. (D.32), and J_{ij} becomes

$$\begin{aligned} J_{ij} &= \frac{1}{(\Omega^{(d-2)})^2} \int \frac{\mathrm{d}\alpha_i \mathrm{d}\beta_i \mathrm{d}\alpha_j \mathrm{d}\beta_j}{(\alpha_i\beta_i\alpha_j\beta_j)^\varepsilon} \, f_i \, f_j \, R(\alpha_i,\beta_i,\alpha_j,\beta_j,\gamma_h) \int \frac{\mathrm{d}\Omega_i^{(d-2)} \mathrm{d}\Omega_j^{(d-2)}}{[k_{ij}^2]^n} \\ &= \int \frac{\mathrm{d}\alpha_i \mathrm{d}\beta_i \mathrm{d}\alpha_j \mathrm{d}\beta_j}{(\alpha_i\beta_i\alpha_j\beta_j)^\varepsilon} \, f_i \, f_j \, \frac{R(\alpha_i,\beta_i,\alpha_j,\beta_j,\gamma_h)}{(\alpha_i\beta_j + \alpha_j\beta_i)^n} \, I_{d-2;n}^{(1)}(\rho_m^2). \end{aligned} \tag{7.7}$$

The function $I_{d,n}^{(1)}$ is defined in eq. (D.36).

Further integrations require us to specify the constraints f_i and f_j. There are five cases to be considered.

(A) If $f_i = \delta(\alpha_i - \beta_i)$ and $f_j = \delta(\alpha_j - \beta_j)$, we integrate over α_i and α_j to obtain

$$J_{ij} = \frac{\Gamma(1-\varepsilon)\,\Gamma(1-2\varepsilon-2n)}{\Gamma(1-\varepsilon-n)\,\Gamma(1-2\varepsilon-n)} \int\limits_0^1 \mathrm{d}\beta_i \mathrm{d}\beta_j \, (\beta_i\beta_j)^{-n-2\varepsilon} \, R(\beta_i,\beta_i,\beta_j,\beta_j,\gamma_h). \tag{7.8}$$

(B) if $f_i = \delta(\alpha_i - \beta_i)$ and $f_j = \theta(\alpha_j - \beta_j)$, we integrate over α_i and perform a variable transformation $\alpha_j \to \beta_j/r_j$. We find

$$J_{ij} = \int\limits_0^1 \mathrm{d}\beta_i \mathrm{d}\beta_j \int\limits_0^1 \mathrm{d}r_j \frac{R\left(\beta_i, \beta_i, \frac{\beta_j}{r_j}, \beta_j, \gamma_h\right)}{\beta_i^{n+2\varepsilon}\beta_j^{n-1+2\varepsilon} r_j^{2-n-\varepsilon}} \, {}_2F_1\left(n, n+\varepsilon; 1-\varepsilon; r_j\right). \tag{7.9}$$

(C) if $f_i = \delta(\alpha_i - \beta_i)$ and $f_j = \theta(\beta_j - \alpha_j)$ we integrate over α_i, and replace $\beta_j = \alpha_j/r_j$

$$J_{ij} = \int\limits_0^1 \mathrm{d}\beta_i \mathrm{d}\alpha_j \int\limits_0^1 \mathrm{d}r_j \frac{R\left(\beta_i, \beta_i, \alpha_j, \frac{\alpha_j}{r_j}, \gamma_h\right)}{\beta_i^{n+2\varepsilon}\alpha_j^{n-1+2\varepsilon} r_j^{2-n-\varepsilon}} \, {}_2F_1\left(n, n+\varepsilon; 1-\varepsilon; r_j\right). \tag{7.10}$$

(D) if $f_i = \theta(\alpha_i - \beta_i)$ and $f_j = \theta(\alpha_j - \beta_j)$, we replace $\alpha_i = \beta_i/r_i$, $\alpha_j \to \beta_j/r_j$, apply the transformation shown in eq. (E.4) to the angular integral, where we also need to split the original integration region into two regions $r_i < r_j$ and $r_j < r_i$. Writing $r_i = r_j\xi$ and $r_j = \xi r_i$ in the first and in the second region, respectively, we obtain the following representation for the integral

$$\begin{aligned} J_{ij} = & \int\limits_0^1 \mathrm{d}\beta_i \mathrm{d}\beta_j \int\limits_0^1 \mathrm{d}r_j \mathrm{d}\xi \frac{R\left(\frac{\beta_i}{\xi r_j}, \beta_i, \frac{\beta_j}{r_j}, \beta_j, \gamma_h\right)}{(\beta_i\beta_j)^{n-1+2\varepsilon} r_j^{3-n-2\varepsilon}\xi^{2-n-\varepsilon}} {}_2F_1\left(n, n+\varepsilon; 1-\varepsilon; \xi\right) \\ & + \int\limits_0^1 \mathrm{d}\beta_i \mathrm{d}\beta_j \int\limits_0^1 \mathrm{d}r_i \mathrm{d}\xi \frac{R\left(\frac{\beta_i}{r_i}, \beta_i, \frac{\beta_j}{\xi r_i}, \beta_j, \gamma_h\right)}{(\beta_i\beta_j)^{n-1+2\varepsilon} r_i^{3-n-2\varepsilon}\xi^{2-n-\varepsilon}} {}_2F_1\left(n, n+\varepsilon; 1-\varepsilon; \xi\right). \end{aligned} \tag{7.11}$$

(E) finally, if $f_i = \theta(\alpha_i - \beta_i)$ and $f_j = \theta(\beta_j - \alpha_j)$, we replace $\alpha_i \to \beta_i/r_i, \beta_j \to \alpha_j/r_j$ and find

$$J_{ij} = \int\limits_0^1 \mathrm{d}\beta_i \mathrm{d}\alpha_j \int\limits_0^1 \mathrm{d}r_i \mathrm{d}r_j \frac{R\left(\frac{\beta_i}{r_i}, \beta_i, \alpha_j, \frac{\alpha_j}{r_j}, \gamma_h\right)}{(\beta_i\alpha_j)^{n-1+2\varepsilon}(r_i r_j)^{2-n-\varepsilon}} \, {}_2F_1\left(n, n+\varepsilon; 1-\varepsilon; r_i r_j\right). \tag{7.12}$$

Further integrations are case specific. Often, integrations over variables r and ξ can be performed in terms of hypergeometric functions, but if mixed propagators of the type $1/(\alpha_i + \alpha_j)$ appear, it becomes impossible to do that. At any rate, the subsequent integrations are performed on the case-by-case basis.

To illustrate the above discussion, we compute the $(m^2)^{-\varepsilon}$ branch of the following integral

$$J = \int \frac{\mathrm{d}\Phi_{\theta\theta\bar{\theta}}}{(k_1 \cdot k_3)\,(k_2 \cdot n)\,(k_{123} \cdot \bar{n})^2\,(k_{123}^2 + m^2)}. \tag{7.13}$$

This integral has three θ-functions and contributes to the $nn\bar{n}$ configuration.

A simple analysis shows that the leading $(m^2)^{-\varepsilon}$ contribution originates from the region where $\beta_3 \sim m^2$; because of that, the integral corresponds to the case (D) above with $i = 1$ and $j = 2$. The integrand in eq. (7.13) has no scalar product $k_1 \cdot k_2$; for this reason, no non-trivial angular integration has to be performed. We use table 3 to read off the simplified propagators, and apply the variable transformations that are explained in item (D) above. We then write the result as the sum of two terms

$$J = J_A + J_B, \tag{7.14}$$

where

$$J_A = 2\int_0^\infty \frac{\mathrm{d}\beta_3}{\beta_3^{1+\varepsilon}} \int_0^1 \mathrm{d}\beta_1 \mathrm{d}\beta_2\, \mathrm{d}\alpha_3 \mathrm{d}r_2 \mathrm{d}\xi \frac{(\beta_1\beta_2)^{-2\varepsilon}(\alpha_3)^{-\varepsilon} r_2^{1+2\varepsilon} \xi^{2+\varepsilon} \delta(1-\beta_1-\beta_2-\alpha_3)}{(\beta_1+(\beta_2+\alpha_3 r_2)\xi)^2((\beta_1+\beta_2\xi)\beta_3+m^2 r_2\xi)}, \tag{7.15}$$

$$J_B = 2\int_0^\infty \frac{\mathrm{d}\beta_3}{\beta_3^{1+\varepsilon}} \int_0^1 \mathrm{d}\beta_1 \mathrm{d}\beta_2 \mathrm{d}\alpha_3 \mathrm{d}r_1 \mathrm{d}\xi \frac{(\beta_1\beta_2)^{-2\varepsilon}(\alpha_3)^{-\varepsilon} r_1^{1+2\varepsilon} \xi^{1+\varepsilon} \delta(1-\beta_1-\beta_2-\alpha_3)}{(\beta_2+(\beta_1+\alpha_3 r_1)\xi)^2((\beta_2+\beta_1\xi)\beta_3+m^2 r_1\xi)}. \tag{7.16}$$

In both integrals, integration over β_3 can be immediately performed using eq. (7.3). Then, the zero-jettiness δ function is removed by integrating over β_2 in J_A and over β_1 in J_B. After that, the variable transformation $\beta_{1,2} = t(1-\alpha_3)$ is performed in integrals $J_{A,B}$, respectively.

To proceed further, it is convenient to treat both integrals on the same footing. To do that, we introduce an auxiliary integral J_n

$$J_n = \frac{2\Gamma(-\varepsilon)\Gamma(1+\varepsilon)}{(m^2)^{1+\varepsilon}} \int_0^1 \mathrm{d}r \mathrm{d}\xi \mathrm{d}\alpha_3 \mathrm{d}t \frac{\xi^n (1-\alpha_3)^{1-3\varepsilon} \alpha_3^{-\varepsilon} r^\varepsilon (1-t)^{-2\varepsilon} t^{-2\varepsilon} (t-\xi-t\xi)^\varepsilon}{(t-\alpha_3 t+\xi-\alpha_3\xi+\alpha_3 r\xi-t\xi+\alpha_3 t\xi)^2}, \tag{7.17}$$

and notice that $J_1 = J_A$ and $J_0 = J_B$, provided that r is identified with $r_{1,2}$ in the two integrals, as appropriate.

To compute J_n, we change the integration variables

$$\xi = \frac{tu}{1-u+tu}, \quad \alpha_3 = \frac{v}{u+v-uv}, \tag{7.18}$$

and obtain

$$J_n = \frac{2\Gamma(-\varepsilon)\Gamma(1+\varepsilon)}{(m^2)^{1+\varepsilon}} \int_0^1 \mathrm{d}r \mathrm{d}t \mathrm{d}u \mathrm{d}v \frac{r^\varepsilon (1-t)^{-2\varepsilon} t^{-1+n-\varepsilon} u^{n-3\varepsilon} (1-v)^{1-3\varepsilon} v^{-\varepsilon}}{(1-u+tu)^{n+\varepsilon} (u+v-uv)^{1-4\varepsilon} (1-v+rv)^2}. \tag{7.19}$$

Integration over v produces the Appell function F_1, see eq. (E.9), which simplifies to ${}_2F_1$, cf. eq. (E.6). The integration over t leads to a hypergeometric function ${}_2F_1$. We obtain

$$\begin{aligned} J_n = &-\frac{2\Gamma(2-3\varepsilon)\Gamma(1-2\varepsilon)\Gamma^2(1-\varepsilon)\Gamma(n-\varepsilon)\Gamma(1+\varepsilon)}{\varepsilon(m^2)^{1+\varepsilon}\Gamma(3-4\varepsilon)\Gamma(1+n-3\varepsilon)} \int_0^1 \mathrm{d}r \mathrm{d}u \frac{r^\varepsilon}{(1-u)^{n+\varepsilon} u^n} \\ &\times {}_2F_1(2,1-\varepsilon;3-4\varepsilon;1-ru)\, {}_2F_1\left(n-\varepsilon,n+\varepsilon;1+n-3\varepsilon;\frac{u}{u-1}\right). \end{aligned} \tag{7.20}$$

It is possible to integrate over r, expressing the result in terms of the hypergeometric function ${}_3F_2$. To do this, we employ eqs. (E.2) and (E.8). We obtain the following one-dimensional integral representation

$$
\begin{aligned}
J_n = & \frac{4(1-4\varepsilon)\Gamma(2-3\varepsilon)\Gamma(2-2\varepsilon)\Gamma(n-\varepsilon)\Gamma^2(1-\varepsilon)\Gamma(1+\varepsilon)}{3\varepsilon^2(m^2)^{1+\varepsilon}(1-3\varepsilon)(1+\varepsilon)\Gamma(3-4\varepsilon)\Gamma(1+n-3\varepsilon)} \\
& \times \int_0^1 \mathrm{d}u\, u^n {}_2F_1(1-2\varepsilon, n+\varepsilon; 1+n-3\varepsilon; u)\, {}_3F_2(2, 1-\varepsilon, 1+\varepsilon; 2+\varepsilon, 1+3\varepsilon; u) \\
& + \frac{2\Gamma(2-3\varepsilon)\Gamma(1-2\varepsilon)\Gamma(n-\varepsilon)\Gamma(-\varepsilon)\Gamma(3\varepsilon)\Gamma(1+\varepsilon)}{(m^2)^{1+\varepsilon}(1-2\varepsilon)\Gamma(1+n-3\varepsilon)} \int_0^1 \mathrm{d}u\, u^{n-3\varepsilon} \\
& \times {}_2F_1(1-2\varepsilon, n+\varepsilon, 1+n-3\varepsilon, u)\, {}_3F_2(1-4\varepsilon, 2-3\varepsilon, 1-2\varepsilon; 1-3\varepsilon, 2-2\varepsilon; u),
\end{aligned}
\tag{7.21}
$$

where we also used eq. (E.3) to simplify the u-dependent hypergeometric function in eq. (7.20).

The integral representation for J_n, $n = 0, 1$ in eq. (7.21) is convenient because integration over u is not singular. Hence, the integrand in that equation can be expanded in powers of ε, and integrated term by term using `HyperInt` [138]. Upon doing that, we obtain the final result for the integral in eq. (7.13)

$$
\begin{aligned}
J = (m^2)^{-1-\varepsilon} \Bigg[& \frac{\pi^2}{3\varepsilon^2} + \frac{10\zeta_3}{\varepsilon} + \frac{29\pi^4}{90} + \varepsilon \left(208\zeta_5 - \frac{38}{3}\pi^2\zeta_3 \right) \\
& + \varepsilon^2 \left(\frac{2239}{5670}\pi^6 - 172\zeta_3^2 \right) + \mathcal{O}(\varepsilon^3) \Bigg].
\end{aligned}
\tag{7.22}
$$

All integrals that possess the $(m^2)^{-\varepsilon}$-branch at large m^2 can be analyzed using similar steps once the large momentum component for one of the partons is identified.

7.3 $(m^2)^{-\varepsilon} \log(m^2)$ boundary integral

All branches of master integrals contain prefactors $(m^2)^{-n\varepsilon}$, with $n = 0, 1, 2$. In addition, we have found that in case $n = 1$, one needs to account for additional sub-branch $(m^2)^{-\varepsilon}\log(m^2)$, where the logarithm appears *before* expansion in ε. This contribution may appear if, in a given integral, two different integration regions over Sudakov parameters contribute to the $(m^2)^{-\varepsilon}$ branch. We will illustrate this phenomenon by considering two integrals. The first integral is quite simple, it can be computed in a closed form and used to understand the origin of such terms. The second is more complex; we discuss it because it was actually used to determine the required boundary condition.

We begin with the following integral

$$
R_1 = \int \frac{\mathrm{d}\Phi_{\delta\theta\bar{\theta}}\, \beta_2}{(k_{123}^2 + m^2)}. \tag{7.23}
$$

It receives two non-vanishing contributions to the branch $(m^2)^{-\varepsilon}$ from the regions with $\alpha_2 \sim m^2$ and $\beta_3 \sim m^2$. Hence, we can write

$$
R_1^{-\varepsilon} = R_{1,\alpha_2} + R_{1,\beta_3}, \tag{7.24}
$$

and a simple analysis shows that, individually, these contributions are not regulated dimensionally.[14]

To proceed with the calculation of individual contributions to the $(m^2)^{-\varepsilon}$ branch, we introduce the factor $\beta_3^{-\nu}$ to the numerator of the original integral eq. (7.23). Considering the contribution of the $\alpha_2 \sim m^2$ region and making use of the integral representation in eq. (7.10) with $n = 0$, we find

$$R_{1,\alpha_2} = \int_0^\infty \mathrm{d}\alpha_2 \int_0^1 \mathrm{d}\beta_1 \mathrm{d}\beta_2 \mathrm{d}\alpha_3 \mathrm{d}r_3 \left(\frac{r_3}{\alpha_3}\right)^\nu \frac{\alpha_3^{1-2\varepsilon}\beta_1^{-2\varepsilon}\beta_2(\alpha_2\beta_2)^{-\varepsilon}\delta(1-\alpha_3-\beta_1-\beta_2)}{r_3^{1-\varepsilon}(r_3(\alpha_2\beta_1+m^2)+\alpha_2\alpha_3)}. \tag{7.25}$$

We continue with the integrations over α_2 and r_3. We remove the δ-function by integrating over β_1, and change variables $\alpha_3 = t(1-\beta_2)$ after that. The integrations over β_2 and t factorize and we obtain

$$\begin{aligned} R_{1,\alpha_2} = & \frac{(1-\varepsilon)\Gamma(1-2\varepsilon)\Gamma^3(1-\varepsilon)\Gamma(1+\varepsilon)\Gamma(2-3\varepsilon-\nu)}{(m^2)^\varepsilon \varepsilon\nu\Gamma(2-3\varepsilon)\Gamma(4-4\varepsilon-\nu)} \\ & \times {}_3F_2\left(1-2\varepsilon, \nu, \varepsilon+\nu; 2-3\varepsilon, 1+\nu; 1\right). \end{aligned} \tag{7.26}$$

The $1/\nu$ pole in the above expression is compensated by the contribution from the region $\beta_3 \sim m^2$, that we now discuss.

We use the representation in eq. (7.9) to obtain

$$R_{1,\beta_3} = \int_0^\infty \mathrm{d}\beta_3 \int_0^1 \mathrm{d}\beta_1 \mathrm{d}\beta_2 \mathrm{d}\alpha_3 \mathrm{d}r_3 \frac{\beta_1^{-2\varepsilon}\beta_2^{2-2\varepsilon}\beta_3^{-\nu}(\alpha_3\beta_3)^{-\varepsilon} r_3^{-1+\varepsilon}\delta(1-\alpha_3-\beta_1-\beta_2)}{r_3(\beta_1\beta_3+m^2)+\beta_2\beta_3}. \tag{7.27}$$

Performing the integrations, we find

$$\begin{aligned} R_{1,\beta_3} = & -\frac{1}{\nu}\frac{(1-\varepsilon)\Gamma(1-2\varepsilon)\Gamma^2(1-\varepsilon)\Gamma(-\varepsilon-\nu+1)\Gamma(3-3\varepsilon+\nu)\Gamma(\varepsilon+\nu)}{(m^2)^{\varepsilon+\nu}\Gamma(3-3\varepsilon)\Gamma(4-4\varepsilon+\nu)} \\ & \times {}_3F_2\left(1-2\varepsilon, \varepsilon, -\nu; 3-3\varepsilon, 1-\nu; 1\right). \end{aligned} \tag{7.28}$$

Finally, combining R_{1,α_2} and R_{1,β_3} and expanding in ν at fixed ε, we find

$$R_1^{-\varepsilon} = R_{1,\alpha_2} + R_{1,\beta_3} = \frac{(1-\varepsilon)\Gamma(1-2\varepsilon)\Gamma^3(1-\varepsilon)\Gamma(\varepsilon)}{\Gamma(4-4\varepsilon)} (m^2)^{-\varepsilon}\log(m^2) + \ldots, \tag{7.29}$$

where ellipses stand for contributions that do not contain the $(m^2)^{-\varepsilon}\log(m^2)$ branch. We note that out of the two terms discussed above, only R_{1,β_3} produces a $\log(m^2)$ contribution whereas another one is only needed for removing the $1/\nu$ pole. This is a generic feature of such integrals, that we exploit in the second example below.

A more complicated integral that is actually employed for the calculation of the relevant boundary constant reads

$$R_2 = \int \frac{\mathrm{d}\Phi_{\theta\theta\bar{\theta}}}{(k_{123}^2 + m^2)(k_{23}\cdot\bar{n})}. \tag{7.30}$$

[14] To avoid confusion, we stress that this integral is regularized dimensionally, in agreement with the discussion in section 3. However, when we *approximate* the integrand to simplify the calculation of the $(m^2)^{-\varepsilon}$ branch at large m^2, the resulting expressions become ill-defined.

JHEP04(2025)084

To compute the $(m^2)^{-\varepsilon}$ branch of this integral, we need to consider two regions, $\alpha_1 \sim m^2$ and $\beta_3 \sim m^2$. We regulate both of these contributions by multiplying the integrand in eq. (7.30) with $\beta_3^{-\nu}$. Similar to the previous example, we find that the region $\alpha_1 \sim m^2$ does not contribute to the $\log(m^2)$ branch, whereas the $\beta_3 \sim m^2$ region does. Both regions contribute to the coefficient of the $1/\nu$ pole, where they cancel each other.

Focusing on the term $(m^2)^{-\varepsilon}\log(m^2)$, we consider the region where $\beta_3 \sim m^2$ and split the relevant integrations into two parts, similar to the representation in eq. (7.11). We write $\alpha_1 = \beta_1/r_1$ and $\alpha_2 = \beta_2/r_2$, consider two regions $r_1 < r_2$ and $r_2 < r_1$ and find that only the first one contributes to the $(m^2)^{-\varepsilon}\log(m^2)$ branch. Hence, changing variables $r_1 = \xi\, r_2$, we arrive at the following representation of the relevant contribution[15] to the integral

$$\tilde{R}_2 = \int\limits_0^\infty \mathrm{d}\beta_3 \int\limits_0^1 \mathrm{d}\beta_1 \mathrm{d}\beta_2 \mathrm{d}\alpha_3 \mathrm{d}r_2 \mathrm{d}\xi \frac{(\beta_1\beta_2)^{1-2\varepsilon}\delta(1-\alpha_3-\beta_1-\beta_2)}{\beta_3^\nu(\alpha_3\beta_3)^\varepsilon r_2^{3-2\varepsilon}\xi^{2-\varepsilon}\left(\alpha_3+\frac{\beta_2}{r_2}\right)\left(m^2+\frac{\beta_2\beta_3}{r_2}+\frac{\beta_1\beta_3}{r_2\xi}\right)}. \tag{7.31}$$

To compute this integral, we integrate over β_3, remove the δ-function by integrating over α_3, and change variables as follows, $\beta_2 = t(1-\beta_1)$ and $\beta_1 = t(1-v)/(t+v-tv)$. Integrating over v and r_2, we obtain the following two-dimensional integral

$$\begin{aligned}\tilde{R}_2 = {}& \frac{\Gamma(2-3\varepsilon)\Gamma(2-2\varepsilon)\Gamma(-\varepsilon-\nu+1)\Gamma(\varepsilon-\nu)\Gamma(\varepsilon+\nu)}{(m^2)^{\varepsilon+\nu}\Gamma(4-5\varepsilon)\Gamma(\varepsilon-\nu+1)} \int\limits_0^1 \mathrm{d}t\mathrm{d}\xi \frac{(1-t)^{-\varepsilon}}{t^{2-\varepsilon}\xi^{3-3\varepsilon+\nu}} \\ & \times {}_2F_1\left(1,\varepsilon-\nu;1+\varepsilon-\nu;1-\frac{1}{t}\right) {}_2F_1\left(2-3\varepsilon,3-4\varepsilon+\nu;4-5\varepsilon;1-\frac{1}{t\xi}\right).\end{aligned} \tag{7.32}$$

Applying the transformations shown in eqs. (E.3), (E.1) to first and second hypergeometric functions, respectively, we find that the integral splits into two parts, where in each part integration over ξ can be performed. Keeping the part that provides the $(m^2)^{-\varepsilon}\log(m^2)$ contribution, we write

$$\tilde{R}_2 = -\frac{\Gamma(2-3\varepsilon)(m^2)^{-\varepsilon-\nu}\Gamma^2(1-\varepsilon)\Gamma(\varepsilon)}{\nu\varepsilon\Gamma(3-4\varepsilon)} \int\limits_0^1 \mathrm{d}x \frac{x^{1-2\varepsilon}}{(1-x)^\varepsilon} {}_2F_1(1,1;1+\varepsilon;1-x) + \dots. \tag{7.33}$$

Integrating over x and extracting the $\log(m^2)$ term, we obtain the final result

$$R_2 = \frac{\Gamma(1-2\varepsilon)\Gamma^3(1-\varepsilon)\Gamma(1+\varepsilon)}{2\varepsilon^2(2-3\varepsilon)\Gamma(2-4\varepsilon)} {}_3F_2(1,1,1-\varepsilon;3-3\varepsilon,1+\varepsilon;1) m^{-2\varepsilon}\log(m^2) + \cdots, \tag{7.34}$$

where ellipses describe terms that do not contain the $\log(m^2)$ term at fixed ε.

7.4 Region $(m^2)^{-2\varepsilon}$

Integrals where *two* light-cone components of partons' momenta can become large simultaneously may possess an $(m^2)^{-2\varepsilon}$ branch.

Similarly to the $(m^2)^{-\varepsilon}$ branch considered earlier, we compute it by removing the θ-functions which involve large light-cone components and extend the relevant integrations

[15] We introduce notation $\tilde{R}_2$ to emphasize that the expression below only gives the relevant $\log(m^2)$ term and not the whole integral R_2.

D_i	$\alpha_1 \sim \alpha_2 \sim m^2$ $q = k_1 + k_2$	$\alpha_2 \sim \alpha_3 \sim m^2$ $q = k_2 + k_3$	$\alpha_1 \sim \alpha_3 \sim m^2$ $q = k_1 + k_3$
$k_{12} \cdot n$	$\beta_{12} = \beta_q$	$\beta_{12} = \beta_2 + \beta_1$	$\beta_{12} = \beta_1 + \beta_2$
$k_{23} \cdot n$	$\beta_{23} = \beta_2 + \beta_3$	$\beta_{23} = \beta_q$	$\beta_{23} = \beta_3 + \beta_2$
$k_{13} \cdot n$	$\beta_{13} = \beta_1 + \beta_3$	$\beta_{13} = \beta_3 + \beta_1$	$\beta_{13} = \beta_q$
$k_{123} \cdot n$	$\beta_{123} = \beta_q + \beta_3$	$\beta_{123} = \beta_q + \beta_1$	$\beta_{123} = \beta_q + \beta_2$
$k_{12} \cdot \bar{n}$	$\alpha_{12} = \alpha_q$	$\boldsymbol{\alpha_2}$	$\boldsymbol{\alpha_1}$
$k_{23} \cdot \bar{n}$	$\boldsymbol{\alpha_2}$	$\alpha_{23} = \alpha_q$	$\boldsymbol{\alpha_3}$
$k_{13} \cdot \bar{n}$	$\boldsymbol{\alpha_1}$	$\boldsymbol{\alpha_3}$	$\alpha_{13} = \alpha_q$
$k_{123} \cdot \bar{n}$	$\boldsymbol{\alpha_{12}} = \alpha_q$	$\boldsymbol{\alpha_{23}} = \alpha_q$	$\boldsymbol{\alpha_{13}} = \alpha_q$
k_{12}^2	$k_{12}^2 = q^2$	$\boldsymbol{\alpha_2 \beta_1}$	$\boldsymbol{\alpha_1 \beta_2}$
k_{23}^2	$\boldsymbol{\alpha_2 \beta_3}$	$k_{23}^2 = q^2$	$\boldsymbol{\alpha_3 \beta_2}$
k_{13}^2	$\boldsymbol{\alpha_1 \beta_3}$	$\boldsymbol{\alpha_3 \beta_1}$	$k_{13}^2 = q^2$
k_{123}^2	$k_{12}^2 + \boldsymbol{\alpha_{12} \beta_3} + m^2$	$k_{23}^2 + \boldsymbol{\alpha_{23} \beta_1} + m^2$	$k_{13}^2 + \boldsymbol{\alpha_{13} \beta_2} + m^2$

Table 4. Possible large integration parameters combinations giving contribution in the region $(m^2)^{-2\varepsilon}$. We do not include contribution of the region with $\alpha_1 \sim \beta_3 \sim m^2$ and $\alpha_2 \sim \beta_3 \sim m^2$ resulting in scaleless integrals.

to the interval $[0, \infty)$. Since in the region where $\alpha_i \sim \alpha_j \sim m^2$, momenta k_i and k_j are not anymore constrained by the θ-functions, it is useful to introduce a new vector $q = k_i + k_j$ and treat an integral over momenta k_i, k_j as a normal phase-space integral at fixed q.

All possible combinations of large Sudakov components, together with simplified propagators, are summarized in table 4. The integration measures for all the relevant cases can be simplified as follows

$$\alpha_2 \sim \alpha_3 \sim m^2 :$$
$$\mathrm{d}\Phi_{\delta\theta\theta} \to \frac{1}{\mathcal{N}_\varepsilon} \mathrm{d}^d q [\mathrm{d}k_1] \delta\left(1 - \beta_q - \beta_1\right) \delta\left(\alpha_1 - \beta_1\right) \mathrm{d}\Phi(q, k_2, k_3), \tag{7.35}$$
$$\alpha_1 \sim \alpha_3 \sim m^2 :$$
$$\mathrm{d}\Phi_{\theta\delta\theta} \to \frac{1}{\mathcal{N}_\varepsilon} \mathrm{d}^d q [\mathrm{d}k_2] \delta\left(1 - \beta_q - \beta_2\right) \delta\left(\alpha_2 - \beta_2\right) \mathrm{d}\Phi(q, k_1, k_3), \tag{7.36}$$
$$\alpha_1 \sim \alpha_2 \sim m^2 :$$
$$\mathrm{d}\Phi_{\theta\theta\delta} \to \frac{1}{\mathcal{N}_\varepsilon} \mathrm{d}^d q [\mathrm{d}k_3] \delta\left(1 - \beta_q - \beta_3\right) \delta\left(\alpha_3 - \beta_3\right) \mathrm{d}\Phi(q, k_1, k_2), \tag{7.37}$$
$$\alpha_1 \sim \alpha_2 \sim m^2 :$$
$$\mathrm{d}\Phi_{\theta\theta\delta} \to \frac{1}{\mathcal{N}_\varepsilon} \mathrm{d}^d q [\mathrm{d}k_3] \delta\left(1 - \beta_q - \alpha_3\right) \delta\left(\beta_3 - \alpha_3\right) \mathrm{d}\Phi(q, k_1, k_2), \tag{7.38}$$
$$\alpha_1 \sim \alpha_2 \sim m^2 :$$
$$\mathrm{d}\Phi_{\theta\theta\bar{\theta}} \to \frac{1}{\mathcal{N}_\varepsilon} \mathrm{d}^d q [\mathrm{d}k_3] \delta\left(1 - \beta_q - \alpha_3\right) \theta\left(\beta_3 - \alpha_3\right) \mathrm{d}\Phi(q, k_1, k_2), \tag{7.39}$$

JHEP04(2025)084

where

$$\mathrm{d}\Phi(q,k_i,k_j) = \frac{1}{\mathcal{N}_\varepsilon^2}[\mathrm{d}k_i][\mathrm{d}k_j]\,\delta^{(d)}\,(q-k_{ij})\,. \tag{7.40}$$

Since integrations over two partons' momenta that add up to q correspond to standard phase-space integrals, it is useful to discuss how to simplify them. To study the most general form of such integrals, we consider the case with $q = k_1 + k_2$, and note that all other momenta assignments can be analyzed similarly. Hence, we consider the following family of integrals

$$J_{a_1\ldots a_6} = \frac{1}{\mathcal{N}_\varepsilon^2}\int \frac{[\mathrm{d}k_1][\mathrm{d}k_2]\delta^{(d)}(q-k_1-k_2)}{(k_1\cdot n)^{a_1}(k_2\cdot n)^{a_2}(k_1\cdot\bar{n})^{a_3}(k_2\cdot\bar{n})^{a_4}(k_1\cdot n+\beta_3)^{a_5}(k_2\cdot n+\beta_3)^{a_6}}\,. \tag{7.41}$$

One can use the integration-by-parts technology to reduce them to the minimal set of master integrals. This approach was employed in the previous (same-hemisphere) calculation as described in refs. [4, 5]. We have also used it in the current computation alongside with an alternative approach that we describe below.

Since the non-trivial part of the integral in eq. (7.41) is the integration over azimuthal angles, we start with discussing it. It is convenient to consider the reference frame where $q = (q_0, \vec{0})$, parametrize momenta of partons 1 and 2 using energies and angles, and integrate over energies removing the δ-functions. As we explain below, remaining integrals over angles can be related to cases familiar from earlier studies [139, 140].

Using energies and angles to parametrize light-like vectors, we write the required inverse propagators as follows

$$\begin{aligned} k_1\cdot n &= \frac{\beta_q}{2}\,(\rho_1\cdot\rho_n)\,, \quad & k_2\cdot n &= \frac{\beta_q}{2}\,(\rho_1\cdot\bar{\rho}_n)\,, \\ k_1\cdot\bar{n} &= \frac{\alpha_q}{2}\,(\rho_1\cdot\rho_{\bar{n}})\,, \quad & k_2\cdot\bar{n} &= \frac{\alpha_q}{2}\,(\rho_1\cdot\bar{\rho}_{\bar{n}})\,. \end{aligned} \tag{7.42}$$

In the above expressions, we introduced the light-like vectors $\rho_1 = (1,\vec{k}_1/|\vec{k}_1|)$, $\rho_n = (1,\vec{n}/|\vec{n}|)$, and $\rho_{\bar{n}} = \left(1,\vec{\bar{n}}/|\vec{\bar{n}}|\right)$, as well as conjugate vectors $\bar{\rho}_n$ and $\bar{\rho}_{\bar{n}}$ which are defined as parity-transformed versions of ρ_n and $\rho_{\bar{n}}$.

Inverse propagators that contain further Sudakov parameters in addition to scalar products shown in eq. (7.42) can be written as scalar products of a light-like vector and a time-like vector. To see this, we introduce two four-vectors $\rho_m = (1,\lambda\vec{n}/|\vec{n}|)$ and $\bar{\rho}_m = (1,-\lambda\vec{n}/|\vec{n}|)$, with

$$\lambda = \frac{\beta_q}{\beta_q+2\beta_3}, \tag{7.43}$$

and write

$$k_1\cdot n+\beta_3 = \left(\frac{\beta_q}{2}+\beta_3\right)(\rho_1\cdot\rho_m)\,, \quad k_2\cdot n+\beta_3 = \left(\frac{\beta_q}{2}+\beta_3\right)(\rho_1\cdot\bar{\rho}_m)\,. \tag{7.44}$$

The integral in eq. (7.41) can be written as follows

$$J_{a_1\ldots a_6} = \frac{1}{\mathcal{N}_\varepsilon^2}\frac{\Omega^{(d-1)}}{(8\pi^2)^{d-1}}\frac{(q^2)^{d/2-2}\,2^a}{\beta_q^{a_1+a_2}\alpha_q^{a_3+a_4}(\beta_q+2\beta_3)^{a_5+a_6}}\Omega^{(d-1)}_{a_1\ldots a_6}(\rho_n,\bar{\rho}_n,\rho_{\bar{n}},\bar{\rho}_{\bar{n}},\rho_m,\bar{\rho}_m)\,, \tag{7.45}$$

where $a = \sum_{i=1}^{6} a_i$ and the angular integral over directions of a light-like vector k with $k_0 = 1$ is defined by the following formula

$$\Omega^{(d-1)}_{a_1 \ldots a_n}[v_1, \ldots, v_n] = \frac{1}{\Omega^{(d-1)}} \int \frac{\mathrm{d}\Omega_k^{(d-1)}}{(k \cdot v_1)^{a_1} (k \cdot v_2)^{a_2} \ldots (k \cdot v_n)^{a_n}}. \tag{7.46}$$

General results for such integrals, alongside with many specific cases, are discussed in refs. [139–141].

For our purposes angular integrals can be further simplified using e.g. the relation between $k \cdot \rho$ and $k \cdot \bar{\rho}$ scalar products. The required partial fractioning rules can be found in appendix D. Once these relations are applied, the final set of Ω-integrals consists of integrals with at most two denominators. Such integrals have been computed in ref. [139] and we provide explicit expressions for them in appendix D. Furthermore, since angular integrals with arbitrary powers of the denominators are known in terms of hypergeometric functions, linear relations between integrals with different powers can easily be constructed [140], and used to simplify the resulting expressions without the need to express hypergeometric functions through elementary functions.

After the partial fractioning and the simplification of angular integrals, the original integral whose $(m^2)^{-2\varepsilon}$ branch defines the required boundary value is given by a linear combination of several simple integrals. Further integrations over components of the vector q can be often performed following the discussion of the nnn case in ref. [4]. However, new challenges arise for the $nn\bar{n}$ case, as we explain below.

The first point is that in the same-hemisphere configuration the zero-jettiness constraint $\delta(1-\beta_{123})$ implies that $\beta_3 = 1-\beta_{12} = 1-\beta_q$ and, therefore, entries in eq. (7.44) simplify. The second point is that in the same hemisphere configuration, integrals with three θ-functions do not appear as master integrals. For the choice of large Sudakov components that we discuss, this implies that not only β_3 but also α_3 is equal to $1 - \beta_q$. All in all, this implies that the integration over k_3 can be easily performed, and only the integration over q remains. For $nn\bar{n}$ integrals with three θ-functions — the examples of which are shown in eq. (7.39) — the required computation is more complex. Below we consider an example which illustrates how such integrals can be calculated.

We are interested in the $(m^2)^{-2\varepsilon}$ branch of the following integral

$$J = \int \frac{\mathrm{d}\Phi_{\theta\theta\bar{\theta}}}{(k_2 \cdot \bar{n})\,(k_{13} \cdot n)\,\left(k_{123}^2 + m^2\right)^2}. \tag{7.47}$$

The relevant contribution comes from the region $\alpha_1 \sim \alpha_2 \sim m^2$. The integration measure in this case is given by eq. (7.39). Simplifying the propagators in the limit $\alpha_{1,2} \sim m^2 \to \infty$, we obtain

$$J \sim \frac{1}{\mathcal{N}_\varepsilon^3} \int \mathrm{d}^d q [\mathrm{d}k_3] \frac{\delta(1-\beta_q-\alpha_3)\theta(\beta_3-\alpha_3)}{(q^2+\alpha_{12}\beta_3+m^2)^2} \int [\mathrm{d}k_1][\mathrm{d}k_2] \frac{\delta^{(d)}(q-k_{12})}{(k_2 \cdot \bar{n})(k_1 \cdot n+\beta_3)}. \tag{7.48}$$

Using eqs. (7.41), (7.45), (D.27), we write the integral over momenta $k_{1,2}$ as follows

$$J_{000110} = \frac{1}{\mathcal{N}_\varepsilon^2} \frac{\Omega^{(d-1)}}{(8\pi^2)^{d-1}} \frac{4\,(q^2)^{-\varepsilon}}{\alpha_q\,(\beta_q + 2\beta_3)} I^{(1)}_{d-1;1,1}\left(\bar{\rho}_{\bar{n}} \cdot \rho_m, \rho_m^2\right). \tag{7.49}$$

Scalar products that appear as arguments of the function $I^{(1)}_{d-1;1,1}$ are given by

$$\rho_{\bar{n}} \cdot \rho_m = 1 - \lambda(1-2u), \quad \rho_m^2 = 1 - \lambda^2, \tag{7.50}$$

where λ can be found in eq. (7.43) and u reads

$$u = \frac{q^2}{(q\cdot n)(q\cdot\bar{n})} = \frac{q^2}{\alpha_q\beta_q}. \tag{7.51}$$

Finally, using the expression for the angular integral in eq. (D.38) and applying the transformation of the Appell function shown in eq. (E.5), we obtain the following result for the angular integral

$$\begin{aligned} I^{(1)}_{d-1;1,1}\left(\bar{\rho}_{\bar{n}} \cdot \rho_m, \rho_m^2\right) = {} & \frac{(2\varepsilon-1)(\beta_q+2\beta_3)}{4\varepsilon(\beta_q+\beta_3)} \\ & \times F_1\left(1;1,-\varepsilon;1-2\varepsilon;\frac{q^2}{(\beta_3+\beta_q)\,\alpha_q},\frac{\beta_q}{\beta_3+\beta_q}\right), \end{aligned} \tag{7.52}$$

so that the complete integral over momenta k_1, k_2 becomes

$$J_{000110} = \frac{1}{\mathcal{N}_\varepsilon^2}\frac{\Omega^{(d-1)}}{(8\pi^2)^{d-1}}\frac{(2\varepsilon-1)\left(q^2\right)^{-\varepsilon}}{\varepsilon(\beta_q+\beta_3)\alpha_q}F_1\left(1;1,-\varepsilon;1-2\varepsilon;\frac{q^2}{(\beta_3+\beta_q)\,\alpha_q},\frac{\beta_q}{\beta_3+\beta_q}\right). \tag{7.53}$$

For the remaining integrations over q and k_3, we employ the Sudakov decomposition for both of these momenta. The integration measure reads

$$\frac{1}{\mathcal{N}_\varepsilon}\mathrm{d}^d q\,[\mathrm{d}k_3] = \frac{\Omega^{(d-2)}}{4}\frac{\mathrm{d}\alpha_3\mathrm{d}\beta_3\mathrm{d}\alpha_q\mathrm{d}\beta_q\mathrm{d}q_\perp^2}{\left(\alpha_3\beta_3 q_\perp^2\right)^\varepsilon}, \tag{7.54}$$

where we used the fact that the integrand is independent of the directions of $q_\perp^\mu$ and $k_{3,\perp}^\mu$. We then change the variable $\beta_3 = \alpha_3/r_3$ eliminating the Heaviside function $\theta(\beta_3-\alpha_3)$, and write $q^2 = \alpha_q\beta_q t, q_\perp^2 = \alpha_q\beta_q(1-t)$. We then find that the integral in eq. (7.48) becomes

$$\begin{aligned} J \sim {} & \frac{2\Gamma^2(1-\varepsilon)\Gamma(1+2\varepsilon)}{(m^2)^{1+2\varepsilon}}\int_0^1 \mathrm{d}\alpha_3\mathrm{d}\beta_q\delta(1-\alpha_3-\beta_q)(\alpha_3\beta_q)^{1-2\varepsilon} \\ & \times\int_0^1 \mathrm{d}t\mathrm{d}r_3\mathrm{d}w\frac{r_3^{-\varepsilon}(\alpha_3+\beta_q r_3)^{-\varepsilon}(\alpha_3+\beta_q r_3 t)^{-1+2\varepsilon}(1-w)^{-1-2\varepsilon}(\alpha_3+\beta_q r_3-\beta_q r_3 w)^\varepsilon}{(\alpha_3+\beta_q r_3-\beta_q r_3 t w)(1-t)^\varepsilon t^\varepsilon}, \end{aligned} \tag{7.55}$$

where we integrated over α_q and introduced the integral representation for the Appell function, cf. eq. (E.9), using an auxiliary variable w. Next, we remove the δ-function integrating over α_3, and change the variable $\beta_q = y/(r_3+y-r_3 y)$. Integration over r_3 can be expressed through the hypergeometric function ${}_2F_1$, cf. eq. (E.7). Applying the transformation in eq. (E.3), we find

$$\begin{aligned} J \sim {} & \frac{2\Gamma^2(1-\varepsilon)\Gamma(1+2\varepsilon)}{(m^2)^{1+2\varepsilon}(1-\varepsilon)}\int_0^1 \mathrm{d}w\mathrm{d}y\frac{(1-y)^{1-2\varepsilon}{}_2F_1\left(1-\varepsilon,\varepsilon;2-\varepsilon;1-y\right)}{y^\varepsilon(1-w)^{1+2\varepsilon}(1-wy)^{-\varepsilon}} \\ & \times\int_0^1 \mathrm{d}t\,\frac{(1-t)^{-\varepsilon}t^{-\varepsilon}}{(1-wty)(1-y(1-t))^{1-2\varepsilon}}. \end{aligned} \tag{7.56}$$

The integral over t can be expressed through the first Appell function (E.9), which reduces to the ${}_2F_1$ function thanks to eq. (E.6). Using the transformation eq. (E.3), we derive the two-dimensional integral representation for the $(m^2)^{-2\varepsilon}$ branch of J

$$\begin{aligned} J \sim &\frac{2\Gamma^4(1-\varepsilon)\Gamma(1+2\varepsilon)}{(m^2)^{1+2\varepsilon}(1-\varepsilon)\Gamma(2-2\varepsilon)} \int_0^1 \mathrm{d}w\mathrm{d}y \frac{(y(1-y))^{1-2\varepsilon}}{(1-w)^{1+2\varepsilon}} \\ &\times {}_2F_1\left(1,2-2\varepsilon;2-\varepsilon;1-y\right) {}_2F_1\left(1-2\varepsilon,1-\varepsilon;2-2\varepsilon;y(1+w(1-y))\right). \end{aligned} \tag{7.57}$$

The only divergence of the integral occurs at the point $w \to 1$, which can be easily subtracted. The subtracted integral is finite, can be expanded in ε under the integral sign and integrated using `HyperInt` [138]. The final result reads

$$\begin{aligned} J \sim &-\frac{\pi^2}{12\varepsilon} - \left(\frac{\pi^2}{6} + \frac{\log(2)\pi^2}{4} + \frac{7}{8}\zeta_3\right) \\ &-\varepsilon\left(\frac{\pi^2}{3} + \frac{\pi^2}{2}\log(2) + \frac{7}{4}\zeta_3 - \frac{3}{8}\log(2)^4 + \frac{\pi^2}{2}\log(2)^2 + \frac{17}{160}\pi^4 - 9\mathrm{Li}_4(1/2)\right) \\ &-\varepsilon^2\left(\frac{2}{3}\pi^2 + \log(2)\pi^2 + \frac{7}{2}\zeta_3 + \frac{17}{80}\pi^4 + \pi^2\log^2(2) - \frac{3}{4}\log^4(2) - 18\mathrm{Li}_4(1/2)\right. \\ &\left.+\frac{211}{480}\pi^4\log(2) + \frac{\pi^2}{6}\log^3(2) - \frac{3}{40}\log^5(2) - \frac{43}{96}\pi^2\zeta_3 - \frac{1023}{64}\zeta_5 + 9\mathrm{Li}_5(1/2)\right) \\ &-\varepsilon^3\left(\frac{4}{3}\pi^2 + 2\pi^2\log(2) + 7\zeta_3 + \frac{17}{40}\pi^4 - \frac{3}{2}\log^4(2) + 2\pi^2\log^2(2) - 36\mathrm{Li}_4(1/2)\right. \\ &-\frac{3}{20}\log^5(2) + \frac{1}{3}\pi^2\log^3(2) + \frac{211}{240}\pi^4\log(2) - \frac{1023}{32}\zeta_5 - \frac{43}{48}\pi^2\zeta_3 + 18\mathrm{Li}_5(1/2) \\ &+\frac{221}{960}\pi^4\log^2(2) - \pi^2\zeta_3\log(2) - \frac{375}{16}\zeta_3^2 + \frac{121}{2016}\pi^6 - \frac{1}{80}\log^6(2) + \frac{1}{32}\pi^2\log^4(2) \\ &\left.-\frac{1}{4}\pi^2\mathrm{Li}_4(1/2) + \frac{159}{4}\zeta_{-5,-1} - 9\mathrm{Li}_6(1/2)\right) + \mathcal{O}(\varepsilon^4). \end{aligned} \tag{7.58}$$

The $(m^2)^{-2\varepsilon}$ branch in all integrals can be calculated once a pair of large parameters is identified, the expansion of denominators is performed according to table 4, angular integrals as in eq. (7.45) introduced and computed, and subsequent integrations over q and the remaining Sudakov parameters are performed.

8 Numerical checks

Calculation of the soft function requires computing a large number of complicated unconventional integrals. Because of this, checking them using alternative methods is critical. Techniques that are usually employed for this purpose include the sector-decomposition [142] and Mellin-Barnes methods [143, 144]. In our case, however, the complex structure of divergencies of the relevant integrals, as well as high perturbative order, makes direct application of public codes based on these methods unfeasible. Hence, care is required to organize the numerical checks to make them manageable. Below we discuss how this can be achieved.

All integrals that we computed numerically can be split into three groups. First, there are integrals without propagators that involve scalar products of soft-parton momenta; such integrals are calculated using the standard sector decomposition approach. Second, there are master integrals with complicated propagators that can be efficiently dealt with using the Mellin-Barnes method. The third group includes integrals that depend on $1/k_{123}^2$ and they pose the biggest challenge. The problem is to find a suitable parametrization that minimizes the number of sectors that appear, if overlapping singularities are treated using the sector decomposition method, or a suitable compact representation if the Mellin-Barnes technology is employed.

All integrals that we may want to check numerically can be written as follows

$$\mathcal{I}[\{f_1,f_2,f_3\},\{a_1\ldots a_7\},\{b_1\ldots b_7\},\{c_1\ldots c_4\}]=\int \frac{\mathrm{d}\Phi_{f_1f_2f_3}}{A_1^{a_1}\ldots A_7^{a_7}B_1^{b_1}\ldots B_7^{b_7}C_1^{c_1}\ldots C_4^{c_4}}, \tag{8.1}$$

where the integration measure is determined by the vector $\{f_1, f_2, f_3\}$

$$\mathrm{d}\Phi_{f_1f_2f_3}=\frac{1}{\mathcal{N}_\varepsilon^3}[\mathrm{d}k_1][\mathrm{d}k_2][\mathrm{d}k_3]f_1(\bar{\gamma}_1-\gamma_1)f_2(\bar{\gamma}_2-\gamma_2)f_3(\bar{\gamma}_3-\gamma_3)\delta(1-\gamma_1-\gamma_2-\gamma_3), \tag{8.2}$$

with $\gamma_i = \beta_i, \bar{\gamma}_i = \alpha_i$ for $f_i = \delta, \theta$ and $\gamma_i = \alpha_i, \bar{\gamma}_i = \beta_i$ for $f_i = \bar{\theta}$. We have split all appearing propagators into three groups. Propagators in the first group involve vector n

$$\begin{aligned}
&A_1 = k_1\cdot n, \quad A_2 = k_2\cdot n, \quad A_3 = k_3\cdot n,\\
&A_4 = k_{12}\cdot n, \quad A_5 = k_{23}\cdot n, \quad A_6 = k_{31}\cdot n, \quad A_7 = k_{123}\cdot n.
\end{aligned} \tag{8.3}$$

The second group contains propagators that depend on vector $\bar{n}$

$$\begin{aligned}
&B_1 = k_1\cdot \bar{n}, \quad B_2 = k_2\cdot \bar{n}, \quad B_3 = k_3\cdot \bar{n},\\
&B_4 = k_{12}\cdot \bar{n}, \quad B_5 = k_{23}\cdot \bar{n}, \quad B_6 = k_{31}\cdot \bar{n}, \quad B_7 = k_{123}\cdot \bar{n}.
\end{aligned} \tag{8.4}$$

The last group contains propagators that depend on the scalar products of soft momenta

$$C_1 = k_1\cdot k_2, \quad C_2 = k_2\cdot k_3, \quad C_3 = k_1\cdot k_3, \quad C_4 = k_{123}^2. \tag{8.5}$$

8.1 Integrals without the $1/k_{123}^2$ propagator

We will discuss first the numerical computation of integrals in eq. (8.1) with $c_3 = c_4 = 0$. This assignment covers all integrals in the soft function that do not contain the propagator $1/k_{123}^2$. To derive a suitable representation for such integrals, we change integration variables $\bar{\gamma}_i = \gamma_i/s_i^2$, $0 < s_i < 1$, to resolve all θ-functions' constraints.[16] Two inverse denominators that involve scalar products between momenta of soft partons read

$$f_i = \theta, f_j = \theta: \qquad k_{ij}^2 = \frac{\gamma_i\gamma_j}{s_i^2 s_j^2}\left((s_i - s_j)^2 + 4s_i s_j \frac{t_{ij}^2}{t_{ij}^2 + \bar{t}_{ij}^2}\right), \tag{8.6}$$

$$f_i = \theta, f_j = \bar{\theta}: \qquad k_{ij}^2 = \frac{\gamma_i\gamma_j}{s_i^2 s_j^2}\left((1 - s_i s_j)^2 + 4s_i s_j \frac{t_{ij}^2}{t_{ij}^2 + \bar{t}_{ij}^2}\right), \tag{8.7}$$

[16] The same variable transformations can be applied to integrals with δ-function constraints. We explain below how the corresponding integral representations can be constructed.

where we introduce angle variables $t_{ij}^2/(t_{ij}^2 + \bar{t}_{ij}^2) = \sin^2(\phi_{ij}/2) \in [0,1]$ and the notation $\bar{x} = 1 - x$ for all variables $0 < x < 1$ appearing in this section. To satisfy the δ-function constraint $\delta(1 - \gamma_1 - \gamma_2 - \gamma_3)$ we apply the variable transformation

$$\{\gamma_{\sigma(1)}, \gamma_{\sigma(2)}, \gamma_{\sigma(3)}\} \to \{x, y\bar{x}, \bar{y}\bar{x}\}, \tag{8.8}$$

where σ is a permutation of the set $\{1,2,3\}$. Different permutations of the set $\{\gamma_1, \gamma_2, \gamma_3\}$ lead to different integrand expressions, which, after the integration, should give identical results, providing useful internal consistency checks of the numerical calculation.

Combining the Jacobians of all transformations described above, we obtain the following expression for the integration measure, where integrations on the right-hand side are confined to a unit hypercube

$$\begin{aligned} \mathrm{d}\Phi_{f_1 f_2 f_3} = \mathrm{d}x \mathrm{d}y \prod_{i=1}^{3} \frac{2\gamma_i \mathrm{d}s_i}{s_i^3} \times \bar{x} \left(\frac{s_1 s_2 s_3}{x y \bar{y} \bar{x}^2}\right)^{2\varepsilon} \\ \times \frac{\Omega^{(d-3)}}{\Omega^{(d-2)}} \frac{\mathrm{d}t_{12}}{(t_{12}\bar{t}_{12})^{2\varepsilon}} \left(\frac{2}{t_{12}^2 + \bar{t}_{12}^2}\right)^{1-2\varepsilon} \frac{\Omega^{(d-3)}}{\Omega^{(d-2)}} \frac{\mathrm{d}t_{23}}{(t_{23}\bar{t}_{23})^{2\varepsilon}} \left(\frac{2}{t_{23}^2 + \bar{t}_{23}^2}\right)^{1-2\varepsilon}. \end{aligned} \tag{8.9}$$

For each constraint $f_i = \theta$ or $f_i = \bar{\theta}$ we replace γ_i according to eq. (8.8) choosing a particular permutation σ, and for each $f_i = \delta$ we set $s_i = 1$ and drop the integration over s_i by setting $\gamma_i \mathrm{d}s_i \to 1$ in eq. (8.9). The propagators $1/A_i$ and $1/B_i$, $i = 1, \ldots, 7$, are expressed in terms of x, y, s_i following the variable change specified by eq. (8.8). The two propagators $1/C_{1,2}$ are written as in eqs. (8.6), (8.7) depending on the relevant constraints. If $f_i = \delta$, the two expressions become equal once $s_i = 1$ is employed.

Using the measure in eq. (8.9) we can, in principle, compute integrals defined in eq. (8.1) without the propagator $1/C_4$, using public codes `FIESTA` [145] or `pySecDec` [142], which implement the sector decomposition approach. However, since the inverse propagator eq. (8.6) has a (line) singularity inside the integration region at $s_i = s_j$, and since such singularities are not automatically found by any of the public codes, we need to consider the cases $s_i < s_j$ and $s_j < s_i$ separately. If we do this, all singularities appear at the boundary of the integration domain, and such cases *are* processed automatically by `FIESTA` [145] and `pySecDec` [142]. Nevertheless, since integrals that we consider are multidimensional, it turns out to be beneficial to analyze the existence of potential singularities at the upper integration boundaries *manually*, avoiding the automatic option for doing that in public codes. We have mostly used `FIESTA` [145] to compute integrals with the analytic regulator and we emphasize that the introduction of the analytic regulator $\mathrm{d}\Phi \to \mathrm{d}\Phi\,(\gamma_1\gamma_2\gamma_3)^{\nu}$ does not impact our discussion. Using these methods, we have checked numerically both regular integrals calculated in section 5.1 and also the $1/\nu$ divergent parts of integrals $I_2^{1/\nu}$ and $I_4^{1/\nu}$ considered in section 5.2.

8.2 Calculation of integrals with $1/k_{123}^2$ using the Mellin-Barnes representation

It turns out to be very difficult to perform numerical checks for integrals with the propagator $1/k_{123}^2$ using the sector decomposition approach because suitable parametrization of angular variables is hard to find. We avoid this by constructing Mellin-Barnes representations for such integrals and using them for the numerical evaluation.

Since the dependence on the momenta directions in the transverse space in such integrals comes only from propagators which contain scalar products of soft momenta, we focus on this part first. The most general form of the considered integral reads

$$\int [\mathrm{d}k_1][\mathrm{d}k_2][\mathrm{d}k_3] \frac{R(\{k_i\cdot n\},\{k_i\cdot\bar{n}\})}{(k_1\cdot k_2)^{a_{12}}(k_2\cdot k_3)^{a_{23}}(k_3\cdot k_1)^{a_{31}}(k_1\cdot k_2+k_2\cdot k_3+k_3\cdot k_1)^{a_{123}}}, \tag{8.10}$$

where the rational function R contains propagators $1/A_{1,\dots,7}$ and $1/B_{1,\dots,7}$, cf. eqs. (8.3), (8.4). We focus on the case $a_{123} > 0$ and, as the first step, we split the $1/k_{123}^2$ propagator using the Mellin-Barnes representation

$$\frac{1}{(k_1\cdot k_2+k_2\cdot k_3+k_3\cdot k_1)^{\lambda}} = \frac{1}{\Gamma(\lambda)} \int\limits_{c-i\infty}^{c+i\infty} \frac{\mathrm{d}z_1\mathrm{d}z_2}{(2\pi i)^2} \frac{\Gamma(\lambda+z_{12})\Gamma(-z_1)\Gamma(-z_2)}{(k_1\cdot k_2)^{z_{12}+\lambda}(k_2\cdot k_3)^{-z_1}(k_3\cdot k_1)^{-z_2}}, \tag{8.11}$$

where $z_{12} = z_1 + z_2$. After this transformation, integration over directions of soft momenta in the transverse space reduces to the calculation of the following integral

$$I(n_1, n_2, n_3) = \int \frac{\mathrm{d}\Omega_1^{(d-2)}\mathrm{d}\Omega_2^{(d-2)}\mathrm{d}\Omega_3^{(d-2)}}{(k_1\cdot k_2)^{n_1}(k_2\cdot k_3)^{n_2}(k_3\cdot k_1)^{n_3}}, \tag{8.12}$$

where powers $n_{1,2,3}$ are arbitrary.

To integrate over angles in the transverse space, it is useful to consider auxiliary $(d-1)$-dimensional (Minkowski) vectors, which contain $(d-2)$-dimensional transverse momenta. We write

$$\rho_i = \left(1, \frac{\vec{k}_{i,\perp}}{|\vec{k}_{i,\perp}|}\right), \quad \rho_i\cdot\rho_j = 1 - \frac{\vec{k}_{i,\perp}\cdot\vec{k}_{j,\perp}}{|\vec{k}_{i,\perp}||\vec{k}_{j,\perp}|}, \quad \rho_i^2 = 0. \tag{8.13}$$

The scalar products in eq. (8.12) take the form

$$(k_i\cdot k_j) = \frac{\left(\sqrt{\alpha_i\beta_j} - \sqrt{\alpha_j\beta_i}\right)^2}{2} + \sqrt{\alpha_i\beta_i\alpha_j\beta_j}(\rho_i\cdot\rho_j). \tag{8.14}$$

If $f_i = f_j = \delta$, the first term in the above equation vanishes. However, in general this does not happen, and we need to split the scalar product further. We write

$$\frac{1}{(k_i\cdot k_j)^{\lambda}} = \frac{1}{\Gamma(\lambda)} \int\limits_{c-i\infty}^{c+i\infty} \frac{\mathrm{d}z}{2\pi i}\Gamma(-z)\Gamma(\lambda+z) \frac{2^{-z}\left(\sqrt{\alpha_i\beta_j} - \sqrt{\alpha_j\beta_i}\right)^{2z}}{(\alpha_i\beta_i\alpha_j\beta_j)^{z/2+\lambda/2}} \frac{1}{(\rho_i\cdot\rho_j)^{z+\lambda}}. \tag{8.15}$$

Hence, to proceed further, we require the following integral

$$J(w_1, w_2, w_3) = \left(\frac{1}{\Omega^{(d-2)}}\right)^3 \int \frac{\mathrm{d}\Omega_1^{(d-2)}\mathrm{d}\Omega_2^{(d-2)}\mathrm{d}\Omega_3^{(d-2)}}{(\rho_1\cdot\rho_2)^{w_1}(\rho_2\cdot\rho_3)^{w_2}(\rho_3\cdot\rho_1)^{w_3}}, \tag{8.16}$$

for arbitrary values of $w_{1,2,3}$. Since, to the best of our knowledge, such integral is not available in the literature, we briefly explain how to compute it. First, we apply eq. (D.37) to integrate over ρ_3. The hypergeometric function that appears in that equation depends on $1 - \rho_1\cdot\rho_2/2$ and obeys the standard series representation $\sum\limits_{n=0}^{\infty} c_n\,(1-(\rho_1\cdot\rho_2)/2)^n$. Writing

$$\sum_{n=0}^{\infty} c_n\,(1-(\rho_1\cdot\rho_2)/2)^n = \sum_{n=0}^{\infty} c_n \sum_{k=0}^{\infty} \frac{\Gamma(k-n)}{\Gamma(-n)k!}\left(\frac{\rho_1\cdot\rho_2}{2}\right)^k, \tag{8.17}$$

we can integrate over directions of ρ_2 using eq. (D.35). Finally, we sum over k and n using the definition of a hypergeometric function, and simplify the result to Γ-functions since after each summation, the obtained hypergeometric function is evaluated at one. We find

$$J(w_1, w_2, w_3) = \frac{\Gamma^3(1-\varepsilon)\Gamma\left(1-2\varepsilon-w_{123}\right)}{\pi^{3/2}2^{6\varepsilon+w_{123}}\Gamma(1-2\varepsilon)} \frac{\prod_{i=1}^{3}\Gamma\left(\frac{1}{2}-\varepsilon-w_i\right)}{\prod_{i=1}^{3}\prod_{j=1}^{i-1}\Gamma\left(1-2\varepsilon-w_{ij}\right)}, \tag{8.18}$$

where $w_{ij} = w_i + w_j$ and $w_{123} = w_1 + w_2 + w_3$. The integral $J(w_1, w_2, w_3)$ is a symmetric function of its arguments; it is normalized to give $J(0, 0, 0) = 1$ and it reduces to known expressions when any of its arguments vanishes.

The Mellin-Barnes representation that we derived so far is five-dimensional since we required two integrations for $1/k_{123}^2$ and then one for each of the three terms $1/k_ik_j$.[17] For each constraint $f_i = \theta$ or $f_i = \bar{\theta}$, we change the large variable $\bar{\gamma}_i = \gamma_i/s_i^2$ and obtain

$$\int_0^\infty \mathrm{d}\bar{\gamma}_i\, \delta(1-\gamma_i-\cdots)\theta(\bar{\gamma}_i-\gamma_i)f(\bar{\gamma}_i) = \int_0^1 ds_i \left(\frac{2\gamma_i}{s_i^3}\right)\delta(1-\gamma_i-\cdots)f\left(\frac{\gamma_i}{s_i^2}\right). \tag{8.19}$$

To resolve the δ-function constraint, we apply a variable transformation from eq. (8.8) choosing a particular permutation. We find

$$\int_0^1 \mathrm{d}\gamma_1\mathrm{d}\gamma_2\mathrm{d}\gamma_3\delta(1-\gamma_1-\gamma_2-\gamma_3)f(\gamma_1,\gamma_2,\gamma_3) = \int_0^1 \mathrm{d}x\mathrm{d}y\,\bar{x}f(x, y\bar{x}, \bar{x}\bar{y}). \tag{8.20}$$

It remains to convert the remaining part of the integral into a Mellin-Barnes representation suitable for numerical integration. To do that, we enable integrations over x, y and s_i by introducing additional Mellin-Barnes integrations to convert sums of these variables, that may appear in the inverse propagators from groups A and B, into variables' products. From eq. (8.14) one notices that for the nnn case, i.e. when $f_i = f_j = \theta$, the representation of $k_i \cdot k_j$ leads to the factor $(s_i - s_j)^p$. We would like to avoid such quantities since, after the application of the Mellin-Barnes splitting formula, they produce a factor $(-1)^z$ which conflicts with the z-integration contour that runs to complex infinity. The solution is to split the integral into two parts where $s_i < s_j$ and $s_i > s_j$.

The remaining integral consists of polynomial factors in variables $x, y, s_1 \ldots s_n$ raised to some powers. We change the integration variables $v_i \to u_i/(1+u_i)$ for all $v_i \in \{x, y, s_1 \ldots s_n\}$, mapping all $[0, 1]$ integration intervals to $[0, \infty)$ intervals. Integrals that we are left with have the following generic representation

$$\int_0^\infty \prod_{i=1}^{n+2}\mathrm{d}u_i \prod_{j=0}^{m} P_j(\vec{u})^{w_j}, \tag{8.21}$$

where $P_j(\vec{u})$ are polynomials of variables $u_1, u_2, \ldots, u_n$. For such integrals, the Mellin-Barnes representations with the minimal number of integrations can be constructed using the package `MBcreate` [144]. This package employs the recursive splitting of polynomials P_j into two parts by introducing a single Mellin-Barnes integration at each step, until all u_i-integrations

[17] If some of the constraints are δ-functions, the number of Mellin-Barnes integrations is smaller.

can be performed using the following formula

$$\int_0^\infty \mathrm{d}u\, u^p (au+b)^q = \frac{\Gamma(p+1)\Gamma(-p-q-1)}{\Gamma(-q)} a^{-p-1} b^{p+q+1}. \tag{8.22}$$

We have found that for successful application of the package `MBcreate` to integrals of interest, we need to extend it by an additional (simple) integration rule

$$\int_0^\infty \mathrm{d}u \frac{u^p(1+u)^q}{((1+u)^2+u^2)^r} = \int_{c-i\infty}^{c+i\infty} \frac{\mathrm{d}z}{2\pi i} \frac{\Gamma(z+r)\Gamma(-z)\Gamma(1+p+2z)\Gamma(2r-p-q-1)}{\Gamma(r)\Gamma(2z+2r-q)}. \tag{8.23}$$

In practice, we use `MBcreate` [144] to construct the representation for all possible permutations σ corresponding to different ways of resolving the δ-function constraints in eq. (8.20), and select one with the minimal number of MB integrations.

The above steps are sufficient to derive the minimal Mellin-Barnes representations for all required integrals. We note that we work with analytically regularized integrals which allows us to check that our master integrals are regulated dimensionally. To find suitable integration contours and to perform analytic continuation of Mellin-Barnes representations, we use the package `MBresolve` [146], which is applicable also when the analytic regulator is present. Furthermore, we find it useful to introduce additional parameter to the angular integral in eq. (8.18) which ensures that all poles of the Mellin-Barnes representation are separated. We do this by shifting all arguments in $J(w_1, w_2, w_3)$ by an infinitesimal positive-definite quantity, which we take to be equal to the analytic regulator. Integrals, analytically continued and expanded in all small parameters, are integrated numerically using the package `MB` [143].[18]

We will illustrate this discussion by describing numerical computation of the integral

$$J = \int \frac{\mathrm{d}\Phi_{\delta\theta\bar{\theta}}}{(k_2\cdot k_3)\ \ (k_{123}^2)\,(k_3\cdot\bar{n})\,(k_{123}\cdot\bar{n})}. \tag{8.24}$$

As the first step, we introduce the factor $\beta_1^\nu \beta_2^\nu \alpha_3^\nu (\rho_1\cdot\rho_2)^{-\nu}(\rho_1\cdot\rho_3)^{-\nu}(\rho_2\cdot\rho_3)^{-\nu}$, $\nu\to 0^+$, into the integrand to achieve the pole separation in the Mellin-Barnes integral. Then, following the steps outlined in this section we obtain the Mellin-Barnes representation

$$J = \int_{c-i\infty}^{c+i\infty} \left(\prod_{n=1}^{10} \frac{\mathrm{d}z_n}{2\pi i}\right) \left(J_a(\vec{z}) + J_b(\vec{z})\right), \tag{8.25}$$

where

$$\begin{aligned} J_a = 2^{3\nu-4\varepsilon-2z_3-2z_4-2z_5} & \frac{\Gamma(1-\varepsilon)^2\Gamma(-z_{10})\Gamma(-z_3)\Gamma(-z_4)\Gamma(-z_5)\Gamma(-z_6)\Gamma(z_6+1)}{\pi\Gamma\left(\frac{1}{2}-\varepsilon\right)\Gamma(-2z_4)\Gamma(3\nu-6\varepsilon)\Gamma(z_1+z_2+2)\Gamma(-2z_5-z_7)} \\ \times & \frac{\Gamma(-z_7)\Gamma(-z_8)\Gamma(z_8+1)\Gamma(z_1+z_2+1)\Gamma(z_3-z_1)\Gamma(z_5-z_2)\Gamma(z_7-2z_4)}{\Gamma(2\nu-2\varepsilon-z_1-z_4-z_5-1)\Gamma(2\nu-2\varepsilon-z_2-z_3-z_4-1)} \\ \times & \frac{\Gamma(3\nu-6\varepsilon+z_9)\Gamma(z_1+z_2+z_4+2)\Gamma(2z_3+2z_4-z_7+1)}{\Gamma(2\varepsilon-2z_{10}+z_2+z_3+z_4+1)\Gamma(2\nu-2\varepsilon+z_1+z_2-z_3-z_5+1)} \end{aligned}$$

[18] We have modified the `MB` package in such a way that a `C` code suitable for numerical integration is generated. The modified package can be downloaded from https://github.com/apik/mbc.

$$\times \frac{\Gamma\left(\nu-\varepsilon+z_1-z_3+\frac{1}{2}\right)\Gamma(\nu-2\varepsilon+z_{10}-z_2)\Gamma\left(\nu-\varepsilon+z_2-z_5+\frac{1}{2}\right)}{\Gamma(2\varepsilon+z_1-z_4+z_5-2z_6+z_7+1)}$$
$$\times \frac{\Gamma\left(\nu-\varepsilon-z_1-z_2-z_4-\frac{3}{2}\right)\Gamma(-2\nu+4\varepsilon-z_1+z_6-z_9)}{\Gamma(4\nu-4\varepsilon+z_1-z_4+z_5-2z_6+z_7+z_8+2z_9+2)}$$
$$\times \Gamma(3\nu-2\varepsilon-z_3-z_4-z_5-1)\Gamma(2\nu-4\varepsilon+z_1+z_{10}-z_6+z_9+1)$$
$$\times \Gamma(2\varepsilon-2z_{10}+z_2-z_3-z_4+z_7)\Gamma(4\nu-4\varepsilon+z_1-z_4-z_5-2z_6+2z_9)$$
$$\times \Gamma(2\varepsilon+z_1-z_4+z_5-2z_6+z_7+z_8+1)\Gamma(-2z_5-z_7-z_8-1)$$
$$\times \Gamma(-\nu+2\varepsilon-z_{10}+z_2-z_9)\Gamma(2z_5+z_7+z_8+2), \tag{8.26}$$

$$J_b = 2^{3\nu-4\varepsilon-2z_3-2z_4-2z_5}\frac{\Gamma(1-\varepsilon)^2\Gamma(-z_{10})\Gamma(-z_3)\Gamma(-z_4)\Gamma(-z_5)\Gamma(-z_6)\Gamma(z_6+1)}{\pi\Gamma\left(\frac{1}{2}-\varepsilon\right)\Gamma(-2z_5)\Gamma(3\nu-6\varepsilon)\Gamma(z_1+z_2+2)}$$
$$\times \frac{\Gamma(-z_7)\Gamma(-z_8)\Gamma(z_8+1)\Gamma(z_1+z_2+1)\Gamma(z_3-z_1)\Gamma(z_5-z_2)\Gamma(z_7-2z_5)}{\Gamma(-2z_4-z_7)\Gamma(2\nu-2\varepsilon-z_1-z_4-z_5-1)\Gamma(2\nu-2\varepsilon-z_2-z_3-z_4-1)}$$
$$\times \frac{\Gamma(z_1+z_2+z_4+2)\Gamma(2z_3+2z_5-z_7+1)\Gamma(-2z_4-z_7-z_8-1)}{\Gamma(2\nu-2\varepsilon+z_1+z_2-z_3-z_5+1)\Gamma(2\varepsilon+z_1+z_4-z_5+2z_6+z_7+3)}$$
$$\times \frac{\Gamma\left(\nu-\varepsilon+z_1-z_3+\frac{1}{2}\right)\Gamma\left(\nu-\varepsilon+z_2-z_5+\frac{1}{2}\right)}{\Gamma(4\varepsilon-z_1+2z_{10}+z_4-z_5+z_7+z_8+2)}$$
$$\times \frac{\Gamma\left(\nu-\varepsilon-z_1-z_2-z_4-\frac{3}{2}\right)\Gamma(3\nu-2\varepsilon-z_3-z_4-z_5-1)}{\Gamma(-4\nu+10\varepsilon+z_1+z_2+z_3+z_5+2z_6-2z_9+3)}$$
$$\times \Gamma(-\nu+2\varepsilon+z_1-z_{10}+z_6-z_9+1)\Gamma(-2\nu+4\varepsilon+z_1+z_2+z_6-z_9+2)$$
$$\times \Gamma(2\nu-4\varepsilon-z_1+z_{10}-z_2-z_6+z_9-1)\Gamma(2z_4+z_7+z_8+2)$$
$$\times \Gamma(-4\nu+10\varepsilon+z_1+z_2-z_3-z_5+2z_6+z_7-2z_9+2)\Gamma(3\nu-6\varepsilon+z_9)$$
$$\times \Gamma(2\varepsilon+z_1+z_4-z_5+2z_6+z_7+z_8+3)\Gamma(4\varepsilon-z_1+2z_{10}-z_4-z_5)$$
$$\times \Gamma(\nu-2\varepsilon-z_1+z_{10}-z_6-1). \tag{8.27}$$

We use the MB package to expand the above integrand in the parameters ν and ε, and take the limit $\nu \to 0^+$, $\varepsilon \to 0$ afterwards. Integrating over Mellin-Barnes parameters, the following numerical result is obtained

$$J_{\rm MB} = \frac{0.104167}{\varepsilon^4} + \frac{0.25}{\varepsilon^3} + \frac{1.7820119(14)}{\varepsilon^2} - \frac{2.077362(8)}{\varepsilon}$$
$$- 100.8647(18) - 1049.07(4)\varepsilon - 8238(2)\varepsilon^2. \tag{8.28}$$

Upon computing the same integral by solving the differential equations in the auxiliary parameter, as described in section 6, we find

$$J_{\rm DE} = \frac{0.104167}{\varepsilon^4} + \frac{0.250000}{\varepsilon^3} + \frac{1.78201}{\varepsilon^2} - \frac{2.07736}{\varepsilon}$$
$$- 100.863 - 1048.99\varepsilon - 8238.03\varepsilon^2. \tag{8.29}$$

The two results are in very good agreement with each other and, in fact, this level of agreement is typical for the many comparisons that we performed.

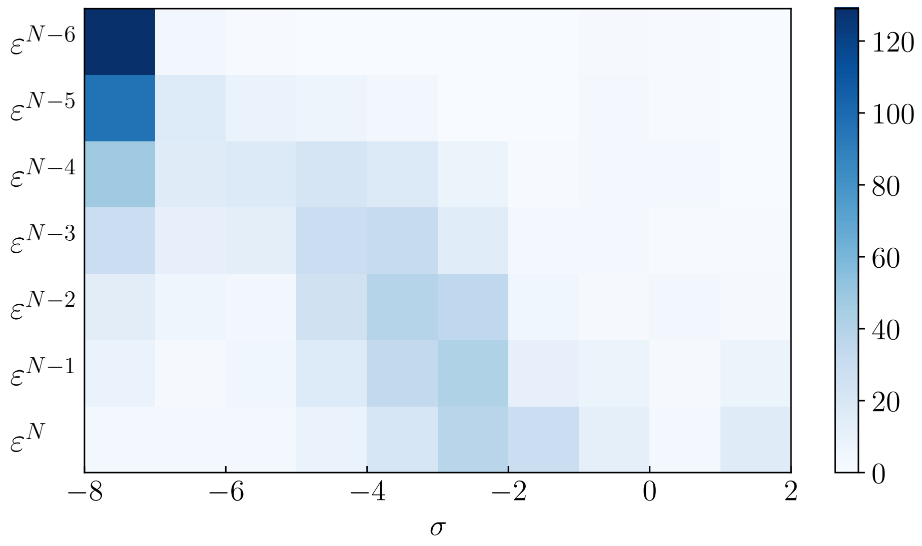

Figure 4. Number of master integrals with propagator $1/k_{123}^2$ that have specific relative errors as defined in eq. (8.30), calculated for each order in ε. Here ε^N denotes the highest order in ε required for each individual integral in the final expression of the soft function.

Out of 139 master integrals with the $1/k_{123}^2$ propagator 107 are checked through all required orders in ε with at most a 5% deviation for the central value. For the remaining 32 integrals the precision rapidly deteriorates once we move to higher terms in the ε expansion. The total number of evaluations used to obtain the value of a particular integral by means of Monte-Carlo integration varies greatly from integral to integral leading to vastly different runtimes needed for obtaining accurate numerical results.

The numerical results are summarized in the density plot figure 4 where the relative error

$$\sigma = \log_{10}\left|\frac{J_{\rm DE} - J_{\rm MB}}{J_{\rm DE}}\right|, \tag{8.30}$$

is calculated for each order in the ε-expansion. We note that results for all integrals expanded through all but the very last order in the ε-expansion are indirectly checked by our ability to reproduce divergencies of the soft function. On the other hand, we do not see anything particular when moving from the ε^{N-1}-row to the ε^N-row in figure 4 strongly suggesting that standard deterioration of the numerical precision occurs for higher orders in the expansion when the Mellin-Barnes method is employed.

8.3 Numerical checks at finite m^2

Determination of complicated integrals from the differential equations at finite m^2, as discussed in section 6, is a critical element of our approach to compute the zero-jettiness soft function. Hence, high-quality numerical checks of integrals at finite m^2 are very much needed. Among other things, they give us confidence in the correctness of the filtered system of differential equations and of the boundary conditions at $m^2 = \infty$. The goal of this section is to discuss how such checks are performed.

JHEP04(2025)084

We note that integrals where a mass-like parameter is introduced into a propagator $1/k_{123}^2$ are less divergent than the original ones, since m^2 acts as an infra-red regulator. It is possible to construct the Mellin-Barnes representations for such integrals, following the discussion in the previous section. However, quite often, this does not allow high-precision evaluation of sufficiently many terms in the ε-expansion, because such representations contain one additional Mellin-Barnes integration in comparison to the $m^2 = 0$ case. Because of this, we look for a way to perform such checks for numerous m^2-dependent integrals, using the sector decomposition methods. The idea is to numerically compute many *nearly-finite* integrals, for which the proliferation of sectors can be avoided, and then use the integration-by-parts reduction to relate them to the master integrals that we actually employ and would like to check.

To explain how this works, we introduce three angles between vectors $k_{1,2,3}$ in the $(d-2)$-dimensional transverse space. The scalar products read

$$\begin{aligned}
(k_1 \cdot k_2) &= \frac{\left(\sqrt{\alpha_1\beta_2} - \sqrt{\alpha_2\beta_1}\right)^2}{2} + \sqrt{\alpha_1\beta_1\alpha_2\beta_2}\,(1-\cos\theta_{12})\,,\\
(k_2 \cdot k_3) &= \frac{\left(\sqrt{\alpha_2\beta_3} - \sqrt{\alpha_3\beta_2}\right)^2}{2} + \sqrt{\alpha_2\beta_2\alpha_3\beta_3}\,(1-\cos\theta_{23})\,,\\
(k_1 \cdot k_3) &= \frac{\left(\sqrt{\alpha_1\beta_3} - \sqrt{\alpha_3\beta_1}\right)^2}{2} + \sqrt{\alpha_1\beta_1\alpha_3\beta_3}\,(1-\cos\theta_{12}\cos\theta_{23} - \sin\theta_{12}\sin\theta_{23}\cos\theta_{13})\,,
\end{aligned} \tag{8.31}$$

where θ_{ij} are the relevant angles. We change variables to map the three angles onto a unit hypercube; the variables are introduced in such a way that the appearance of square roots in the integrand is avoided. Explicit formulas read

$$\sin\theta_{12} = \frac{2t_1\bar{t}_1}{\bar{t}_1^2 + t_1^2}, \qquad \cos\theta_{12} = \frac{\bar{t}_1 - t_1}{\bar{t}_1^2 + t_1^2}, \tag{8.32}$$

$$\sin\theta_{23} = \frac{2t_2\bar{t}_2}{\bar{t}_2^2 + t_2^2}, \qquad \cos\theta_{23} = \frac{\bar{t}_2 - t_2}{\bar{t}_2^2 + t_2^2}, \tag{8.33}$$

$$\sin\theta_{13} = 2\sqrt{\lambda_3\bar{\lambda}_3}, \quad \cos\theta_{13} = 1 - 2\lambda_3, \tag{8.34}$$

where, as before, $\bar{x} = 1 - x$, for all variables. The integration measure becomes

$$\begin{aligned}
&\left(\Omega^{(d-2)}\right)^{-3} \mathrm{d}\Omega_1^{(d-2)}\mathrm{d}\Omega_2^{(d-2)}\mathrm{d}\Omega_3^{(d-2)} = \\
&\frac{\Omega^{(d-3)}\Omega^{(d-4)}}{\left(\Omega^{(d-2)}\right)^2}\,\frac{\mathrm{d}t_1\, 2^{1-2\varepsilon}}{\left(t_1\bar{t}_1\right)^{2\varepsilon}\left(t_1^2+\bar{t}_1^2\right)^{1-2\varepsilon}}\,\frac{\mathrm{d}t_2\, 2^{1-2\varepsilon}}{\left(t_2\bar{t}_2\right)^{2\varepsilon}\left(t_2^2+\bar{t}_2^2\right)^{1-2\varepsilon}}\,\frac{\mathrm{d}\lambda_3\, 2^{-1-2\varepsilon}}{\left(\lambda_3\bar{\lambda}_3\right)^{1+\varepsilon}},
\end{aligned} \tag{8.35}$$

where all integrations on the right -hand side are restricted to the $[0,1]$ intervals. The remaining integrals over the light-cone components are simplified using eq. (8.19) to resolve θ-function constraints, and eq. (8.20) to eliminate the jettiness δ-function. For each pair of same-hemisphere emissions with $f_i = f_j = \theta$, we split the integration into two regions $s_i < s_j$ and $s_j < s_i$ to avoid the line singularity. Since in the most complex integrals with three θ-functions, only two partons can be emitted into the same hemisphere, there is only one scalar product where such a splitting is required. Performing these steps, we obtain an eight-dimensional integral over a unit hyper-cube in variables $x, y, s_1, \ldots, s_n, t_1, t_2, \lambda_3$. In general, these integrals have a complicated structure of infra-red divergences and even if some divergences are "screened" because of the m^2 parameter in the $1/k_{123}^2$ propagator, they are still very difficult to calculate. Part of the reason for this is an interplay of ultra-violet and infra-red divergences in many master integrals, which becomes hidden if all integration variables are mapped onto a unit hypercube. This observation suggests that one possibility to simplify the computation of mass-dependent integrals, is to choose them to be ultra-violet-finite.

Hence, instead of calculating m^2-dependent master integrals, we find it more beneficial to find a (large) set of less divergent integrals, compute them numerically with high precision, and express them through master integrals to obtain constraints on the latter. In fact, by calculating a large enough number of such quasi-finite integrals and comparing them with the results of the reduction and with the solutions of the differential equations, we obtain a very powerful tool for checking master integrals at finite m^2.

Because we need many integrals for such checks, it is useful to develop an automated procedure to construct them. To this end, we note that since we have access to numerical solutions for all master integrals with m^2, we can select a subset of integrals $\vec{F}$ which are ε-finite. Because we work at finite m^2, any derivative of any such integral with respect to m^2, is also finite. Hence, it can be "easily" computed numerically and also expressed through the master integrals using the integration-by-parts reduction.

Although the procedure described above is relatively straightforward, it is important to notice that the construction of the ε-expansion requires care since the integration measure in eq. (8.35) exhibits artificial divergences at $\lambda_3 \to 0$ and $\lambda_3 \to 1$. We have found it to be convenient to subtract these divergences from the integrands and add integrated subtracted terms back. Properly subtracted integrands can be expanded in ε and integrated numerically with `CUBA` [147]. Results for finite integrals obtained in this way provide the most accurate numerical checks of the finite-m^2 master integrals, especially for higher orders of the ε-expansion.

Two comments are in order here. First, one can extend the list of integrals $\vec{F}$ by including there also integrals with simple divergences, e.g. the ultra-violet ones. Second, it is convenient to express the derivatives of integrals $\vec{F}$ through master integrals recursively, using the differential equation, instead of performing the real reduction, see eq. (6.13)

Finally, we note that for some integrals and their derivatives, that enter the differential equations, it was not possible to find finite or easily-calculable divergent integrals that would allow the above checks. In such cases we had to work with integrals whose divergence structure is complex, and involves overlapping divergences. Unfortunately, the numerical integration rapidly becomes very challenging due to a large number of terms that appear after the sector decomposition of all possible overlapping divergences.

To reduce the complexity of the integration, it is crucial to find integrals with as simple a divergence structure as possible. We do such an analysis before the actual integral calculation using the following technique. Our starting point is the parametrization of the $(d-2)$-dimensional transverse momenta integration measure shown in eq. (8.35), complemented with integrations over other variables over the unit hypercube. After splitting the integration domain in case of the same-hemisphere emissions to avoid the "line singularities", all divergencies of the integral are located at the boundaries of the integration domain, i.e. either at zero or at one.

Our approach to detecting potential divergences of the integrals is inspired by techniques developed for the analytical regularization of parametric integrals [148] and for finding finite integrals [149]. Suppose we integrate over a set of variables $\{v_i\}$ over the unit hypercube. It is useful to switch to new variables $v_i = z_i/(1+z_i)$ remapping all divergences from $v_i = 1$ to $z_i = \infty$. Integrals of interest become

$$\int_0^\infty \prod_{i=1}^{n} \frac{\mathrm{d}z_i}{z_i^{1-\nu_i}} \prod_{j=1}^{m} P_j^{a_j}(z_1, \ldots, z_n) \,. \tag{8.36}$$

Potential divergences of such integrals can be identified by considering subsets of variables $\{z_1, \ldots, z_n\}$ and studying limits when the variables from the subset approach zero or infinity. Specifically, we consider two non-intersecting subsets of $Z_n = \{z_1, \ldots, z_n\}$, that we will refer to as Z_0 and Z_∞, such that $Z_0 \cup Z_\infty \in Z_n$. We then rescale all variables $z_i \in Z_0$ by $z_i \to \lambda z_i$ and all $z_i \in Z_\infty$ by $z_i \to z_i/\lambda$, and consider the limit $\lambda \to 0$. Upon doing this, the integral receives an overall factor λ^w. The integral is divergent in the above limit if

$$w \leq 0. \tag{8.37}$$

By considering all possible subsets $\{Z_0, Z_\infty\}$, it is possible to detect all potential divergences of the integral. If divergences with a non-empty set Z_∞ are detected, we split the integration domain for each variable $z_i \in Z_\infty$ and remap divergences that arise at $z_i \to \infty$ to zero by an appropriate change of variables. Continuing this procedure, we obtain the set of integrals where *all* potential divergencies are located at the origin.

To select candidates that are best suited for numerical evaluation, we choose integrals for which *the minimal number of such splittings is needed*. Since the remaining integrals after the splitting can only have divergences at the origin, we prefer integrals with the smallest number of shortest Z_0 lists. The resulting integrals are computed numerically with `FIESTA` [145].[19]

9 Soft function renormalization and checks from the renormalization group equation

The result for the N3LO soft function has been already presented in ref. [1]. In this section and in a few appendices, we collect all the different contributions that are needed to obtain this result.

We start with the bare soft function. Restoring the dependencies on τ, $s_{ab} = 2p_a \cdot p_b$, and the normalization factor P, we write

$$S_{\tau,B} = \delta(\tau) + \frac{A_s}{\tau}\left(\frac{s_{ab}}{P^2\tau^2}\right)^{\varepsilon} S_1 + \frac{A_s^2}{\tau}\left(\frac{s_{ab}}{P^2\tau^2}\right)^{2\varepsilon} S_2 + \frac{A_s^3}{\tau}\left(\frac{s_{ab}}{P^2\tau^2}\right)^{3\varepsilon} S_3 + \mathcal{O}\left(A_s^4\right), \tag{9.1}$$

where the expansion parameter reads

$$A_s = \frac{g_s^2}{(4\pi)^{2-\varepsilon}\Gamma(1-\varepsilon)}, \tag{9.2}$$

[19] We note that some finite-m^2 master integrals have also been checked with a patched version of `pySecDec` [142].

and g_s is the bare strong coupling constant. The NLO and NNLO contributions $S_{1,2}$, needed through higher orders in ε, have been computed in refs. [2, 94, 95], and can be found in eq. (A.8). The N3LO part S_3 is comprised out of three terms

$$S_3 = S_{\tau,B}^{\rm RVV} + S_{\tau,B}^{\rm RRV} + S_{\tau,B}^{\rm RRR}, \tag{9.3}$$

which refer to the two-loop corrections to single-real emission, the one-loop corrections to double-real emission, and the triple-real emission, respectively.

It is straightforward to compute the two-loop correction to the single-gluon emission because the corresponding soft current is simple and because the integration over the single-gluon phase space is easy. This contribution was calculated in ref. [3]; we present its independent computation in appendix B.

One-loop corrections to real-emission amplitudes with two soft partons ($q\bar{q}$ and gg) were calculated in refs. [3, 6]. The RRV contribution in eq. (9.3) can be written as

$$S_{\tau,B}^{\rm RRV} = \cos(\pi\varepsilon)\left(S^{(3)}_{{\rm RRV},gg} + S^{(3)}_{{\rm RRV},q\bar{q}}\right), \tag{9.4}$$

where the two quantities $S^{(3)}_{{\rm RRV},gg}, S^{(3)}_{{\rm RRV},q\bar{q}}$ can be found in ancillary files to ref. [6].

Triple-real emission contribution to the N3LO soft function, $S_{\tau,B}^{\rm RRR}$, whose calculation is described in this paper, is quite demanding. To describe it, we note that each of the perturbative contributions in eq. (9.1) admits a Laurent expansion in ε

$$S_n = \sum_{k=1-2n}^{\infty} S_{n,k}\,\varepsilon^k. \tag{9.5}$$

We also note that it is possible to predict all contributions to the N3LO soft function S_3 through $S_{3,0}$ from the renormalization group equation that the soft function satisfies, cf. eq. (9.10). Hence, using these predictions, the results for $S_3^{\rm RVV}$ and $S_3^{\rm RRV}$, and eq. (9.3), it is possible to predict all terms in the expansion of $S_{\tau,B}^{\rm RRR}$ in ε through $\mathcal{O}(\varepsilon^0)$. For this reason, we do not show these terms and only say that our calculation of the triple-real contribution does reproduce them. The coefficient $S_{3,1}^{\rm RRR}$, which cannot be predicted from the renormalization group equation and the knowledge of other contributions to the soft function, reads

$$\begin{aligned} S_{3,1}^{\rm RRR} = {} & C_R^3\left(131072\zeta_3^2 - \frac{156928}{945}\pi^6\right) - C_R^2 n_f T_F\left(\frac{277376}{243} - \frac{21440}{81}\pi^2\right. \\ & \left. + \frac{70912}{9}\zeta_3 + \frac{12544}{135}\pi^4 - \frac{12800}{3}\pi^2\zeta_3 + 61184\zeta_5\right) - C_R^2 C_A\left(\frac{540224}{243}\right. \\ & - \frac{10496}{81}\pi^2 - \frac{218048}{9}\zeta_3 - \frac{9112}{27}\pi^4 + \frac{35200}{3}\pi^2\zeta_3 - 168256\zeta_5 - \frac{13928}{105}\pi^6 \\ & \left. + 73104\zeta_3^2\right) - 18285.58462095074 C_R C_A^2 + 3809.242380482391 C_R C_A n_f T_F \\ & - 556.5414878890519 C_R C_F n_f T_F. \end{aligned} \tag{9.6}$$

We note that the C_R^3 and C_R^2 terms in eq. (9.6) originate from iterated emissions; their calculation is discussed in appendix C. Combining $S_{3,1}^{\rm RRR}$ with contributions from the RVV result in (B.22), and the RRV result from [6], we obtain

$$\begin{aligned} S_{3,1} = {} & C_R^3\left(131072\zeta_3^2 - \frac{156928}{945}\pi^6\right) - C_R^2 n_f T_F\left(\frac{277376}{243} - \frac{21440}{81}\pi^2 + \frac{70912}{9}\zeta_3\right. \\ & \left. + \frac{12544}{135}\pi^4 - \frac{12800}{3}\pi^2\zeta_3 + 61184\zeta_5\right) - C_R^2 C_A\left(\frac{540224}{243} - \frac{10496}{81}\pi^2\right. \\ & \left. - \frac{218048}{9}\zeta_3 - \frac{9112}{27}\pi^4 + \frac{35200}{3}\pi^2\zeta_3 - 168256\zeta_5 + \frac{1024}{35}\pi^6 + 13104\zeta_3^2\right. \\ & + C_R n_f^2 T_F^2\left(\frac{224512}{81}\zeta_3 - \frac{839552}{2187} - \frac{1664}{27}\pi^2 - \frac{9664}{405}\pi^4\right) \\ & - 8308.681872115387535516222257 1 C_R C_A^2 \\ & + 4352.641895772148064259428875 1 C_R C_A n_f T_F \\ & - 158.2157843893941593818080121 4 C_R C_F n_f T_F . \end{aligned} \tag{9.7}$$

We need to renormalize the bare soft function and the bare strong coupling constant that appear in eq. (9.1). The renormalization of the strong coupling constant amounts to expressing the bare coupling A_s through the $\overline{\text{MS}}$ coupling $\alpha_s(\mu)$ with the help of the following formula

$$A_s = a_s(\mu)\frac{\mu^{2\varepsilon}e^{\varepsilon\gamma_E}}{\Gamma(1-\varepsilon)}Z_{a_s}, \quad Z_{a_s} = 1 - a_s\frac{\beta_0}{\varepsilon} + a_s^2\left(\frac{\beta_0^2}{\varepsilon^2} - \frac{\beta_1}{2\varepsilon}\right) + \mathcal{O}\left(a_s^3\right), \tag{9.8}$$

where $\beta_{0,1}$ are the expansion coefficients of the QCD β-function that can be found in appendix A, and $a_s(\mu) = \alpha_s(\mu)/(4\pi)$.

The remaining divergences of the soft function are removed by a dedicated $\overline{\text{MS}}$ renormalization. It is convenient to perform this renormalization working with the Laplace-transformed soft function, defined as

$$\tilde{S}_B\left(a_s(\mu), L_S\right) = \int\limits_0^\infty \mathrm{d}\tau e^{-\tau u} S_{\tau,B}(a_s(\mu)). \tag{9.9}$$

In the above equation $L_S = \log\left(\mu\bar{u}\sqrt{s_{ab}}/P\right)$ and $\bar{u} = ue^{\gamma_E}$.

The renormalized soft function reads

$$\tilde{S}\left(a_s, L_S\right) = Z_s\left(a_s, L_S\right)\tilde{S}_B\left(a_s, L_S\right), \tag{9.10}$$

where both a_s and L_S depend on the scale μ. The constant Z_s fulfills the renormalization group equation [95, 150–152]

$$\left(\frac{\partial}{\partial L_S} + \beta_{a_s}\frac{\partial}{\partial a_s}\right)\log Z_s\left(a_s, L_S\right) = -4\Gamma_{\text{cusp}}(a_s)L_S - 2\gamma^s(a_s), \tag{9.11}$$

where the β-function and the anomalous dimensions can be found in appendix A. Solving the renormalization group equation, we find the renormalization constant Z_s; the result is given in appendix A. Using it in eq. (9.10), we obtain the renormalized soft function.

It is convenient to write the renormalized soft function in an exponential form. To this end, we define the logarithm of the soft function $\tilde{s}(L_S) = \log\tilde{S}(L_S)$ and write its perturbative expansion as

$$\tilde{s}(L_S) = \log\left[\tilde{S}(L_S)\right] = \sum_{i=1}^{\infty} a_s^i \sum_{j=0}^{i+1} C_{i,j}L_S^j\,. \tag{9.12}$$

Coefficients of terms with non-vanishing powers of logarithm L_s in eq. (9.12) follow from the renormamlization group analysis and can be calculated from the following recurrence relation

$$C_{i,j} = \left(\frac{2}{j} \sum_{k=1}^{i-1} C_{k,j-1} \beta_{i-1-k} \right) - 2 \left(\delta_{j,2} \Gamma_{i-1} + \delta_{j,1} \gamma^s_{i-1} \right). \tag{9.13}$$

In eq. (9.13), β_i, Γ_i and γ_i^s are the A_s-expansion coefficients of the β-function, cusp anomalous dimension and soft anomalous dimension, respectively. They can be found in appendix A, cf. eqs. (A.2), (A.4), (A.6). Explicit expressions for coefficients C_{ij} in eq. (9.13) are presented in appendix A as well.

The coefficients $C_{i,0}$, $i = 1, 2, 3$, have already been provided in ref. [1]. We repeat them here for completeness

$$\begin{aligned} C_{1,0} &= -C_R \pi^2, \quad C_{2,0} = C_R \left[n_f T_F \left(\frac{80}{81} + \frac{154\pi^2}{27} - \frac{104\zeta_3}{9} \right) \right. \\ &\qquad \left. - C_A \left(\frac{2140}{80} + \frac{871\pi^2}{54} - \frac{286\zeta_3}{9} - \frac{14\pi^4}{15} \right) \right], \\ C_{3,0} &= C_R \left[n_f^2 T_F^2 \left(\frac{265408}{6561} - \frac{400\pi^2}{243} - \frac{51904\zeta_3}{243} + \frac{328\pi^4}{1215} \right) \right. \\ &\qquad \left. + n_f T_F \left(C_F X_{FF} + C_A X_{FA} \right) + C_A^2 X_{AA} \right], \end{aligned} \tag{9.14}$$

The numerical constants truncated to sixteen significant digits are given by [1]

$$\begin{aligned} X_{FF} &= 68.9425849800376, \\ X_{FA} &= 839.7238523813981, \\ X_{AA} &= -753.7757872704537. \end{aligned} \tag{9.15}$$

10 Conclusion

Recently [1], we have presented the calculation of N3LO QCD corrections to the zero-jettiness soft function. The technical details of the computation were not discussed in that reference. The goal of this paper is to fill this gap and to provide a detailed discussion of the theoretical methods employed and developed by us in the course of that computation. A particularly challenging contribution at N3LO QCD is the triple real-emission correction since in this case the phase space includes one Heaviside functions per soft parton making it especially complex.

Methods discussed in this paper encompass the extension of reverse unitarity [129] to real-emission integrals with θ-function constraints, the need to introduce an analytic regulator and the idea of "filtering", which allows us to remove this regulator from the properly-constructed integration-by-parts identities, computation of phase-space integrals using differential equations obtained by introducing an auxiliary parameter, calculation of boundary conditions as well as numerical computation of zero-jettiness phase-space integrals which turns out to be quite demanding. We hope that theoretical methods developed by us in the context of the zero-jettiness soft function computation and presented in this and earlier papers [5, 6, 93], will be useful for extending the N-jettiness slicing scheme to arbitrary number of hard partons at N3LO in perturbative QCD.

JHEP04(2025)084

Acknowledgments

We acknowledge useful conversation with Arnd Behring and Fabian Lange. Parts of the computation reported in this paper were performed at the HPC system at the Max Planck Computing and Data Facility (MPCDF) in Garching.

The research of KM and AP was partially supported by the Deutsche Forschungsgemeinschaft (DFG, German Research Foundation) under grant 396021762-TRR 257. The research of MD was supported by the European Research Council (ERC) under the European Union's research and innovation programme grant agreement 949279 (ERC Starting Grant HighPHun). The work of DB is supported in part by the Swiss National Science Foundation (SNSF) under contract 200020_219367.

A Perturbative expansion coefficients

In this appendix, we collect the various quantities that are needed for the calculation of the N3LO zero-jettiness soft function, see e.g. ref. [152]. The QCD β-function is defined as follows

$$\beta_{a_s} = -2\varepsilon a_s - 2a_s^2 \sum_{k=0}^{\infty} \beta_k a_s^k, \tag{A.1}$$

where $a_s = \alpha_s/(4\pi)$. The two coefficients, relevant for the computation of the soft function at N3LO, read

$$\beta_0 = \frac{11}{3}C_A - \frac{4}{3}n_f T_F, \quad \beta_1 = \frac{34}{3}C_A^2 - \frac{20}{3}C_A n_f T_F - 4C_F n_f T_F. \tag{A.2}$$

We write the α_s expansion of the cusp anomalous dimension as

$$\Gamma_{\text{cusp}} = a_s\left[\Gamma_0 + a_s\Gamma_1 + a_s^2\Gamma_2 + \mathcal{O}\left(a_s^3\right)\right], \tag{A.3}$$

with the expansion coefficients

$$\begin{aligned}
\Gamma_0 &= 4C_R, \\
\Gamma_1 &= C_R C_A\left(\frac{268}{9} - \frac{4}{3}\pi^2\right) - \frac{80}{9}C_R n_f T_F, \\
\Gamma_2 &= C_R C_A^2\left(\frac{88}{3}\zeta_3 + \frac{490}{3} - \frac{536}{27}\pi^2 + \frac{44}{45}\pi^4\right) \\
&\quad + C_R C_A n_f T_F\left(-\frac{224}{3}\zeta_3 - \frac{1672}{27} + \frac{160}{27}\pi^2\right) \\
&\quad + C_R C_F n_f T_F\left(64\zeta_3 - \frac{220}{3}\right) - \frac{64}{27}C_R n_f^2 T_F^2.
\end{aligned} \tag{A.4}$$

The soft anomalous dimension γ^s reads

$$\gamma^s = a_s\left[\gamma_0^s + a_s\gamma_1^s + a_s^2\gamma_2^s + \mathcal{O}\left(a_s^3\right)\right], \tag{A.5}$$

where

$$\begin{aligned}
\gamma_0^s &= 0,\\
\gamma_1^s &= C_R C_A\left(-28\zeta_3+\frac{808}{27}-\frac{11}{9}\pi^2\right)+\left(\frac{4}{9}\pi^2-\frac{224}{27}\right)C_R n_f T_F,\\
\gamma_2^s &= C_R C_A^2\left(-\frac{1316}{3}\zeta_3+\frac{88}{9}\pi^2\zeta_3+192\zeta_5+\frac{136781}{729}-\frac{6325}{243}\pi^2+\frac{88}{45}\pi^4\right)\\
&\quad+C_R C_A n_f T_F\left(\frac{1456}{27}\zeta_3-\frac{23684}{729}+\frac{2828}{243}\pi^2-\frac{16}{15}\pi^4\right)\\
&\quad+C_R C_F n_f T_F\left(\frac{608}{9}\zeta_3-\frac{3422}{27}+\frac{4}{3}\pi^2+\frac{16}{45}\pi^4\right)\\
&\quad+C_R n_f^2 T_F^2\left(\frac{448}{27}\zeta_3-\frac{8320}{729}-\frac{80}{81}\pi^2\right).
\end{aligned}\tag{A.6}$$

Using these quantities and the renormalization group equation, we compute the soft-function renormalization constant. We find

$$\begin{aligned}
Z_s &= 1+a_s\left[\frac{\Gamma_0}{\varepsilon^2}+\frac{2\Gamma_0}{\varepsilon}L_S\right]+a_s^2\left[\frac{\Gamma_0^2}{2\varepsilon^4}-\frac{3\beta_0\Gamma_0}{4\varepsilon^3}+\frac{\Gamma_1}{4\varepsilon^2}+\frac{\gamma_1^s}{2\varepsilon}+\left(\frac{2\Gamma_0^2}{\varepsilon^3}-\frac{\beta_0\Gamma_0}{\varepsilon^2}\right.\right.\\
&\quad\left.\left.+\frac{\Gamma_1}{\varepsilon}\right)L_S+\frac{2\Gamma_0^2}{\varepsilon^2}L_S^2\right]+a_s^3\left[\frac{\Gamma_0^3}{6\varepsilon^6}-\frac{3\beta_0\Gamma_0^2}{4\varepsilon^5}+\left(\frac{11}{18}\beta_0^2\Gamma_0+\frac{1}{4}\Gamma_0\Gamma_1\right)\frac{1}{\varepsilon^4}\right.\\
&\quad-\left(\frac{4}{9}\beta_1\Gamma_0+\frac{5}{18}\beta_0\Gamma_1-\frac{1}{2}\Gamma_0\gamma_1^s\right)\frac{1}{\varepsilon^3}+\left(\frac{\Gamma_2}{9}-\frac{1}{3}\beta_0\gamma_1^s\right)\frac{1}{\varepsilon^2}+\frac{\gamma_2^s}{3\varepsilon}+\left(\frac{\Gamma_0^3}{\varepsilon^5}\right.\\
&\quad-\frac{5\beta_0\Gamma_0^2}{2\varepsilon^4}+\left(\frac{2}{3}\beta_0^2\Gamma_0+\frac{3}{2}\Gamma_0\Gamma_1\right)\frac{1}{\varepsilon^3}-\left(\frac{2}{3}\beta_1\Gamma_0+\frac{2}{3}\beta_0\Gamma_1-\Gamma_0\gamma_1^s\right)\frac{1}{\varepsilon^2}+\left.\frac{2\Gamma_2}{3\varepsilon}\right)L_S\\
&\quad\left.+\left(\frac{2\Gamma_0^3}{\varepsilon^4}-\frac{2\beta_0\Gamma_0^2}{\varepsilon^3}+\frac{2\Gamma_1\Gamma_0}{\varepsilon^2}\right)L_S^2+\frac{4\Gamma_0^3}{3\varepsilon^3}L_S^3\right]+\mathcal{O}(a_s^4).
\end{aligned}\tag{A.7}$$

The last two ingredients that one needs are the soft functions at NLO and NNLO. The coefficients of the ε-expansion through the required orders are [2]

$$\begin{aligned}
S_{1,-1} &= 8C_R,\\
S_{2,-3} &= -32C_R^2,\\
S_{2,-2} &= -\frac{16}{3}C_R n_f T_F+\frac{44}{3}C_R C_A,\\
S_{2,-1} &= \frac{64}{3}\pi^2 C_R^2-\frac{80}{9}C_R n_f T_F+C_R C_A\left(\frac{268}{9}-\frac{4}{3}\pi^2\right),\\
S_{2,0} &= 512C_R^2\zeta_3+C_R n_f T_F\left(\frac{16}{9}\pi^2-\frac{448}{27}\right)+C_R C_A\left(-56\zeta_3+\frac{1616}{27}-\frac{44}{9}\pi^2\right),\\
S_{2,1} &= \frac{64}{5}\pi^4 C_R^2+C_R n_f T_F\left(\frac{320}{3}\zeta_3-\frac{320}{81}-\frac{112}{9}\pi^2\right)\\
&\quad+C_R C_A\left(-\frac{880}{3}\zeta_3+\frac{8560}{81}-\frac{98}{45}\pi^4+\frac{268}{9}\pi^2\right),\\
S_{2,2} &= C_R^2\left(6144\zeta_5-\frac{1024}{3}\pi^2\zeta_3\right)\\
&\quad+C_R n_f T_F\left(-\frac{1408}{3}\zeta_3+\frac{8576}{243}+\frac{208}{45}\pi^4+\frac{640}{81}\pi^2\right)\\
&\quad+C_R C_A\left(-680\zeta_5+1072\zeta_3+\frac{32}{3}\pi^2\zeta_3+\frac{49664}{243}-\frac{572}{45}\pi^4-\frac{1472}{81}\pi^2\right),
\end{aligned}$$

JHEP04(2025)084

$$S_{2,3} = C_R^2\left(\frac{10112}{945}\pi^6 - 4096\zeta_3^2\right) + C_R n_f T_F\Bigg(\frac{9088}{3}\zeta_5 + \frac{13952}{27}\zeta_3 - \frac{1280}{9}\pi^2\zeta_3 + \frac{138688}{729} - \frac{832}{45}\pi^4 - \frac{4000}{81}\pi^2\Bigg) + C_R C_A\Bigg(- \frac{24992}{3}\zeta_5 - 504\zeta_3^2 - \frac{31456}{27}\zeta_3 + \frac{3520}{9}\pi^2\zeta_3 + \frac{270112}{729} - \frac{40}{63}\pi^6 + \frac{1876}{45}\pi^4 + \frac{9664}{81}\pi^2\Bigg). \tag{A.8}$$

Divergent contributions to the soft function are related to anomalous dimensions and β-function coefficients. We summarize these relations below

$$\begin{aligned}
S_{1,-1} &= 2\Gamma_0, \quad S_{1,0} = 0,\\
S_{2,-3} &= -2\Gamma_0^2, \quad S_{2,-2} = \beta_0\Gamma_0,\\
S_{2,-1} &= -2\boxed{S_{1,1}}\Gamma_0 + \frac{4}{3}\pi^2\Gamma_0^2 + \Gamma_1,\\
S_{2,0} &= -2\boxed{S_{1,2}}\Gamma_0 + 2\beta_0\boxed{S_{1,1}} - \frac{1}{6}\pi^2\beta_0\Gamma_0 + 32\zeta_3\Gamma_0^2 + 2\gamma_1^s,\\
S_{3,-5} &= \Gamma_0^3, \quad S_{3,-4} = -\frac{3}{2}\beta_0\Gamma_0^2,\\
S_{3,-3} &= \frac{3}{2}\boxed{S_{1,1}}\Gamma_0^2 + \frac{2}{3}\beta_0^2\Gamma_0 - 2\pi^2\Gamma_0^3 - \frac{3}{2}\Gamma_1\Gamma_0,\\
S_{3,-2} &= \frac{3}{2}\boxed{S_{1,2}}\Gamma_0^2 - \frac{15}{4}\beta_0\boxed{S_{1,1}}\Gamma_0 + \frac{9}{4}\pi^2\beta_0\Gamma_0^2 + \frac{1}{3}\beta_1\Gamma_0 + \frac{4}{3}\beta_0\Gamma_1 - 3\Gamma_0\gamma_1^s - 64\zeta_3\Gamma_0^3,\\
S_{3,-1} &= -\frac{3}{2}\boxed{S_{2,1}}\Gamma_0 - \frac{3}{2}\boxed{S_{1,3}}\Gamma_0^2 - \frac{3}{4}\beta_0\boxed{S_{1,2}}\Gamma_0 + \boxed{S_{1,1}}\left(-\frac{3}{4}\Gamma_1 + 3\beta_0^2 - \pi^2\Gamma_0^2\right)\\
&\quad - \frac{1}{3}\pi^2\beta_0^2\Gamma_0 - \frac{4}{15}\pi^4\Gamma_0^3 + 2\pi^2\Gamma_1\Gamma_0 + \frac{2}{3}\Gamma_2 + 72\beta_0\zeta_3\Gamma_0^2 + 4\beta_0\gamma_1^s,\\
S_{3,0} &= -\frac{3}{2}\boxed{S_{2,2}}\Gamma_0 + 3\beta_0\boxed{S_{2,1}} - \frac{3}{2}\boxed{S_{1,4}}\Gamma_0^2 + \frac{21}{4}\beta_0\boxed{S_{1,3}}\Gamma_0 + \boxed{S_{1,2}}\Bigg(-\pi^2\Gamma_0^2\\
&\quad - \frac{3}{4}\Gamma_1 - 3\beta_0^2\Bigg) + \boxed{S_{1,1}}\left(+\frac{9}{8}\pi^2\beta_0\Gamma_0 - 48\zeta_3\Gamma_0^2 - \frac{3}{2}\gamma_1^s + \frac{3}{2}\beta_1\right)\\
&\quad + \frac{1}{5}\pi^4\beta_0\Gamma_0^2 - \frac{1}{6}\pi^2\beta_1\Gamma_0 - \frac{1}{6}\pi^2\beta_0\Gamma_1 + 4\pi^2\Gamma_0\gamma_1^s + \frac{2}{3}\beta_0^2\zeta_3\Gamma_0 - 960\zeta_5\Gamma_0^3\\
&\quad + 96\pi^2\zeta_3\Gamma_0^3 + 72\zeta_3\Gamma_1\Gamma_0 + 2\gamma_2^s.
\end{aligned} \tag{A.9}$$

Contributions that cannot be obtained from the renormalization group equation alone are marked with boxes.

Terms in the soft function that are multiplied by powers of the logarithm L_S are

$$\begin{aligned}
C_{1,1} &= 0,\\
C_{1,2} &= -8C_R,\\
C_{2,1} &= C_A C_R\left(56\zeta_3 - \frac{1616}{27} - \frac{44}{9}\pi^2\right) + C_R n_f T_F\left(\frac{448}{27} + \frac{16}{9}\pi^2\right),\\
C_{2,2} &= C_R C_A\left(\frac{8}{3}\pi^2 - \frac{536}{9}\right) + \frac{160}{9}C_R n_f T_F,\\
C_{2,3} &= -\frac{176}{9}C_R C_A + \frac{64}{9}C_R n_f T_F,
\end{aligned}$$

$$\sum_{f=\theta,\bar{\theta}} \int \mathrm{d}\Phi_f \mathrm{Re}\left[\boldsymbol{J}^{(l)\dagger}_{\mu,a}\boldsymbol{J}^{(m)}_{\mu,a}\right] \sim$$

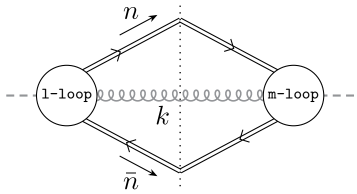

Figure 5. Soft amplitude squared $(l \times m)$-loop contribution with single soft gluon emission.

$$\begin{aligned}
C_{3,1} &= C_A^2 C_R\left(\frac{36272}{27}\zeta_3 - \frac{176}{9}\pi^2\zeta_3 - 384\zeta_5 - \frac{556042}{729} - \frac{50344}{243}\pi^2 + \frac{88}{9}\pi^4\right) \\
&\quad + C_R C_A n_f T_F\left(-\frac{12064}{27}\zeta_3 + \frac{160648}{729} + \frac{38816}{243}\pi^2 - \frac{128}{45}\pi^4\right) \\
&\quad + C_R C_F n_f T_F\left(-\frac{1216}{9}\zeta_3 + \frac{6844}{27} + \frac{16}{3}\pi^2 - \frac{32}{45}\pi^4\right) \\
&\quad + C_R n_f^2 T_F^2\left(\frac{256}{9}\zeta_3 + \frac{12800}{729} - \frac{256}{9}\pi^2\right), \\
C_{3,2} &= C_A^2 C_R\left(352\zeta_3 - \frac{62012}{81} + \frac{104}{27}\pi^2 - \frac{88}{45}\pi^4\right) + C_R C_A n_f T_F\left(\frac{32816}{81}\right. \\
&\quad \left. + \frac{128}{9}\pi^2\right) + C_R C_F n_f T_F\left(\frac{440}{3} - 128\zeta_3\right) + C_R n_f^2 T_F^2\left(-\frac{3200}{81} - \frac{128}{27}\pi^2\right), \\
C_{3,3} &= C_R C_A^2\left(\frac{352}{27}\pi^2 - \frac{28480}{81}\right) + C_R C_A n_f T_F\left(\frac{18496}{81} - \frac{128}{27}\pi^2\right) \\
&\quad + \frac{64}{3} C_R C_F n_f T_F - \frac{2560}{81} C_R n_f^2 T_F^2, \\
C_{3,4} &= -\frac{1936}{27} C_R C_A^2 + \frac{1408}{27} C_R C_A n_f T_F - \frac{256}{27} C_R n_f^2 T_F^2.
\end{aligned} \tag{A.10}$$

B Single soft-gluon emission corrections

In this appendix we compute the single-gluon N3LO QCD contribution to the zero-jettiness soft function. It follows from eq. (2.4) that in order to do that, we need to integrate the square of the single-soft eikonal current, truncated at $\mathcal{O}(\alpha_s^3)$, over single-gluon phase space subject to the zero-jettiness constraint.

To facilitate this computation, we write perturbative corrections to the soft current

$$\boldsymbol{J}_{\mu,a}(k) = g_s \sum_{l=0}^{\infty} g_s^{2l} \boldsymbol{J}^{(l)}_{\mu,a}(k), \tag{B.1}$$

and define the product of l- and m-loop currents

$$w_{l,m}(k) = -g^{\mu\nu}\mathrm{Re}\left[\boldsymbol{J}^{(l)\dagger}_{\mu,a}(k)\boldsymbol{J}^{(m)}_{\nu,a}(k)\right], \tag{B.2}$$

where summation over all color degrees of freedom, as well as over gluon polarizations, is assumed. Thanks to the simple dependence of the soft currents on the external momenta, this quantity reads

$$w_{l,m}(k) = \mathcal{C}_{l,m}\mathrm{Re}\left[e^{-i\pi l\varepsilon}e^{i\pi m\varepsilon}\right]\left(\frac{n\cdot\bar{n}}{2(k\cdot n)(k\cdot\bar{n})}\right)^{1+(l+m)\varepsilon}, \tag{B.3}$$

where the constant $\mathcal{C}_{l,m}$ contains all the information about colors and other quantities that depend on l and m but not on momenta k, n and $\bar{n}$.

To calculate soft-function contribution $s_{l,m}$ from diagrams with $l\times m$ loops we sum over two hemisphere configurations and integrate over the gluon momentum k

$$\begin{aligned} s_{l,m} &= \mathcal{N}_\varepsilon \sum_{f=\theta,\bar{\theta}} \int \mathrm{d}\Phi_f w_{l,m}(k) \\ &= \mathcal{N}_\varepsilon \mathcal{C}_{l,m}\cos\left[(l-m)\pi\varepsilon\right]\sum_{f=\theta,\bar{\theta}}\int \mathrm{d}\Phi_f\left(\frac{n\cdot\bar{n}}{2(k\cdot n)(k\cdot\bar{n})}\right)^{1+(l+m)\varepsilon} \\ &= 2\mathcal{N}_\varepsilon\cos\left[(l-m)\pi\varepsilon\right]\mathcal{C}_{l,m}\,F(l+m)\,\left(\frac{n\cdot\bar{n}}{2}\right)^{1+(l+m)\varepsilon}. \end{aligned} \tag{B.4}$$

Using the following expressions for the integration measures,

$$\mathrm{d}\Phi_\theta = \frac{1}{\mathcal{N}_\varepsilon}[\mathrm{d}k]\delta(1-k\cdot n)\theta(k\cdot\bar{n}-k\cdot n), \quad \mathrm{d}\Phi_{\bar{\theta}} = \frac{1}{\mathcal{N}_\varepsilon}[\mathrm{d}k]\delta(1-k\cdot\bar{n})\theta(k\cdot n-k\cdot\bar{n}), \tag{B.5}$$

and the fact that the integrand is symmetric under $n\leftrightarrow\bar{n}$ replacement, we find

$$F(m) = \int\frac{\mathrm{d}\alpha\mathrm{d}\beta}{\alpha^\varepsilon\beta^\varepsilon}\delta(1-\beta)\theta(\alpha-\beta)\frac{1}{\alpha^{1+m\varepsilon}\beta^{1+m\varepsilon}} = \int_1^\infty\frac{\mathrm{d}\alpha}{\alpha^{1+\varepsilon+m\varepsilon}} = \frac{1}{(m+1)\varepsilon}. \tag{B.6}$$

The final expression for $n\cdot\bar{n} = 2$ reads

$$s_{l,m} = 2\mathcal{N}_\varepsilon\cos\left[(l-m)\pi\varepsilon\right]\frac{\mathcal{C}_{l,m}}{(1+l+m)\varepsilon}. \tag{B.7}$$

To find corrections at N3LO, we require $s_{0,2}$, $s_{2,0}$ and $s_{1,1}$. To fix the normalization, we start with the lowest order contribution. Writing the leading order current as

$$\boldsymbol{J}^{(0)}_{\mu,a}(k) = \boldsymbol{T}_a\left(\frac{n_\mu}{k\cdot n}-\frac{\bar{n}_\mu}{k\cdot\bar{n}}\right), \tag{B.8}$$

and using it in eqs. (B.1), (B.3), it is easy to fix the constant $\mathcal{C}_{0,0} = 4C_R$. The one-loop current was computed in ref. [153] and we borrow it from that reference. It reads[20]

$$\boldsymbol{J}^{(1)}_{\mu,a}(k) = \mathcal{N}_\varepsilon\mathcal{X}\left[\frac{-(n\cdot\bar{n})}{2(k\cdot n)(k\cdot\bar{n})}\right]^\varepsilon\boldsymbol{J}^{(0)}_{\mu,a}(k), \tag{B.9}$$

with

$$\mathcal{X} = -C_A\frac{\Gamma^4(1-\varepsilon)\Gamma^2(1+\varepsilon)}{\varepsilon^2\Gamma(1-2\varepsilon)}. \tag{B.10}$$

[20]Since we consider n, $\bar{n}$ and k to be final-state momenta, the $(-1)^\varepsilon$ factor should be understood as $e^{+i\pi\varepsilon}$, see ref. [153].

Then, using eq. (B.8) and eq. (B.9), we calculate the NLO contribution

$$w_{1,0} = w_{0,1} = w_{0,0}\, \mathcal{N}_\varepsilon \mathcal{X} \left[\frac{-n\cdot\bar{n}}{2(k\cdot n)(k\cdot\bar{n})}\right]^\varepsilon, \tag{B.11}$$

and use eq. (B.3) to fix the following constants.

$$\mathcal{C}_{0,1} = \mathcal{C}_{1,0} = \mathcal{N}_\varepsilon \mathcal{X} \mathcal{C}_{0,0}. \tag{B.12}$$

Similarly, using eq. (B.9) we can calculate $w_{1,1}$ and extract the corresponding constant

$$\mathcal{C}_{1,1} = (\mathcal{N}_\varepsilon \mathcal{X})^2\, \mathcal{C}_{0,0}. \tag{B.13}$$

The result for the two-loop contribution is [113–115]. We use ref. [113] and eq. (B.3) to fix two remaining constants

$$\mathcal{C}_{0,2} = \mathcal{C}_{2,0} = 4C_R \left(\frac{\mathcal{N}_\varepsilon \Gamma^3(1-\varepsilon)\Gamma(1+\varepsilon)}{\Gamma(1-2\varepsilon)}\right)^2 r^{(2)}_{\text{soft}}. \tag{B.14}$$

The constant $r^{(2)}_{\text{soft}}$ is defined in [113]; it reads

$$r^{(2)}_{\text{soft}} = 2C_A n_f T_F \mathcal{R}_1 + C_A^2 \mathcal{R}_2, \tag{B.15}$$

where

$$\begin{aligned}
\mathcal{R}_1 &= \frac{1}{6\varepsilon^3} + \frac{5}{18\varepsilon^2} + \left(\frac{19}{54} + \frac{\pi^2}{18}\right)\frac{1}{\varepsilon} \\
&\quad + \left(\frac{65}{162} + \frac{5}{54}\pi^2 - \frac{8}{3}\zeta_3\right) + \varepsilon\left(\frac{211}{486} - \frac{4}{81}\pi^2 - \frac{40}{9}\zeta_3 - \frac{\pi^4}{15}\right) \\
&\quad - \varepsilon^2\left(\frac{287\zeta_3}{27} + \frac{8\pi^2\zeta_3}{9} + 32\zeta_5 - \frac{665}{1458} + \frac{151\pi^2}{486} + \frac{\pi^4}{9}\right) + \mathcal{O}\left(\varepsilon^3\right),
\end{aligned} \tag{B.16}$$

$$\begin{aligned}
\mathcal{R}_2 &= \frac{1}{2\varepsilon^4} - \frac{11}{12\varepsilon^3} - \left(\frac{67}{36} - \frac{1}{4}\pi^2\right)\frac{1}{\varepsilon^2} - \left(\frac{193}{54} + \frac{11}{36}\pi^2 - \frac{1}{2}\zeta_3\right)\frac{1}{\varepsilon} \\
&\quad - \left(\frac{571}{81} + \frac{67}{108}\pi^2 - \frac{44}{3}\zeta_3 - \frac{29}{360}\pi^4\right) - \varepsilon\left(\frac{3410}{243} + \frac{83}{81}\pi^2 - \frac{268}{9}\zeta_3 - \frac{11}{30}\pi^4 \right.\\
&\quad \left. - \frac{2}{3}\pi^2\zeta_3 + \frac{37}{2}\zeta_5\right) - \varepsilon^2\left(\frac{20428}{729} + \frac{1007}{486}\pi^2 - \frac{1679}{27}\zeta_3 - \frac{67}{90}\pi^4 - \frac{44}{9}\pi^2\zeta_3 \right.\\
&\quad \left. - 176\zeta_5 + \frac{451}{11340}\pi^6 + \frac{29}{2}\zeta_3^2\right) + \mathcal{O}\left(\varepsilon^3\right).
\end{aligned} \tag{B.17}$$

Finally, we use the above results to compute the single-gluon contribution to the soft function through N3LO. Writing

$$S_g = A_s S_g^{(1)} + A_s^2 S_g^{(2)} + A_s^3 S_g^{(3)} + \mathcal{O}\left(A_s^4\right), \tag{B.18}$$

where the strong coupling constant A_s is defined in eq. (9.2), we obtain

$$S_g^{(1)} = \frac{s_{0,0}}{\mathcal{N}_\varepsilon} = \frac{8}{\varepsilon} C_R, \tag{B.19}$$

$$S_g^{(2)} = \frac{1}{\mathcal{N}_\varepsilon^2} \left(s_{1,0} + s_{0,1}\right) = \frac{8}{\varepsilon} C_R \cos\left(\pi\varepsilon\right) \mathcal{X}, \tag{B.20}$$

$$\begin{aligned} S_g^{(3)} &= \frac{1}{\mathcal{N}_\varepsilon^3} \left(s_{2,0} + s_{1,1} + s_{0,2}\right) \\ &= \frac{8}{3\varepsilon} C_R \left(\mathcal{X}^2 + 2\cos\left(2\pi\varepsilon\right) \left(\frac{\Gamma^3(1-\varepsilon)\Gamma(1+\varepsilon)}{\Gamma(1-2\varepsilon)} \right)^2 r_{\text{soft}}^{(2)} \right). \end{aligned} \tag{B.21}$$

To conclude, we explicitly write the result for $S_3^{RVV} = S_g^{(3)}$ expanded through the required order in ε

$$\begin{aligned} S_3^{\text{RVV}} = S_g^{(3)} &= \frac{16}{3\varepsilon^5} C_R C_A^2 + \left(\frac{16}{9} C_A C_R n_f T_F - \frac{44}{9} C_A^2 C_R \right) \frac{1}{\varepsilon^4} \\ &- \left(\left(\frac{268}{27} + \frac{28\pi^2}{9} \right) C_A^2 C_R - \frac{80}{27} C_A C_R n_f T_F \right) \frac{1}{\varepsilon^3} \\ &- \left(C_A^2 C_R \left(\frac{1544}{81} - \frac{220}{27}\pi^2 + \frac{56}{3}\zeta_3 \right) - C_R C_A n_f T_F \left(\frac{304}{81} - \frac{80}{27}\pi^2 \right) \right) \frac{1}{\varepsilon^2} \\ &- \left(+ C_A^2 C_R \left(\frac{9136}{243} - \frac{1340}{81}\pi^2 - \frac{880}{9}\zeta_3 + \frac{86}{135}\pi^4 \right) + C_A C_R n_f T_F \left(\frac{320}{9}\zeta_3 \right.\right. \\ &\left.\left. - \frac{1040}{243} + \frac{400}{81}\pi^2 \right) \right) \frac{1}{\varepsilon} - \left(C_R C_A^2 \left(\frac{54560}{729} - \frac{7936}{243}\pi^2 - \frac{5360}{27}\zeta_3 - \frac{308}{135}\pi^4 \right.\right. \\ &\left.\left. - \frac{32}{3}\pi^2\zeta_3 + \frac{488}{3}\zeta_5 \right) - C_R C_A n_f T_F \left(\frac{3376}{729} - \frac{1952}{243}\pi^2 - \frac{1600}{27}\zeta_3 - \frac{112}{135}\pi^4 \right) \right) \\ &- \varepsilon \left(C_R C_A^2 \left(\frac{326848}{2187} - \frac{46760}{729}\pi^2 - \frac{33040}{81}\zeta_3 - \frac{1876}{405}\pi^4 + \frac{4400}{27}\pi^2\zeta_3 \right.\right. \\ &\left. - \frac{2992}{3}\zeta_5 + \frac{2524}{8505}\pi^6 + \frac{136}{3}\zeta_3^2 \right) - C_A C_R n_f T_F \left(\frac{10640}{2187} - \frac{8656}{729}\pi^2 - \frac{10400}{81}\zeta_3 \right. \\ &\left.\left. - \frac{112}{81}\pi^4 + \frac{1600}{27}\pi^2\zeta_3 - \frac{1088}{3}\zeta_5 \right) \right) + \mathcal{O}\left(\varepsilon^2\right). \end{aligned} \tag{B.22}$$

C Iterated real-emission contributions

As we explain in this appendix, some of the real-emission contributions to the N3LO soft function can be computed with a relative ease. To this end, we consider the real-emission contribution to the n-th order term in the expansion of the soft function in α_s, cf. eq. (2.3), and write it as

$$S_\tau^{(n)} = \int \prod_{i=1}^{n} [\mathrm{d}k_i]\ \delta(\tau - \mathcal{T}_0(n))\ \xi_n(k_1, \ldots, k_n). \tag{C.1}$$

The functions ξ_n contain contributions from all possible final states and color structures and, in general, they cannot be predicted from similar functions at lower orders. However, for certain color structures, their form simplifies. Following refs. [116, 118], we write

$$\xi_1(k_1) = C_R w_g(k_1), \tag{C.2}$$

$$\xi_2(k_1,k_2) = \frac{1}{2!}\Big(C_R^2 w_g(k_1)w_g(k_2) + C_R C_A w_{gg}(k_1,k_2)\Big) + C_R n_f T_F w_{q\bar{q}}(k_1,k_2), \tag{C.3}$$

$$\begin{aligned}\xi_3(k_1,k_2,k_3) = \frac{1}{3!}\Big(&C_R^3 w_g(k_1)w_g(k_2)w_g(k_3)\\ &+ C_R^2 C_A\left[w_g(k_1)w_{gg}(k_2,k_3) + (1\leftrightarrow 2) + (1\leftrightarrow 3)\right]\Big)\\ &+ C_R^2 n_f T_F w_g(k_1) w_{q\bar{q}}(k_2,k_3) + \dots,\end{aligned} \tag{C.4}$$

where ellipses stand for contributions that are unrelated to lower order ones. The functions $w_g(k_1)$ and $w_{gg}(k_1,k_2)$ are called $w_{BC}^{(1)}(k_1)$ and $w_{BC}^{(2)}(k_1,k_2)$ in ref. [116]; the function $w_{q\bar{q}}(k_1,k_2)$ is called $w_{BC}^{(2)}(k_1,k_2)$ in ref. [118]; they can be extracted from those references. The common feature of the contributions to $\bar{\zeta}_3$ shown explicitly in eq. (C.4) is that the single-gluon emission contribution w_g factorizes as least once.

Since the zero-jettiness $\mathcal{T}_0$ is a *linear* function of the soft partons' momenta, the factorization property can be exploited by computing the Laplace transform of the soft function. We introduce it by considering the C_R^3 contribution to $S_\tau^{(3)}$. We write

$$S_u^{(3),C_R^3} = \frac{1}{3!}\int \mathrm{d}\tau\, e^{-u\tau}\prod_{i=1}^{3}[\mathrm{d}k_i]\delta(\tau - \mathcal{T}_0)\; w_g(k_1)w_g(k_2)w_g(k_3). \tag{C.5}$$

Integrating over τ and using the fact that $\mathcal{T}_0 = \mathcal{T}_0(k_1) + \mathcal{T}_0(k_2) + \mathcal{T}_0(k_3)$, we obtain

$$S_u^{(3),C_R^3} = \frac{1}{3!}\left[S_u^{(1),C_R}\right]^3. \tag{C.6}$$

Subleading contributions $C_R^2 C_A$ and $C_R^2 n_f T_F$ are obtained in the same way. Computing the Laplace transform and accounting for the permutations, we find

$$S_u^{(3),C_R^2 C_A} = S_u^{(1),C_R} S_u^{(2),C_R C_A}, \qquad S_u^{(3),C_R^2 n_f T_F} = S_u^{(1),C_R} S_u^{(2),C_R n_f T_F}. \tag{C.7}$$

Because the scaling of the soft function $S_\tau^{(n)}$ with respect to τ is fully determined by n, the following relation between the soft function and its Laplace image holds

$$S_u^{(n)} = \Gamma(-2n\varepsilon)\, u^{2n\varepsilon} S_\tau^{(n)}\Big|_{\tau=1}. \tag{C.8}$$

Hence, once the Laplace imagine is known, it is straightforward to reconstruct the τ-dependent soft function from the above equation. When writing the soft function S_τ below, we will always assume that τ is taken to be one and we will not indicate this further.

Required NLO contribution to eq. (C.7) can be easily calculated from the exact result for $S_\tau^{(1)}$

$$S_\tau^{(1),C_R} = \frac{8}{\varepsilon} \quad\to\quad S_u^{(1),C_R} = \frac{8\Gamma(-2\varepsilon)}{\varepsilon}u^{2\varepsilon}. \tag{C.9}$$

Using eq. (C.6) and eq. (C.8), we find the part of the N3LO soft function proportional to C_R^3 to be

$$S_\tau^{(3),C_R^3} = \frac{\Gamma^3(-2\varepsilon)}{6\Gamma(-6\varepsilon)}\left[S_\tau^{(1),C_R}\right]^3 = \frac{256\Gamma^3(-2\varepsilon)}{3\varepsilon^3\Gamma(-6\varepsilon)}. \tag{C.10}$$

To calculate contributions proportional to C_R^2 using eq. (C.7), we can extract the required parts $S_u^{(2),C_RC_A}$ and $S_u^{(2),C_Rn_fT_F}$ from the NNLO soft function in eq. (A.8). To get the real-emission contribution for the final-state gluons, we need to subtract virtual corrections from the NNLO soft function. On the contrary, in case of the $q\bar{q}$, no subtraction is needed, and we can use the NNLO contribution $S_\tau^{(2),C_Rn_fT_F}$ directly. We obtain

$$\begin{aligned}
S_\tau^{(3),C_R^2n_fT_F} &= \frac{\Gamma(-2\varepsilon)\Gamma(-4\varepsilon)}{\Gamma(-6\varepsilon)}S_\tau^{(1),C_R}S_\tau^{(2),C_Rn_fT_F} \\
&= \frac{32}{\varepsilon^4}+\frac{160}{3\varepsilon^3}+\frac{1}{\varepsilon^2}\left(\frac{896}{9}-\frac{160}{3}\pi^2\right)+\frac{1}{\varepsilon}\left(-2176\zeta_3+\frac{640}{27}+\frac{32}{9}\pi^2\right) \\
&\quad+\left(256\zeta_3-\frac{17152}{81}-\frac{4864}{27}\pi^2-\frac{3424}{45}\pi^4\right)+\left(-\frac{70912}{9}\zeta_3\right. \\
&\quad\left.+\frac{12800}{3}\pi^2\zeta_3-61184\zeta_5-\frac{277376}{243}+\frac{21440}{81}\pi^2-\frac{12544}{135}\pi^4\right)\varepsilon+\mathcal{O}\left(\varepsilon^2\right).
\end{aligned} \tag{C.11}$$

As we mentioned earlier, to obtain the $C_R^2C_A$ part of the soft function, we need to subtract the real-virtual corrections from the $\mathcal{O}(C_RC_A)$ term in the NNLO soft function. The real-virtual contribution reads

$$S_{\tau,\mathrm{RV}}^{(2)} = -\frac{8\Gamma^5(1-\varepsilon)\Gamma^3(1+\varepsilon)}{\varepsilon^3\Gamma^2(1-2\varepsilon)\Gamma(1+2\varepsilon)}, \tag{C.12}$$

where the color factor C_RC_A is not shown. By combining the relevant contributions, we obtain the final result for the coefficient of the $C_R^2C_A$ color structure

$$\begin{aligned}
S_\tau^{(3),C_R^2C_A} &= \frac{\Gamma(-2\varepsilon)\Gamma(-4\varepsilon)}{\Gamma(-6\varepsilon)}S_\tau^{(1),C_R}\left[S_\tau^{(2),C_RC_A}-S_{\mathrm{RV}}^{(2)}\right] \\
&= -\frac{48}{\varepsilon^5}-\frac{88}{\varepsilon^4}+\frac{1}{\varepsilon^3}\left(88\pi^2-\frac{536}{3}\right)+\frac{1}{\varepsilon^2}\left(2736\zeta_3-\frac{3232}{9}+\frac{440}{3}\pi^2\right) \\
&\quad+\left(5984\zeta_3-\frac{17120}{27}+\frac{536}{9}\pi^2+\frac{388}{5}\pi^4\right)\frac{1}{\varepsilon}+\left(2144\zeta_3-4896\pi^2\zeta_3\right. \\
&\quad\left.+68880\zeta_5-\frac{99328}{81}+\frac{15872}{27}\pi^2+\frac{9416}{45}\pi^4\right)+\left(\frac{218048}{9}\zeta_3-\frac{35200}{3}\pi^2\zeta_3\right. \\
&\quad-73104\zeta_3^2+168256\zeta_5-\frac{540224}{243}+\frac{10496}{81}\pi^2+\frac{9112}{27}\pi^4 \\
&\quad\left.+\frac{13928}{105}\pi^6\right)\varepsilon+\mathcal{O}\left(\varepsilon^2\right).
\end{aligned} \tag{C.13}$$

D Angular integrations

Partial fractioning identities

$$\frac{1}{(\rho_1\cdot\rho_{\bar{n}})(\rho_1\cdot\bar{\rho}_{\bar{n}})}=\frac{1}{2}\frac{1}{(\rho_1\cdot\rho_{\bar{n}})}+\frac{1}{2}\frac{1}{(\rho_1\cdot\bar{\rho}_{\bar{n}})}, \tag{D.1}$$

$$\frac{1}{(\rho_1\cdot\rho_{n})(\rho_1\cdot\bar{\rho}_{n})}=\frac{1}{2}\frac{1}{(\rho_1\cdot\rho_{n})}+\frac{1}{2}\frac{1}{(\rho_1\cdot\bar{\rho}_{n})}, \tag{D.2}$$

$$\frac{1}{(\rho_1\cdot\rho_{n})(\rho_1\cdot\rho_{m})}=\frac{1}{1-\lambda}\frac{1}{(\rho_1\cdot\rho_{n})}-\frac{\lambda}{1-\lambda}\frac{1}{(\rho_1\cdot\rho_{m})}, \tag{D.3}$$

$$\frac{1}{(\rho_1\cdot\rho_{n})(\rho_1\cdot\bar{\rho}_{m})}=\frac{1}{1+\lambda}\frac{1}{(\rho_1\cdot\rho_{n})}+\frac{\lambda}{1+\lambda}\frac{1}{(\rho_1\cdot\bar{\rho}_{m})}, \tag{D.4}$$

$$\frac{1}{(\rho_1\cdot\bar{\rho}_{n})(\rho_1\cdot\rho_{m})}=\frac{1}{1+\lambda}\frac{1}{(\rho_1\cdot\bar{\rho}_{n})}+\frac{\lambda}{1+\lambda}\frac{1}{(\rho_1\cdot\rho_{m})}, \tag{D.5}$$

$$\frac{1}{(\rho_1\cdot\bar{\rho}_{n})(\rho_1\cdot\bar{\rho}_{m})}=\frac{1}{1-\lambda}\frac{1}{(\rho_1\cdot\bar{\rho}_{n})}-\frac{\lambda}{1-\lambda}\frac{1}{(\rho_1\cdot\bar{\rho}_{m})}, \tag{D.6}$$

$$\frac{1}{(\rho_1\cdot\rho_{m})(\rho_1\cdot\bar{\rho}_{m})}=\frac{1}{2}\frac{1}{(\rho_1\cdot\rho_{m})}+\frac{1}{2}\frac{1}{(\rho_1\cdot\bar{\rho}_{m})}. \tag{D.7}$$

$$\frac{(\rho_1\cdot\rho_{\bar{n}})}{(\rho_1\cdot\bar{\rho}_{\bar{n}})}=-1+2\frac{1}{(\rho_1\cdot\bar{\rho}_{\bar{n}})},\qquad \frac{(\rho_1\cdot\bar{\rho}_{\bar{n}})}{(\rho_1\cdot\rho_{\bar{n}})}=-1+2\frac{1}{(\rho_1\cdot\rho_{\bar{n}})}, \tag{D.8}$$

$$\frac{(\rho_1\cdot\rho_{n})}{(\rho_1\cdot\bar{\rho}_{n})}=-1+2\frac{1}{(\rho_1\cdot\bar{\rho}_{n})},\qquad \frac{(\rho_1\cdot\bar{\rho}_{n})}{(\rho_1\cdot\rho_{n})}=-1+2\frac{1}{(\rho_1\cdot\rho_{n})}, \tag{D.9}$$

$$\frac{(\rho_1\cdot\rho_{n})}{(\rho_1\cdot\rho_{m})}=\frac{1}{\lambda}-\frac{1-\lambda}{\lambda}\frac{1}{(\rho_1\cdot\rho_{m})},\qquad \frac{(\rho_1\cdot\rho_{m})}{(\rho_1\cdot\rho_{n})}=\lambda+(1-\lambda)\frac{1}{(\rho_1\cdot\rho_{n})}, \tag{D.10}$$

$$\frac{(\rho_1\cdot\rho_{n})}{(\rho_1\cdot\bar{\rho}_{m})}=-\frac{1}{\lambda}+\frac{1+\lambda}{\lambda}\frac{1}{(\rho_1\cdot\bar{\rho}_{m})},\qquad \frac{(\rho_1\cdot\bar{\rho}_{m})}{(\rho_1\cdot\rho_{n})}=-\lambda+(1+\lambda)\frac{1}{(\rho_1\cdot\rho_{n})}, \tag{D.11}$$

$$\frac{(\rho_1\cdot\bar{\rho}_{n})}{(\rho_1\cdot\rho_{m})}=-\frac{1}{\lambda}+\frac{1+\lambda}{\lambda}\frac{1}{(\rho_1\cdot\rho_{m})},\qquad \frac{(\rho_1\cdot\rho_{m})}{(\rho_1\cdot\bar{\rho}_{n})}=-\lambda+(1+\lambda)\frac{1}{(\rho_1\cdot\bar{\rho}_{n})}, \tag{D.12}$$

$$\frac{(\rho_1\cdot\bar{\rho}_{n})}{(\rho_1\cdot\bar{\rho}_{m})}=\frac{1}{\lambda}-\frac{1-\lambda}{\lambda}\frac{1}{(\rho_1\cdot\bar{\rho}_{m})},\qquad \frac{(\rho_1\cdot\bar{\rho}_{m})}{(\rho_1\cdot\bar{\rho}_{n})}=\lambda+(1-\lambda)\frac{1}{(\rho_1\cdot\bar{\rho}_{n})}, \tag{D.13}$$

$$\frac{(\rho_1\cdot\rho_{m})}{(\rho_1\cdot\bar{\rho}_{m})}=-1+2\frac{1}{(\rho_1\cdot\bar{\rho}_{m})},\qquad \frac{(\rho_1\cdot\bar{\rho}_{m})}{(\rho_1\cdot\rho_{m})}=-1+2\frac{1}{(\rho_1\cdot\rho_{m})}. \tag{D.14}$$

Integrals defined in (7.46) after partial fractioning identities application

$$\Omega^{(d-1)}_{000000}=1, \tag{D.15}$$

$$\Omega^{(d-1)}_{a_1 00000}=I^{(0)}_{d-1;a_1}, \tag{D.16}$$

$$\Omega^{(d-1)}_{0a_2 0000}=I^{(0)}_{d-1;a_2}, \tag{D.17}$$

$$\Omega^{(d-1)}_{00a_3 000}=I^{(0)}_{d-1;a_3}, \tag{D.18}$$

$$\Omega^{(d-1)}_{000a_4 00}=I^{(0)}_{d-1;a_4}, \tag{D.19}$$

$$\Omega^{(d-1)}_{0000a_5 0}=I^{(1)}_{d-1;a_5}\left(\rho_m^2\right), \tag{D.20}$$

$$\Omega^{(d-1)}_{00000a_6}=I^{(1)}_{d-1;a_6}\left(\bar{\rho}_m^2\right), \tag{D.21}$$

$$\Omega^{(d-1)}_{a_1 0a_3 000}=I^{(0)}_{d-1;a_1,a_3}\left(\rho_n\cdot\rho_{\bar{n}}\right), \tag{D.22}$$

$$\Omega^{(d-1)}_{a_1 00 a_4 00} = I^{(0)}_{d-1;a_1,a_4}\left(\rho_n \cdot \bar{\rho}_{\bar{n}}\right), \tag{D.23}$$
$$\Omega^{(d-1)}_{0 a_2 a_3 000} = I^{(0)}_{d-1;a_2,a_3}\left(\bar{\rho}_n \cdot \rho_{\bar{n}}\right), \tag{D.24}$$
$$\Omega^{(d-1)}_{0 a_2 0 a_4 00} = I^{(0)}_{d-1;a_2,a_4}\left(\bar{\rho}_n \cdot \bar{\rho}_{\bar{n}}\right), \tag{D.25}$$
$$\Omega^{(d-1)}_{00 a_3 0 a_5 0} = I^{(1)}_{d-1;a_3,a_5}\left(\rho_{\bar{n}} \cdot \rho_m, \rho_m^2\right), \tag{D.26}$$
$$\Omega^{(d-1)}_{000 a_4 a_5 0} = I^{(1)}_{d-1;a_4,a_5}\left(\bar{\rho}_{\bar{n}} \cdot \rho_m, \rho_m^2\right), \tag{D.27}$$
$$\Omega^{(d-1)}_{00 a_3 00 a_6} = I^{(1)}_{d-1;a_3,a_6}\left(\rho_{\bar{n}} \cdot \bar{\rho}_m, \bar{\rho}_m^2\right), \tag{D.28}$$
$$\Omega^{(d-1)}_{000 a_4 0 a_6} = I^{(1)}_{d-1;a_4,a_6}\left(\bar{\rho}_{\bar{n}} \cdot \bar{\rho}_m, \bar{\rho}_m^2\right). \tag{D.29}$$

All considered angle integrals are normalized by full solid angle, so

$$I_0^{(0)} = I_0^{(1)}\left(\rho^2\right) = I_{0,0}^{(0)}\left(\rho_1 \cdot \rho_2\right) = I_{0,0}^{(1)}\left(\rho_1 \cdot \rho_2, \rho_2^2\right) = 1. \tag{D.30}$$

$$I^{(0)}_{d-1;n} = \frac{1}{\Omega^{(d-1)}} \int \frac{\mathrm{d}\Omega_v^{(d-1)}}{(v \cdot \rho)^n}, \quad \rho^2 = 0, \tag{D.31}$$
$$I^{(1)}_{d-1;n}\left(\rho^2\right) = \frac{1}{\Omega^{(d-1)}} \int \frac{\mathrm{d}\Omega_v^{(d-1)}}{(v \cdot \rho)^n}, \quad \rho^2 \neq 0, \tag{D.32}$$
$$I^{(0)}_{d-1;a,b}\left(\rho_1 \cdot \rho_2\right) = \frac{1}{\Omega^{(d-1)}} \int \frac{\mathrm{d}\Omega_v^{(d-1)}}{(v \cdot \rho_1)^a (v \cdot \rho_2)^b}, \quad \rho_1^2 = \rho_2^2 = 0, \tag{D.33}$$
$$I^{(1)}_{d-1;a,b}\left(\rho_1 \cdot \rho_2, \rho_2^2\right) = \frac{1}{\Omega^{(d-1)}} \int \frac{\mathrm{d}\Omega_v^{(d-1)}}{(v \cdot \rho_1)^a (v \cdot \rho_2)^b}, \quad \rho_1^2 = 0, \rho_2^2 \neq 0, \tag{D.34}$$

where v is a light-like vector.

$$I^{(0)}_{d-1;n} = \frac{\Gamma(2-2\varepsilon)\Gamma(1-\varepsilon-n)}{\Gamma(1-\varepsilon)\Gamma(2-2\varepsilon-n)}, \tag{D.35}$$

$$I^{(1)}_{d-1;n}\left(\rho^2\right) = (1+\beta)^{-n} {}_2F_1\left(n, 1-\varepsilon, 2-2\varepsilon; \frac{2\beta}{1+\beta}\right), \quad \beta = \sqrt{1-\rho^2}, \tag{D.36}$$

$$I^{(0)}_{d-1;a,b}(\rho_1 \cdot \rho_2) = \frac{\Gamma(2-2\varepsilon)\Gamma(1-\varepsilon-a)\Gamma(1-\varepsilon-b)}{2^{a+b}\Gamma^2(1-\varepsilon)\Gamma(2-2\varepsilon-a-b)} {}_2F_1\left(a, b, 1-\varepsilon; 1-\frac{\rho_1 \cdot \rho_2}{2}\right), \tag{D.37}$$

$$\begin{aligned} I^{(1)}_{d-1;a,b}\left(\rho_1 \cdot \rho_2, \rho_2^2\right) = {} & \frac{2^{(-a)}}{(\rho_1 \cdot \rho_2)^b} \frac{\Gamma(2-2\varepsilon)\Gamma(1-\varepsilon-a)}{\Gamma(1-\varepsilon)\Gamma(2-2\varepsilon-a)} \times \\ & F_1\left(b, 1-\varepsilon-a, 1-\varepsilon-a, 2-2\varepsilon-a; 1-\frac{1+\beta}{\rho_1 \cdot \rho_2}, 1-\frac{1-\beta}{\rho_1 \cdot \rho_2}\right), \quad \beta = \sqrt{1-\rho_2^2}. \end{aligned} \tag{D.38}$$

E Special functions

In this appendix we collect various identities for (generalized) hypergeometric functions, see e.g. ref. [154], that we have used in this paper.

Transformation rules.

$$
\begin{aligned}
{}_2F_1(a,b;c;z) &= (1-z)^{-a}\frac{\Gamma(b-a)\Gamma(c)}{\Gamma(c-a)\Gamma(b)}\,{}_2F_1\left(a,c-b;1+a-b;\frac{1}{1-z}\right) \\
&\quad + (1-z)^{-b}\frac{\Gamma(a-b)\Gamma(c)}{\Gamma(c-b)\Gamma(a)}\,{}_2F_1\left(b,c-a;1-a+b;\frac{1}{1-z}\right),
\end{aligned}
\tag{E.1}
$$

$$
\begin{aligned}
{}_2F_1(a,b;c;z) &= \frac{\Gamma(c-a-b)\Gamma(c)}{\Gamma(c-a)\Gamma(c-b)}\,{}_2F_1(a,b;a+b+1-c;1-z) \\
&\quad + (1-z)^{c-a-b}\frac{\Gamma(a+b-c)\Gamma(c)}{\Gamma(a)\Gamma(b)}\,{}_2F_1(c-a,c-b;c+1-a-b;1-z),
\end{aligned}
\tag{E.2}
$$

$$
{}_2F_1(a,b;c;z) = (1-z)^{-b}\,{}_2F_1\left(c-a,b;c;\frac{z}{z-1}\right), \tag{E.3}
$$

$$
{}_2F_1(a,b;2b;z) = \left(\frac{1+\sqrt{1-z}}{2}\right)^{-2a}{}_2F_1\left(a,a-b+\frac{1}{2};b+\frac{1}{2};\frac{1-\sqrt{1-z}}{1+\sqrt{1-z}}\right), \tag{E.4}
$$

$$
F_1(a;b,b';c;w,z) = (1-w)^{-a}F_1\left(a;c-b-b',b';c;\frac{w}{w-1},\frac{z-w}{1-w}\right), \tag{E.5}
$$

$$
F_1(a;b,b';b+b';w,z) = (1-z)^{-a}\,{}_2F_1\left(a,b;b+b';\frac{w-z}{1-z}\right). \tag{E.6}
$$

Integral representations.

$$
{}_2F_1(a,b;c;z) = \frac{\Gamma(c)}{\Gamma(b)\Gamma(c-b)}\int_0^1 \mathrm{d}t\, t^{b-1}(1-t)^{c-b-1}(1-tz)^{-a}, \tag{E.7}
$$

$$
{}_pF_q((a_p);(b_q);z) = \frac{\Gamma(b_q)}{\Gamma(a_p)\Gamma(b_q-a_p)}\int_0^1 \mathrm{d}t \frac{t^{a_p-1}}{(1-t)^{1+a_p-b_q}}\,{}_{p-1}F_{q-1}((a_{p-1});(b_{q-1});tz), \tag{E.8}
$$

$$
F_1(a;b,b';c;w,z) = \frac{\Gamma(c)}{\Gamma(a)\Gamma(c-a)}\int_0^1 \mathrm{d}t \frac{t^{a-1}(1-t)^{c-a-1}}{(1-wt)^b(1-zt)^{b'}}. \tag{E.9}
$$

Data Availability Statement. This article has no associated data or the data will not be deposited.

Code Availability Statement. This article has no associated code or the code will not be deposited.

References

[1] D. Baranowski et al., *Zero-jettiness soft function to third order in perturbative QCD*, arXiv:2409.11042 [INSPIRE].

[2] D. Baranowski, *NNLO zero-jettiness beam and soft functions to higher orders in the dimensional-regularization parameter* ϵ, *Eur. Phys. J. C* **80** (2020) 523 [arXiv:2004.03285] [INSPIRE].

[3] W. Chen, F. Feng, Y. Jia and X. Liu, *Double-real-virtual and double-virtual-real corrections to the three-loop thrust soft function*, *JHEP* **12** (2022) 094 [arXiv:2206.12323] [INSPIRE].

[4] D. Baranowski, M. Delto, K. Melnikov and C.-Y. Wang, *On phase-space integrals with Heaviside functions*, *JHEP* **02** (2022) 081 [arXiv:2111.13594] [INSPIRE].

[5] D. Baranowski, M. Delto, K. Melnikov and C.-Y. Wang, *Same-hemisphere three-gluon-emission contribution to the zero-jettiness soft function at N3LO QCD*, *Phys. Rev. D* **106** (2022) 014004 [arXiv:2204.09459] [INSPIRE].

[6] D. Baranowski et al., *One-loop corrections to the double-real emission contribution to the zero-jettiness soft function at N3LO in QCD*, *JHEP* **04** (2024) 114 [arXiv:2401.05245] [INSPIRE].

[7] F. Bloch and A. Nordsieck, *Note on the Radiation Field of the electron*, *Phys. Rev.* **52** (1937) 54 [INSPIRE].

[8] T. Kinoshita, *Mass singularities of Feynman amplitudes*, *J. Math. Phys.* **3** (1962) 650 [INSPIRE].

[9] T.D. Lee and M. Nauenberg, *Degenerate Systems and Mass Singularities*, *Phys. Rev.* **133** (1964) B1549 [INSPIRE].

[10] R.K. Ellis, D.A. Ross and A.E. Terrano, *The Perturbative Calculation of Jet Structure in e^+e^- Annihilation*, *Nucl. Phys. B* **178** (1981) 421 [INSPIRE].

[11] K. Fabricius, I. Schmitt, G. Krämer and G. Schierholz, *Higher Order Perturbative QCD Calculation of Jet Cross-Sections in e^+e^- Annihilation*, *Z. Phys. C* **11** (1981) 315 [INSPIRE].

[12] S. Frixione, Z. Kunszt and A. Signer, *Three jet cross-sections to next-to-leading order*, *Nucl. Phys. B* **467** (1996) 399 [hep-ph/9512328] [INSPIRE].

[13] S. Frixione, *A general approach to jet cross-sections in QCD*, *Nucl. Phys. B* **507** (1997) 295 [hep-ph/9706545] [INSPIRE].

[14] S. Catani and M.H. Seymour, *A general algorithm for calculating jet cross-sections in NLO QCD*, *Nucl. Phys. B* **485** (1997) 291 [hep-ph/9605323] [INSPIRE].

[15] S. Catani, S. Dittmaier, M.H. Seymour and Z. Trócsányi, *The dipole formalism for next-to-leading order QCD calculations with massive partons*, *Nucl. Phys. B* **627** (2002) 189 [hep-ph/0201036] [INSPIRE].

[16] Z. Nagy and D.E. Soper, *General subtraction method for numerical calculation of one loop QCD matrix elements*, *JHEP* **09** (2003) 055 [hep-ph/0308127] [INSPIRE].

[17] Z. Nagy and D.E. Soper, *Parton showers with quantum interference*, *JHEP* **09** (2007) 114 [arXiv:0706.0017] [INSPIRE].

[18] C.H. Chung, M. Krämer and T. Robens, *An alternative subtraction scheme for next-to-leading order QCD calculations*, *JHEP* **06** (2011) 144 [arXiv:1012.4948] [INSPIRE].

[19] C.-H. Chung and T. Robens, *Nagy-Soper subtraction scheme for multiparton final states*, *Phys. Rev. D* **87** (2013) 074032 [arXiv:1209.1569] [INSPIRE].

[20] G. Bevilacqua, M. Czakon, M. Kubocz and M. Worek, *Complete Nagy-Soper subtraction for next-to-leading order calculations in QCD*, *JHEP* **10** (2013) 204 [arXiv:1308.5605] [INSPIRE].

[21] S. Catani and M. Grazzini, *An NNLO subtraction formalism in hadron collisions and its application to Higgs boson production at the LHC*, *Phys. Rev. Lett.* **98** (2007) 222002 [hep-ph/0703012] [INSPIRE].

[22] R. Bonciani et al., *The q_T subtraction method for top quark production at hadron colliders*, *Eur. Phys. J. C* **75** (2015) 581 [arXiv:1508.03585] [INSPIRE].

[23] M. Grazzini, S. Kallweit and M. Wiesemann, *Fully differential NNLO computations with MATRIX*, *Eur. Phys. J. C* **78** (2018) 537 [arXiv:1711.06631] [INSPIRE].

[24] S. Catani et al., *Top-quark pair hadroproduction at next-to-next-to-leading order in QCD*, *Phys. Rev. D* **99** (2019) 051501 [arXiv:1901.04005] [INSPIRE].

[25] S. Catani et al., *Top-quark pair production at the LHC: Fully differential QCD predictions at NNLO*, *JHEP* **07** (2019) 100 [arXiv:1906.06535] [INSPIRE].

[26] S. Kallweit, V. Sotnikov and M. Wiesemann, *Triphoton production at hadron colliders in NNLO QCD*, *Phys. Lett. B* **812** (2021) 136013 [arXiv:2010.04681] [INSPIRE].

[27] S. Catani et al., *Bottom-quark production at hadron colliders: fully differential predictions in NNLO QCD*, *JHEP* **03** (2021) 029 [arXiv:2010.11906] [INSPIRE].

[28] S. Catani, I. Fabre, M. Grazzini and S. Kallweit, *$t\bar{t}H$ production at NNLO: the flavour off-diagonal channels*, *Eur. Phys. J. C* **81** (2021) 491 [arXiv:2102.03256] [INSPIRE].

[29] R. Boughezal, C. Focke, X. Liu and F. Petriello, *W-boson production in association with a jet at next-to-next-to-leading order in perturbative QCD*, *Phys. Rev. Lett.* **115** (2015) 062002 [arXiv:1504.02131] [INSPIRE].

[30] R. Boughezal et al., *Higgs boson production in association with a jet at NNLO using jettiness subtraction*, *Phys. Lett. B* **748** (2015) 5 [arXiv:1505.03893] [INSPIRE].

[31] J. Gaunt, M. Stahlhofen, F.J. Tackmann and J.R. Walsh, *N-jettiness Subtractions for NNLO QCD Calculations*, *JHEP* **09** (2015) 058 [arXiv:1505.04794] [INSPIRE].

[32] R. Boughezal et al., *Color singlet production at NNLO in MCFM*, *Eur. Phys. J. C* **77** (2017) 7 [arXiv:1605.08011] [INSPIRE].

[33] A. Gehrmann-De Ridder, T. Gehrmann and E.W.N. Glover, *Antenna subtraction at NNLO*, *JHEP* **09** (2005) 056 [hep-ph/0505111] [INSPIRE].

[34] A. Gehrmann-De Ridder, T. Gehrmann and E.W.N. Glover, *Gluon-gluon antenna functions from Higgs boson decay*, *Phys. Lett. B* **612** (2005) 49 [hep-ph/0502110] [INSPIRE].

[35] A. Gehrmann-De Ridder, T. Gehrmann and E.W.N. Glover, *Quark-gluon antenna functions from neutralino decay*, *Phys. Lett. B* **612** (2005) 36 [hep-ph/0501291] [INSPIRE].

[36] A. Daleo, T. Gehrmann and D. Maitre, *Antenna subtraction with hadronic initial states*, *JHEP* **04** (2007) 016 [hep-ph/0612257] [INSPIRE].

[37] A. Gehrmann-De Ridder, T. Gehrmann, E.W.N. Glover and G. Heinrich, *Second-order QCD corrections to the thrust distribution*, *Phys. Rev. Lett.* **99** (2007) 132002 [arXiv:0707.1285] [INSPIRE].

[38] A. Daleo, A. Gehrmann-De Ridder, T. Gehrmann and G. Luisoni, *Antenna subtraction at NNLO with hadronic initial states: initial-final configurations*, *JHEP* **01** (2010) 118 [arXiv:0912.0374] [INSPIRE].

[39] T. Gehrmann and P.F. Monni, *Antenna subtraction at NNLO with hadronic initial states: real-virtual initial-initial configurations*, *JHEP* **12** (2011) 049 [arXiv:1107.4037] [INSPIRE].

[40] R. Boughezal, A. Gehrmann-De Ridder and M. Ritzmann, *Antenna subtraction at NNLO with hadronic initial states: double real radiation for initial-initial configurations with two quark flavours*, *JHEP* **02** (2011) 098 [arXiv:1011.6631] [INSPIRE].

JHEP04(2025)084

[41] A. Gehrmann-De Ridder, T. Gehrmann and M. Ritzmann, *Antenna subtraction at NNLO with hadronic initial states: double real initial-initial configurations*, *JHEP* **10** (2012) 047 [arXiv:1207.5779] [INSPIRE].

[42] J. Currie, E.W.N. Glover and S. Wells, *Infrared Structure at NNLO Using Antenna Subtraction*, *JHEP* **04** (2013) 066 [arXiv:1301.4693] [INSPIRE].

[43] J. Currie, T. Gehrmann and J. Niehues, *Precise QCD predictions for the production of dijet final states in deep inelastic scattering*, *Phys. Rev. Lett.* **117** (2016) 042001 [arXiv:1606.03991] [INSPIRE].

[44] J. Currie et al., *Precise predictions for dijet production at the LHC*, *Phys. Rev. Lett.* **119** (2017) 152001 [arXiv:1705.10271] [INSPIRE].

[45] J. Currie et al., *Infrared sensitivity of single jet inclusive production at hadron colliders*, *JHEP* **10** (2018) 155 [arXiv:1807.03692] [INSPIRE].

[46] F. Herzog, *Geometric IR subtraction for final state real radiation*, *JHEP* **08** (2018) 006 [arXiv:1804.07949] [INSPIRE].

[47] M. Czakon, *A novel subtraction scheme for double-real radiation at NNLO*, *Phys. Lett. B* **693** (2010) 259 [arXiv:1005.0274] [INSPIRE].

[48] M. Czakon, *Double-real radiation in hadronic top quark pair production as a proof of a certain concept*, *Nucl. Phys. B* **849** (2011) 250 [arXiv:1101.0642] [INSPIRE].

[49] M. Czakon, P. Fiedler and A. Mitov, *Total Top-Quark Pair-Production Cross Section at Hadron Colliders Through $O(\alpha_S^4)$*, *Phys. Rev. Lett.* **110** (2013) 252004 [arXiv:1303.6254] [INSPIRE].

[50] M. Czakon and D. Heymes, *Four-dimensional formulation of the sector-improved residue subtraction scheme*, *Nucl. Phys. B* **890** (2014) 152 [arXiv:1408.2500] [INSPIRE].

[51] M. Czakon, A. van Hameren, A. Mitov and R. Poncelet, *Single-jet inclusive rates with exact color at $\mathcal{O}$ (α_s^4)*, *JHEP* **10** (2019) 262 [arXiv:1907.12911] [INSPIRE].

[52] H.A. Chawdhry, M.L. Czakon, A. Mitov and R. Poncelet, *NNLO QCD corrections to three-photon production at the LHC*, *JHEP* **02** (2020) 057 [arXiv:1911.00479] [INSPIRE].

[53] L. Magnea et al., *Local analytic sector subtraction at NNLO*, *JHEP* **12** (2018) 107 [*Erratum ibid.* **06** (2019) 013] [arXiv:1806.09570] [INSPIRE].

[54] L. Magnea et al., *Factorisation and Subtraction beyond NLO*, *JHEP* **12** (2018) 062 [arXiv:1809.05444] [INSPIRE].

[55] L. Magnea et al., *Analytic integration of soft and collinear radiation in factorised QCD cross sections at NNLO*, *JHEP* **02** (2021) 037 [arXiv:2010.14493] [INSPIRE].

[56] G. Somogyi, Z. Trócsányi and V. Del Duca, *Matching of singly- and doubly-unresolved limits of tree-level QCD squared matrix elements*, *JHEP* **06** (2005) 024 [hep-ph/0502226] [INSPIRE].

[57] G. Somogyi and Z. Trócsányi, *A new subtraction scheme for computing QCD jet cross sections at next-to-leading order accuracy*, hep-ph/0609041 [INSPIRE].

[58] G. Somogyi, Z. Trócsányi and V. Del Duca, *A subtraction scheme for computing QCD jet cross sections at NNLO: Regularization of doubly-real emissions*, *JHEP* **01** (2007) 070 [hep-ph/0609042] [INSPIRE].

[59] G. Somogyi and Z. Trócsányi, *A subtraction scheme for computing QCD jet cross sections at NNLO: Regularization of real-virtual emission*, *JHEP* **01** (2007) 052 [hep-ph/0609043] [INSPIRE].

[60] G. Somogyi and Z. Trócsányi, *A subtraction scheme for computing QCD jet cross sections at NNLO: Integrating the subtraction terms. I*, *JHEP* **08** (2008) 042 [arXiv:0807.0509] [INSPIRE].

[61] U. Aglietti et al., *Analytic integration of real-virtual counterterms in NNLO jet cross sections. I*, *JHEP* **09** (2008) 107 [arXiv:0807.0514] [INSPIRE].

[62] G. Somogyi, *Subtraction with hadronic initial states at NLO: An NNLO-compatible scheme*, *JHEP* **05** (2009) 016 [arXiv:0903.1218] [INSPIRE].

[63] P. Bolzoni, S.-O. Moch, G. Somogyi and Z. Trócsányi, *Analytic integration of real-virtual counterterms in NNLO jet cross sections. II*, *JHEP* **08** (2009) 079 [arXiv:0905.4390] [INSPIRE].

[64] P. Bolzoni, G. Somogyi and Z. Trócsányi, *A subtraction scheme for computing QCD jet cross sections at NNLO: integrating the iterated singly-unresolved subtraction terms*, *JHEP* **01** (2011) 059 [arXiv:1011.1909] [INSPIRE].

[65] V. Del Duca, G. Somogyi and Z. Trócsányi, *Integration of collinear-type doubly unresolved counterterms in NNLO jet cross sections*, *JHEP* **06** (2013) 079 [arXiv:1301.3504] [INSPIRE].

[66] G. Somogyi, *A subtraction scheme for computing QCD jet cross sections at NNLO: integrating the doubly unresolved subtraction terms*, *JHEP* **04** (2013) 010 [arXiv:1301.3919] [INSPIRE].

[67] V. Del Duca et al., *Jet production in the CoLoRFulNNLO method: event shapes in electron-positron collisions*, *Phys. Rev. D* **94** (2016) 074019 [arXiv:1606.03453] [INSPIRE].

[68] T. Han, G. Valencia and S. Willenbrock, *Structure function approach to vector boson scattering in p p collisions*, *Phys. Rev. Lett.* **69** (1992) 3274 [hep-ph/9206246] [INSPIRE].

[69] M. Brucherseifer, F. Caola and K. Melnikov, *On the NNLO QCD corrections to single-top production at the LHC*, *Phys. Lett. B* **736** (2014) 58 [arXiv:1404.7116] [INSPIRE].

[70] M. Cacciari et al., *Fully Differential Vector-Boson-Fusion Higgs Production at Next-to-Next-to-Leading Order*, *Phys. Rev. Lett.* **115** (2015) 082002 [*Erratum ibid.* **120** (2018) 139901] [arXiv:1506.02660] [INSPIRE].

[71] X. Chen et al., *Dilepton Rapidity Distribution in Drell-Yan Production to Third Order in QCD*, *Phys. Rev. Lett.* **128** (2022) 052001 [arXiv:2107.09085] [INSPIRE].

[72] T. Neumann and J. Campbell, *Fiducial Drell-Yan production at the LHC improved by transverse-momentum resummation at N^4LLp+N^3LO*, *Phys. Rev. D* **107** (2023) L011506 [arXiv:2207.07056] [INSPIRE].

[73] X. Chen et al., *Third-Order Fiducial Predictions for Drell-Yan Production at the LHC*, *Phys. Rev. Lett.* **128** (2022) 252001 [arXiv:2203.01565] [INSPIRE].

[74] X. Chen et al., *Transverse mass distribution and charge asymmetry in W boson production to third order in QCD*, *Phys. Lett. B* **840** (2023) 137876 [arXiv:2205.11426] [INSPIRE].

[75] J. Campbell and T. Neumann, *Third order QCD predictions for fiducial W-boson production*, *JHEP* **11** (2023) 127 [arXiv:2308.15382] [INSPIRE].

[76] D.E. Soper, *Techniques for QCD calculations by numerical integration*, *Phys. Rev. D* **62** (2000) 014009 [hep-ph/9910292] [INSPIRE].

[77] D.E. Soper, *Choosing integration points for QCD calculations by numerical integration*, *Phys. Rev. D* **64** (2001) 034018 [hep-ph/0103262] [INSPIRE].

[78] M. Krämer and D.E. Soper, *Next-to-leading order numerical calculations in Coulomb gauge*, *Phys. Rev. D* **66** (2002) 054017 [hep-ph/0204113] [INSPIRE].

[79] M. Krämer and D.E. Soper, *Next-to-leading order QCD calculations with parton showers. I. Collinear singularities*, *Phys. Rev. D* **69** (2004) 054019 [hep-ph/0306222] [INSPIRE].

[80] D.E. Soper, *Next-to-leading order QCD calculations with parton showers. II. Soft singularities*, *Phys. Rev. D* **69** (2004) 054020 [hep-ph/0306268] [INSPIRE].

[81] Z. Capatti, V. Hirschi, A. Pelloni and B. Ruijl, *Local Unitarity: a representation of differential cross-sections that is locally free of infrared singularities at any order*, *JHEP* **04** (2021) 104 [arXiv:2010.01068] [INSPIRE].

[82] A. A H et al., *Light-by-light scattering at next-to-leading order in QCD and QED*, *Phys. Lett. B* **851** (2024) 138555 [arXiv:2312.16956] [INSPIRE].

[83] G. Heinrich, *Collider Physics at the Precision Frontier*, *Phys. Rept.* **922** (2021) 1 [arXiv:2009.00516] [INSPIRE].

[84] I.W. Stewart, F.J. Tackmann and W.J. Waalewijn, *Factorization at the LHC: From PDFs to Initial State Jets*, *Phys. Rev. D* **81** (2010) 094035 [arXiv:0910.0467] [INSPIRE].

[85] I.W. Stewart, F.J. Tackmann and W.J. Waalewijn, *N-Jettiness: An Inclusive Event Shape to Veto Jets*, *Phys. Rev. Lett.* **105** (2010) 092002 [arXiv:1004.2489] [INSPIRE].

[86] J. Gaunt, M. Stahlhofen and F.J. Tackmann, *The Gluon Beam Function at Two Loops*, *JHEP* **08** (2014) 020 [arXiv:1405.1044] [INSPIRE].

[87] J.R. Gaunt, M. Stahlhofen and F.J. Tackmann, *The Quark Beam Function at Two Loops*, *JHEP* **04** (2014) 113 [arXiv:1401.5478] [INSPIRE].

[88] R. Boughezal, F. Petriello, U. Schubert and H. Xing, *Spin-dependent quark beam function at NNLO*, *Phys. Rev. D* **96** (2017) 034001 [arXiv:1704.05457] [INSPIRE].

[89] R. Brüser, Z.L. Liu and M. Stahlhofen, *Three-Loop Quark Jet Function*, *Phys. Rev. Lett.* **121** (2018) 072003 [arXiv:1804.09722] [INSPIRE].

[90] M.A. Ebert, B. Mistlberger and G. Vita, *Collinear expansion for color singlet cross sections*, *JHEP* **09** (2020) 181 [arXiv:2006.03055] [INSPIRE].

[91] M.A. Ebert, B. Mistlberger and G. Vita, *N-jettiness beam functions at N^3LO*, *JHEP* **09** (2020) 143 [arXiv:2006.03056] [INSPIRE].

[92] A. Behring et al., *Quark beam function at next-to-next-to-next-to-leading order in perturbative QCD in the generalized large-N_c approximation*, *Phys. Rev. D* **100** (2019) 114034 [arXiv:1910.10059] [INSPIRE].

[93] D. Baranowski et al., *Beam functions for N-jettiness at N^3LO in perturbative QCD*, *JHEP* **02** (2023) 073 [arXiv:2211.05722] [INSPIRE].

[94] R. Kelley, M.D. Schwartz, R.M. Schabinger and H.X. Zhu, *The two-loop hemisphere soft function*, *Phys. Rev. D* **84** (2011) 045022 [arXiv:1105.3676] [INSPIRE].

[95] P.F. Monni, T. Gehrmann and G. Luisoni, *Two-Loop Soft Corrections and Resummation of the Thrust Distribution in the Dijet Region*, *JHEP* **08** (2011) 010 [arXiv:1105.4560] [INSPIRE].

[96] R. Boughezal, X. Liu and F. Petriello, *N-jettiness soft function at next-to-next-to-leading order*, *Phys. Rev. D* **91** (2015) 094035 [arXiv:1504.02540] [INSPIRE].

[97] H.T. Li and J. Wang, *Next-to-Next-to-Leading Order N-Jettiness Soft Function for One Massive Colored Particle Production at Hadron Colliders*, *JHEP* **02** (2017) 002 [arXiv:1611.02749] [INSPIRE].

JHEP04(2025)084

[98] J.M. Campbell, R.K. Ellis, R. Mondini and C. Williams, *The NNLO QCD soft function for 1-jettiness*, *Eur. Phys. J. C* **78** (2018) 234 [arXiv:1711.09984] [INSPIRE].

[99] P. Banerjee, P.K. Dhani and V. Ravindran, *Gluon jet function at three loops in QCD*, *Phys. Rev. D* **98** (2018) 094016 [arXiv:1805.02637] [INSPIRE].

[100] S. Jin and X. Liu, *Two-loop N-jettiness soft function for $pp \to 2j$ production*, *Phys. Rev. D* **99** (2019) 114017 [arXiv:1901.10935] [INSPIRE].

[101] G. Bell, B. Dehnadi, T. Mohrmann and R. Rahn, *The NNLO soft function for N-jettiness in hadronic collisions*, *JHEP* **07** (2024) 077 [arXiv:2312.11626] [INSPIRE].

[102] P. Agarwal, K. Melnikov and I. Pedron, *N-jettiness soft function at next-to-next-to-leading order in perturbative QCD*, *JHEP* **05** (2024) 005 [arXiv:2403.03078] [INSPIRE].

[103] F. Caola, K. Melnikov and R. Röntsch, *Nested soft-collinear subtractions in NNLO QCD computations*, *Eur. Phys. J. C* **77** (2017) 248 [arXiv:1702.01352] [INSPIRE].

[104] F. Caola, M. Delto, H. Frellesvig and K. Melnikov, *The double-soft integral for an arbitrary angle between hard radiators*, *Eur. Phys. J. C* **78** (2018) 687 [arXiv:1807.05835] [INSPIRE].

[105] T. Binoth and G. Heinrich, *An automatized algorithm to compute infrared divergent multiloop integrals*, *Nucl. Phys. B* **585** (2000) 741 [hep-ph/0004013] [INSPIRE].

[106] F.V. Tkachov, *A theorem on analytical calculability of 4-loop renormalization group functions*, *Phys. Lett. B* **100** (1981) 65 [INSPIRE].

[107] K.G. Chetyrkin and F.V. Tkachov, *Integration by parts: The algorithm to calculate β-functions in 4 loops*, *Nucl. Phys. B* **192** (1981) 159 [INSPIRE].

[108] A.V. Kotikov, *Differential equations method: New technique for massive Feynman diagrams calculation*, *Phys. Lett. B* **254** (1991) 158 [INSPIRE].

[109] A.V. Kotikov, *Differential equations method: The calculation of vertex type Feynman diagrams*, *Phys. Lett. B* **259** (1991) 314 [INSPIRE].

[110] A.V. Kotikov, *Differential equation method: The calculation of N point Feynman diagrams*, *Phys. Lett. B* **267** (1991) 123 [INSPIRE].

[111] E. Remiddi, *Differential equations for Feynman graph amplitudes*, *Nuovo Cim. A* **110** (1997) 1435 [hep-th/9711188] [INSPIRE].

[112] T. Gehrmann and E. Remiddi, *Differential equations for two-loop four-point functions*, *Nucl. Phys. B* **580** (2000) 485 [hep-ph/9912329] [INSPIRE].

[113] C. Duhr and T. Gehrmann, *The two-loop soft current in dimensional regularization*, *Phys. Lett. B* **727** (2013) 452 [arXiv:1309.4393] [INSPIRE].

[114] Y. Li and H.X. Zhu, *Single soft gluon emission at two loops*, *JHEP* **11** (2013) 080 [arXiv:1309.4391] [INSPIRE].

[115] S.D. Badger and E.W.N. Glover, *Two loop splitting functions in QCD*, *JHEP* **07** (2004) 040 [hep-ph/0405236] [INSPIRE].

[116] S. Catani, D. Colferai and A. Torrini, *Triple (and quadruple) soft-gluon radiation in QCD hard scattering*, *JHEP* **01** (2020) 118 [arXiv:1908.01616] [INSPIRE].

[117] V. Del Duca, C. Duhr, R. Haindl and Z. Liu, *Tree-level soft emission of a quark pair in association with a gluon*, *JHEP* **01** (2023) 040 [arXiv:2206.01584] [INSPIRE].

[118] S. Catani, L. Cieri, D. Colferai and F. Coradeschi, *Soft gluon-quark-antiquark emission in QCD hard scattering*, *Eur. Phys. J. C* **83** (2023) 38 [arXiv:2210.09397] [INSPIRE].

[119] M. Tentyukov and J. Fleischer, *A Feynman diagram analyzer DIANA*, Comput. Phys. Commun. **132** (2000) 124 [hep-ph/9904258] [INSPIRE].

[120] P. Nogueira, *Automatic Feynman Graph Generation*, J. Comput. Phys. **105** (1993) 279 [INSPIRE].

[121] S. Catani and M. Grazzini, *Infrared factorization of tree level QCD amplitudes at the next-to-next-to-leading order and beyond*, Nucl. Phys. B **570** (2000) 287 [hep-ph/9908523] [INSPIRE].

[122] J.A.M. Vermaseren, *New features of FORM*, math-ph/0010025 [INSPIRE].

[123] J. Kuipers, T. Ueda, J.A.M. Vermaseren and J. Vollinga, *FORM version 4.0*, Comput. Phys. Commun. **184** (2013) 1453 [arXiv:1203.6543] [INSPIRE].

[124] J. Kuipers, T. Ueda and J.A.M. Vermaseren, *Code Optimization in FORM*, Comput. Phys. Commun. **189** (2015) 1 [arXiv:1310.7007] [INSPIRE].

[125] B. Ruijl, T. Ueda and J. Vermaseren, *FORM version 4.2*, arXiv:1707.06453 [INSPIRE].

[126] J.C. Collins and F.V. Tkachov, *Breakdown of dimensional regularization in the Sudakov problem*, Phys. Lett. B **294** (1992) 403 [hep-ph/9208209] [INSPIRE].

[127] Y. Li, D. Neill and H.X. Zhu, *An exponential regulator for rapidity divergences*, Nucl. Phys. B **960** (2020) 115193 [arXiv:1604.00392] [INSPIRE].

[128] W. Chen, *Unregulated divergences of Feynman integrals*, Phys. Lett. B **862** (2025) 139299 [arXiv:2406.12051] [INSPIRE].

[129] C. Anastasiou and K. Melnikov, *Higgs boson production at hadron colliders in NNLO QCD*, Nucl. Phys. B **646** (2002) 220 [hep-ph/0207004] [INSPIRE].

[130] S. Laporta, *High-precision calculation of multiloop Feynman integrals by difference equations*, Int. J. Mod. Phys. A **15** (2000) 5087 [hep-ph/0102033] [INSPIRE].

[131] C. Anastasiou, L.J. Dixon, K. Melnikov and F. Petriello, *High precision QCD at hadron colliders: Electroweak gauge boson rapidity distributions at NNLO*, Phys. Rev. D **69** (2004) 094008 [hep-ph/0312266] [INSPIRE].

[132] V. Maheria, *Semi- and Fully-Inclusive Phase-Space Integrals at Four Loops*, Ph.D. thesis, Universität Hamburg, 22761 Hamburg, Germany (2022) [INSPIRE].

[133] P. Maierhöfer, J. Usovitsch and P. Uwer, *Kira — A Feynman integral reduction program*, Comput. Phys. Commun. **230** (2018) 99 [arXiv:1705.05610] [INSPIRE].

[134] P. Maierhöfer and J. Usovitsch, *Kira 1.2 Release Notes*, arXiv:1812.01491 [INSPIRE].

[135] J. Klappert, F. Lange, P. Maierhöfer and J. Usovitsch, *Integral reduction with Kira 2.0 and finite field methods*, Comput. Phys. Commun. **266** (2021) 108024 [arXiv:2008.06494] [INSPIRE].

[136] T. Huber and D. Maitre, *HypExp: A Mathematica package for expanding hypergeometric functions around integer-valued parameters*, Comput. Phys. Commun. **175** (2006) 122 [hep-ph/0507094] [INSPIRE].

[137] T. Huber and D. Maitre, *HypExp 2, Expanding Hypergeometric Functions about Half-Integer Parameters*, Comput. Phys. Commun. **178** (2008) 755 [arXiv:0708.2443] [INSPIRE].

[138] E. Panzer, *Algorithms for the symbolic integration of hyperlogarithms with applications to Feynman integrals*, Comput. Phys. Commun. **188** (2015) 148 [arXiv:1403.3385] [INSPIRE].

[139] G. Somogyi, *Angular integrals in d dimensions*, *J. Math. Phys.* **52** (2011) 083501 [arXiv:1101.3557] [INSPIRE].

[140] V.E. Lyubovitskij, F. Wunder and A.S. Zhevlakov, *New ideas for handling of loop and angular integrals in D-dimensions in QCD*, *JHEP* **06** (2021) 066 [arXiv:2102.08943] [INSPIRE].

[141] T. Ahmed, S.M. Hasan and A. Rapakoulias, *Phase-space integrals through Mellin-Barnes representation*, arXiv:2410.18886 [INSPIRE].

[142] S. Borowka et al., *pySecDec: a toolbox for the numerical evaluation of multi-scale integrals*, *Comput. Phys. Commun.* **222** (2018) 313 [arXiv:1703.09692] [INSPIRE].

[143] M. Czakon, *Automatized analytic continuation of Mellin-Barnes integrals*, *Comput. Phys. Commun.* **175** (2006) 559 [hep-ph/0511200] [INSPIRE].

[144] A.V. Belitsky, A.V. Smirnov and V.A. Smirnov, *MB tools reloaded*, *Nucl. Phys. B* **986** (2023) 116067 [arXiv:2211.00009] [INSPIRE].

[145] A.V. Smirnov, N.D. Shapurov and L.I. Vysotsky, *FIESTA5: Numerical high-performance Feynman integral evaluation*, *Comput. Phys. Commun.* **277** (2022) 108386 [arXiv:2110.11660] [INSPIRE].

[146] A.V. Smirnov and V.A. Smirnov, *On the Resolution of Singularities of Multiple Mellin-Barnes Integrals*, *Eur. Phys. J. C* **62** (2009) 445 [arXiv:0901.0386] [INSPIRE].

[147] T. Hahn, *CUBA: A library for multidimensional numerical integration*, *Comput. Phys. Commun.* **168** (2005) 78 [hep-ph/0404043] [INSPIRE].

[148] E. Panzer, *On hyperlogarithms and Feynman integrals with divergences and many scales*, *JHEP* **03** (2014) 071 [arXiv:1401.4361] [INSPIRE].

[149] A. von Manteuffel, E. Panzer and R.M. Schabinger, *A quasi-finite basis for multi-loop Feynman integrals*, *JHEP* **02** (2015) 120 [arXiv:1411.7392] [INSPIRE].

[150] G.P. Korchemsky and G. Marchesini, *Resummation of large infrared corrections using Wilson loops*, *Phys. Lett. B* **313** (1993) 433 [INSPIRE].

[151] G.P. Korchemsky and G. Marchesini, *Structure function for large × and renormalization of Wilson loop*, *Nucl. Phys. B* **406** (1993) 225 [hep-ph/9210281] [INSPIRE].

[152] G. Billis, M.A. Ebert, J.K.L. Michel and F.J. Tackmann, *A toolbox for q_T and 0-jettiness subtractions at N^3LO*, *Eur. Phys. J. Plus* **136** (2021) 214 [arXiv:1909.00811] [INSPIRE].

[153] S. Catani and M. Grazzini, *The soft gluon current at one loop order*, *Nucl. Phys. B* **591** (2000) 435 [hep-ph/0007142] [INSPIRE].

[154] M. Abramowitz and I. Stegun, *Handbook of Mathematical Functions, With Formulas, Graphs, and Mathematical Tables*, Dover Publications, Incorporated (1974) [ISBN: 9780486612720].

JHEP04(2025)084